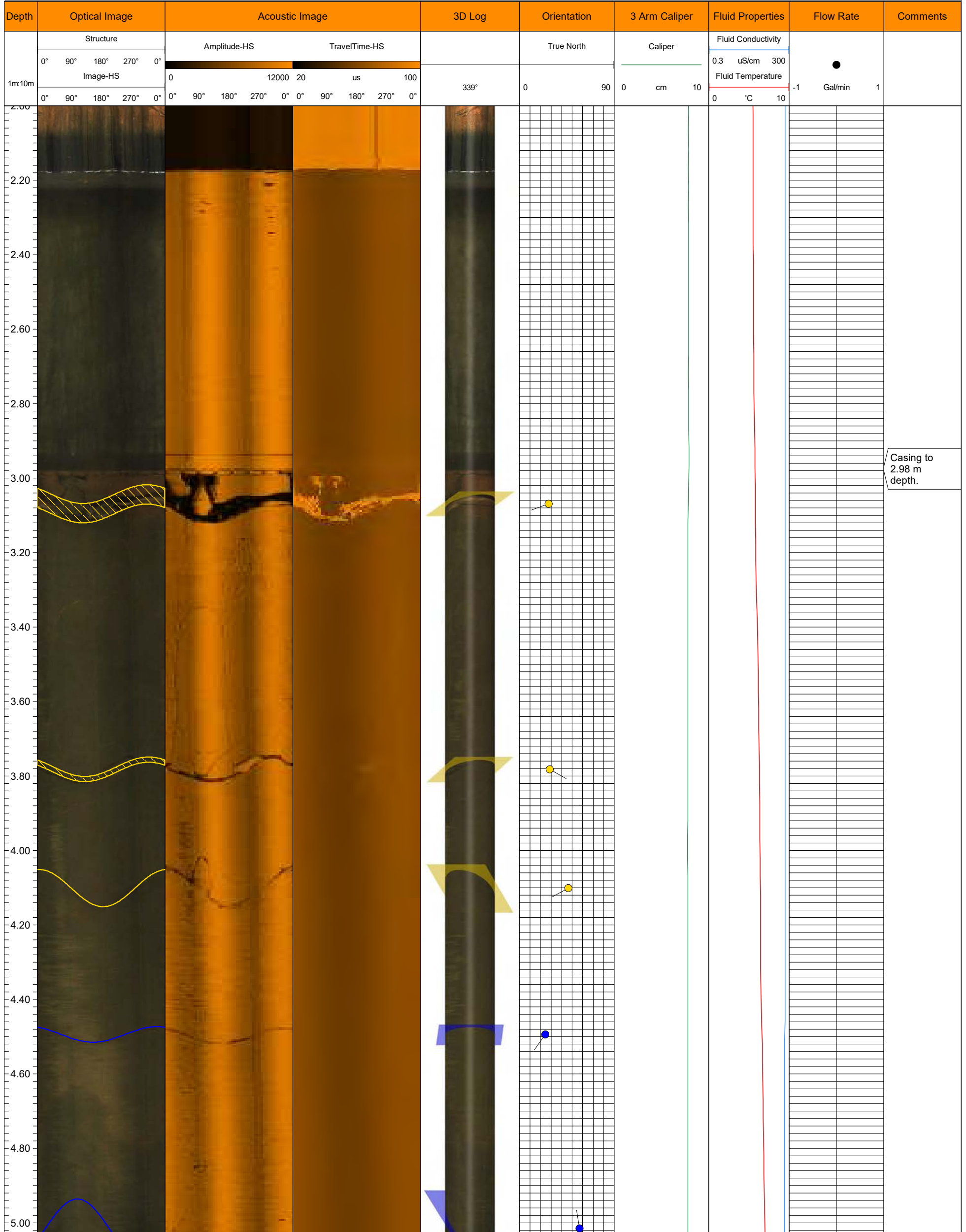


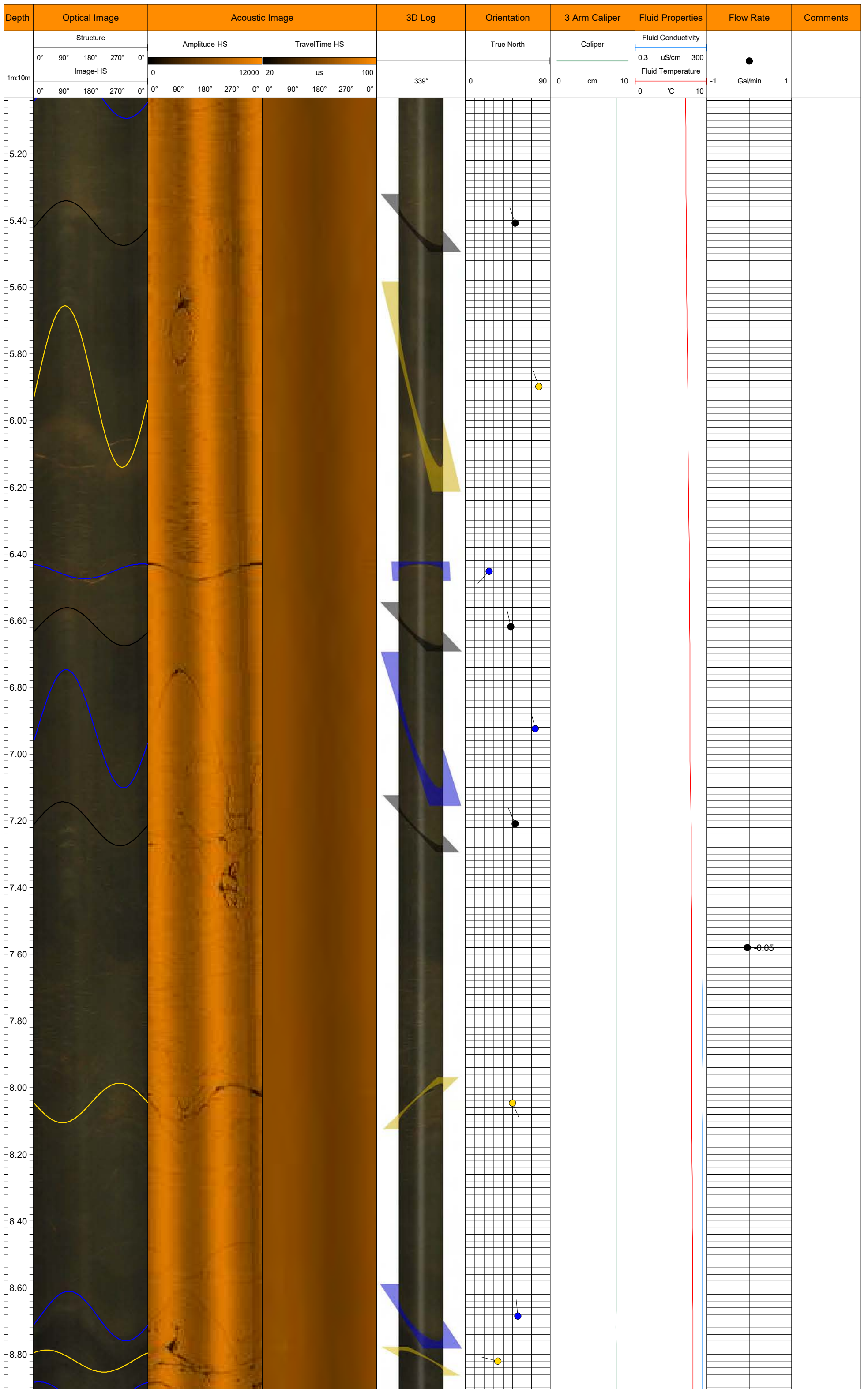
Client: Stantec Consulting Inc				
Project: Downhole Geophysical Investigation Mooseland, Nova Scotia 21-100-H				
Area: Mooseland		Hole ID: BH21-12		
Location: N: 4980999 E: 504225 Z: 110		Azimuth: 0		Dip: -90
Hole Depth (m): 110	Log Depth (m): 40	Logged By: P.Ramlochund	Logged Date: 01/02/22	Water Level: 2.1 m

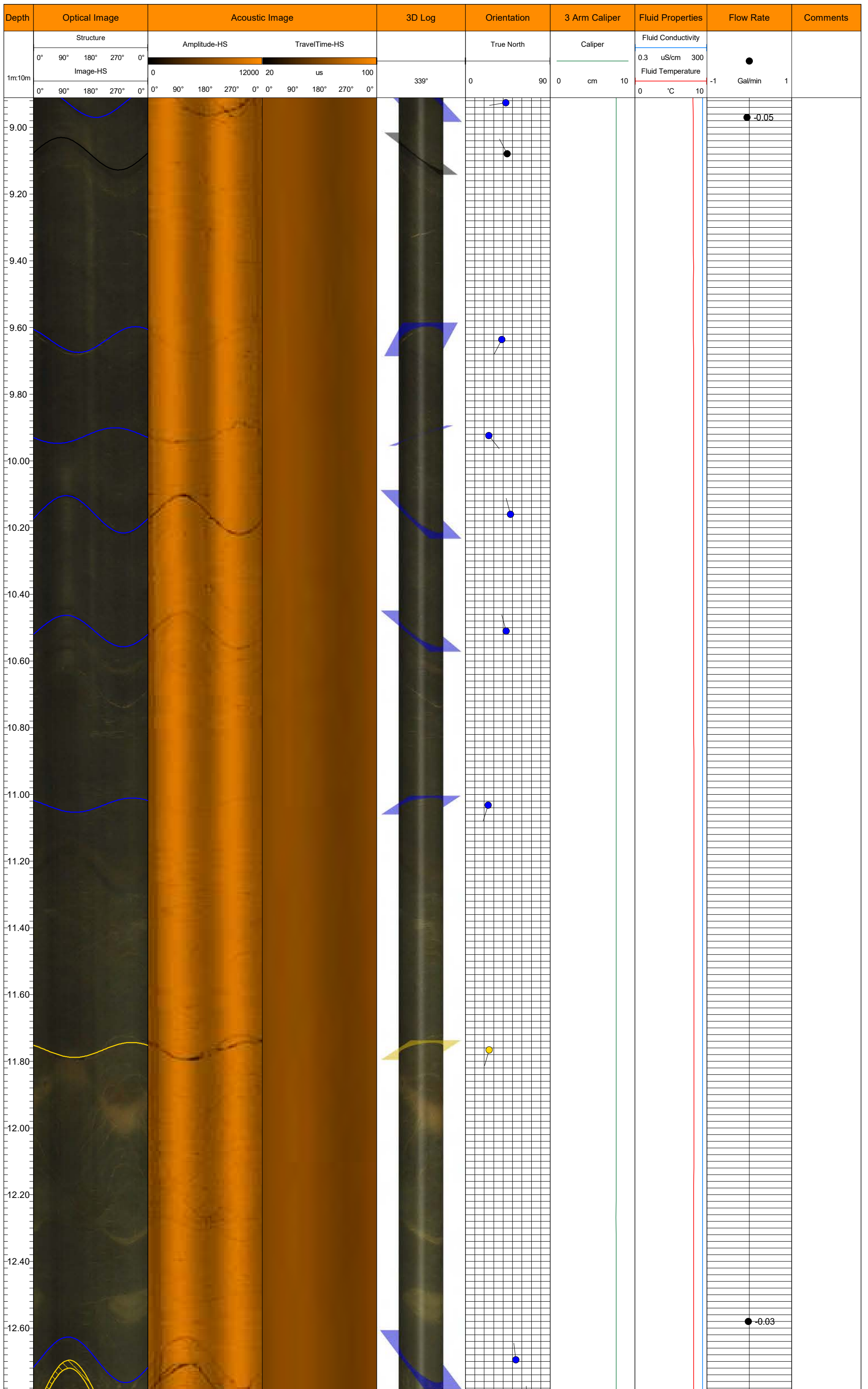


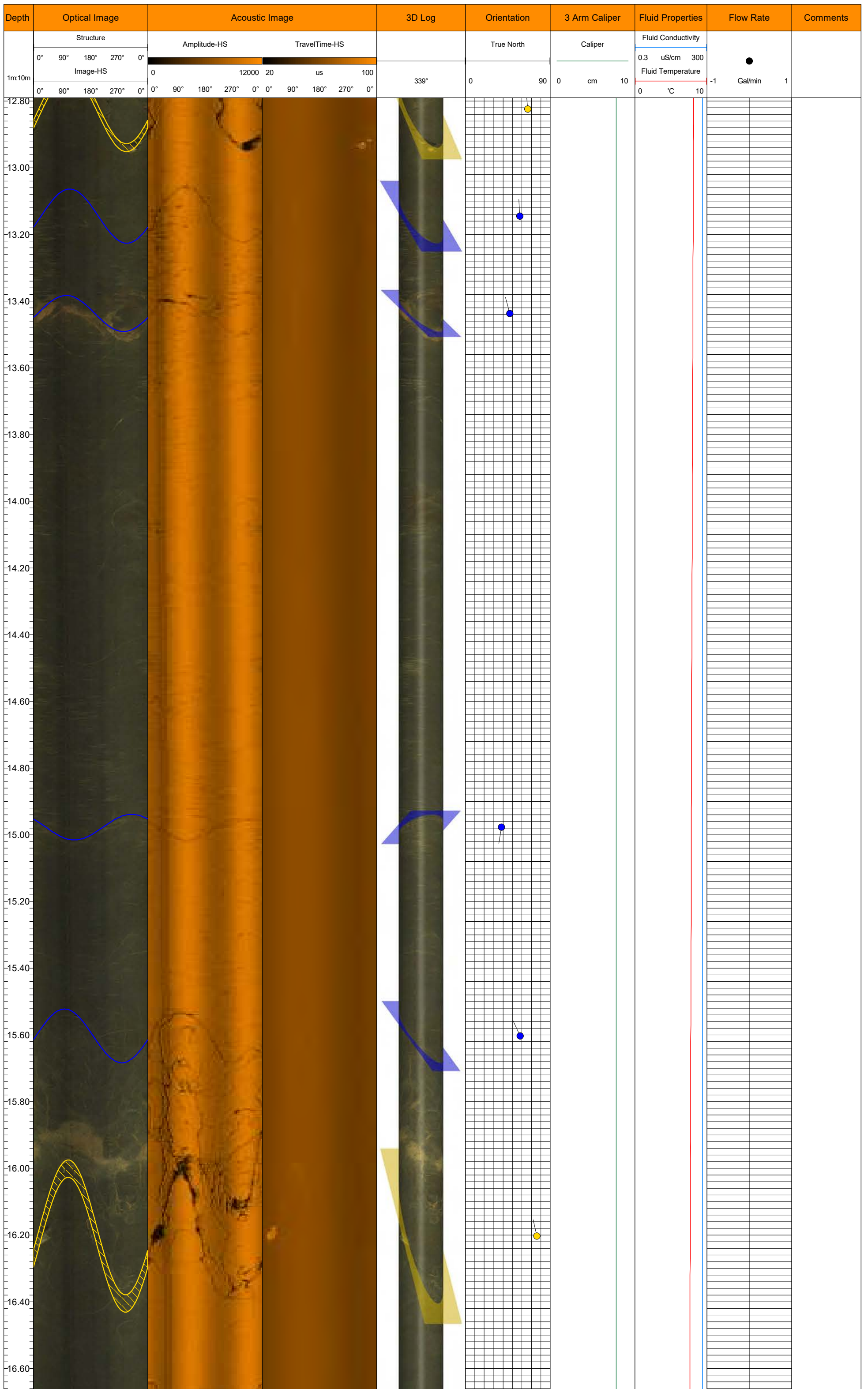
OJT - Open Joint	JC - Cemented Joint	JS - Joint	VN - Vein
FLT_m - Minor Fault	FLT_M - Fault Zone	BD - Bedding	CL - Cleavage
SZ - Shear	FO - Foliation	FOc - Foliation Closed	RZ - Rubble Zone
CNT - Contact	IAP - Interpreted Axial Plane		

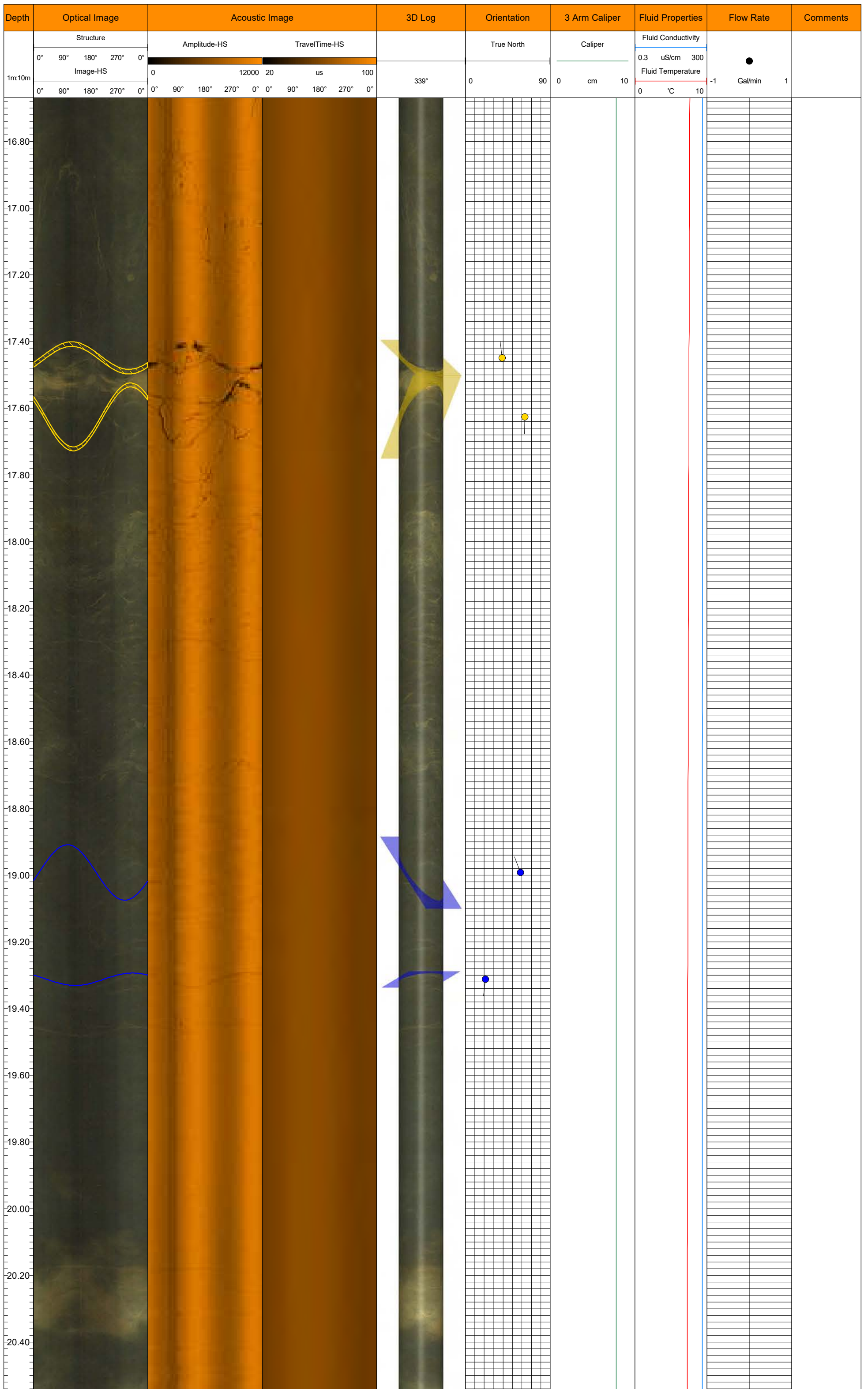
Notes:

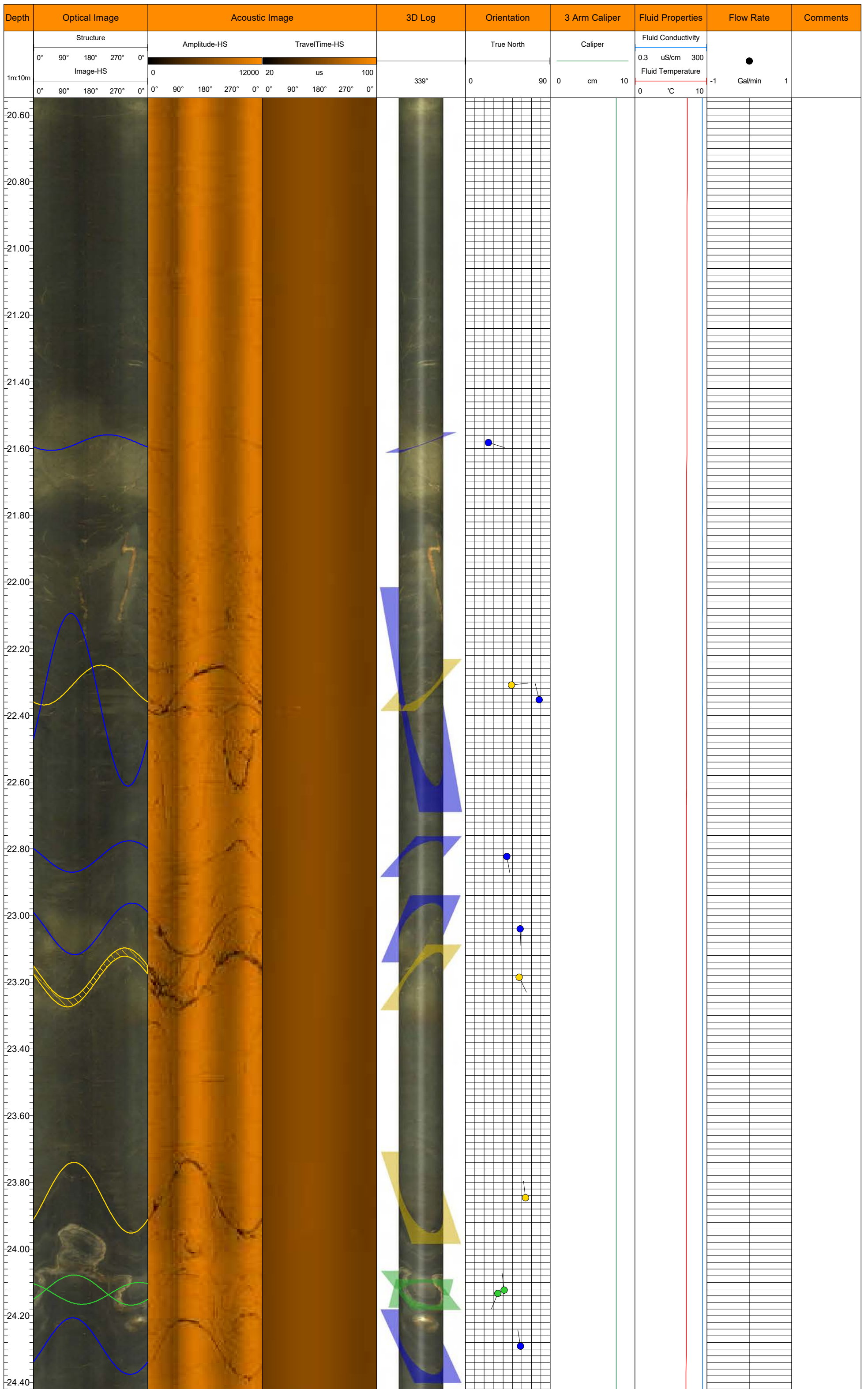


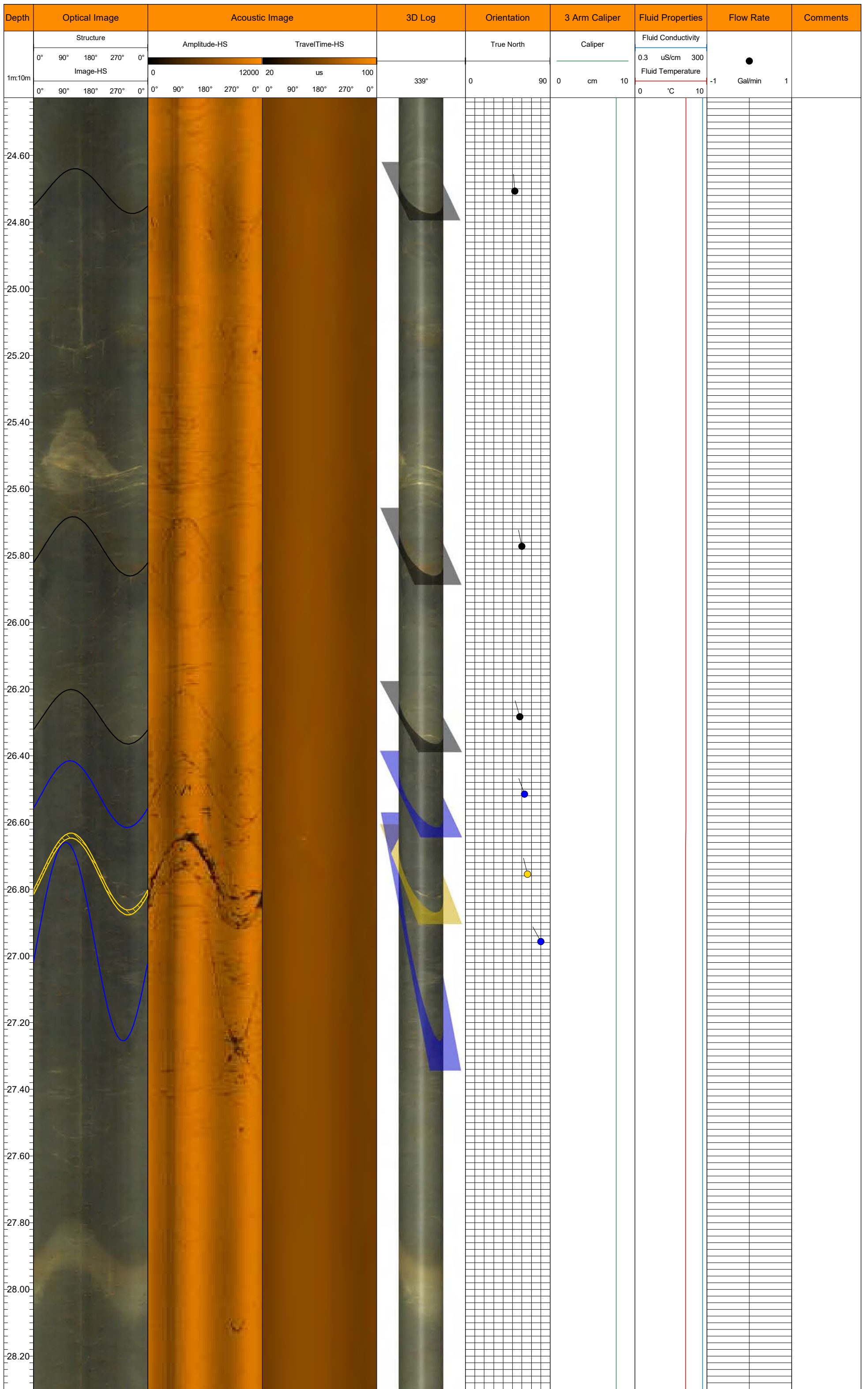


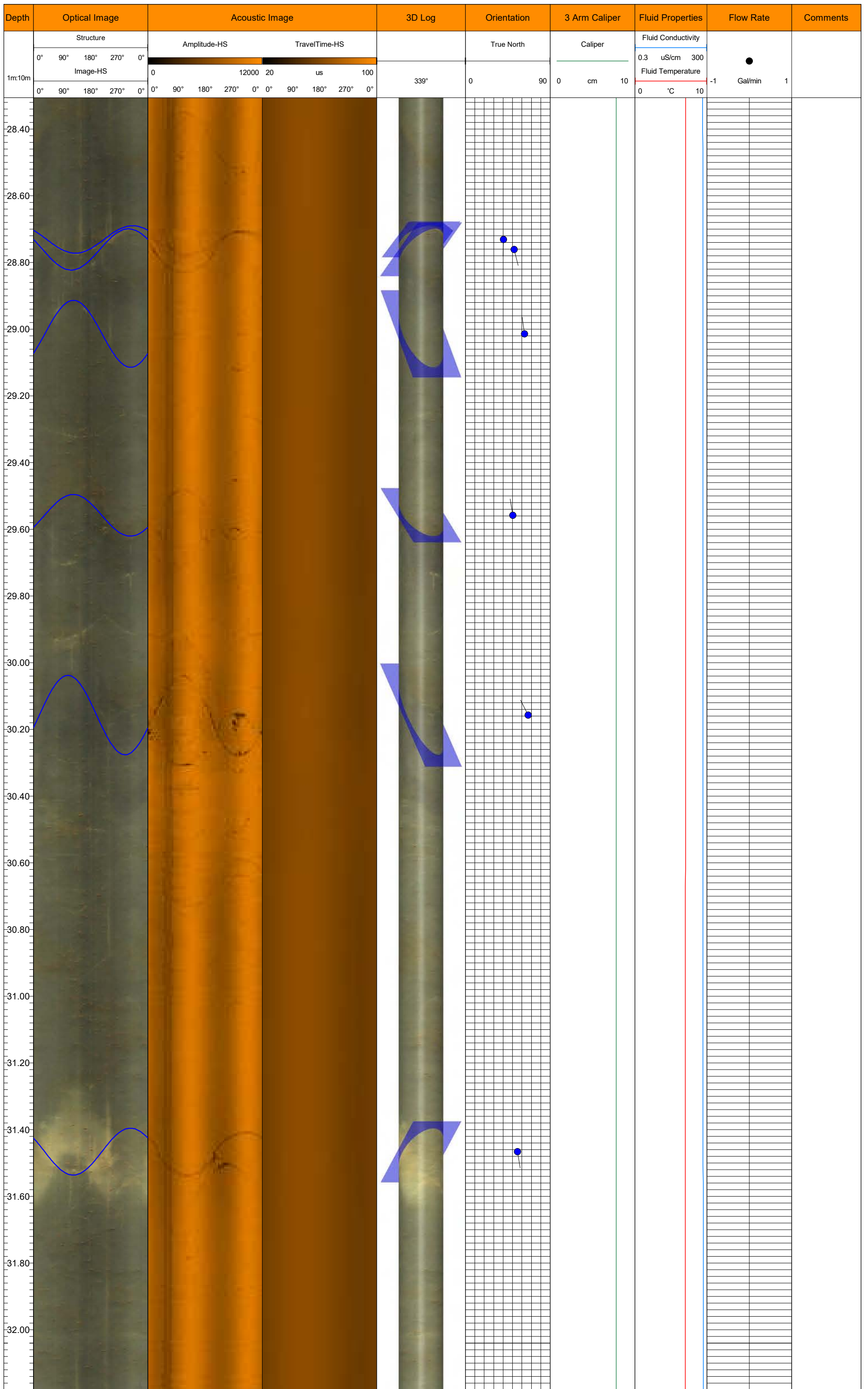




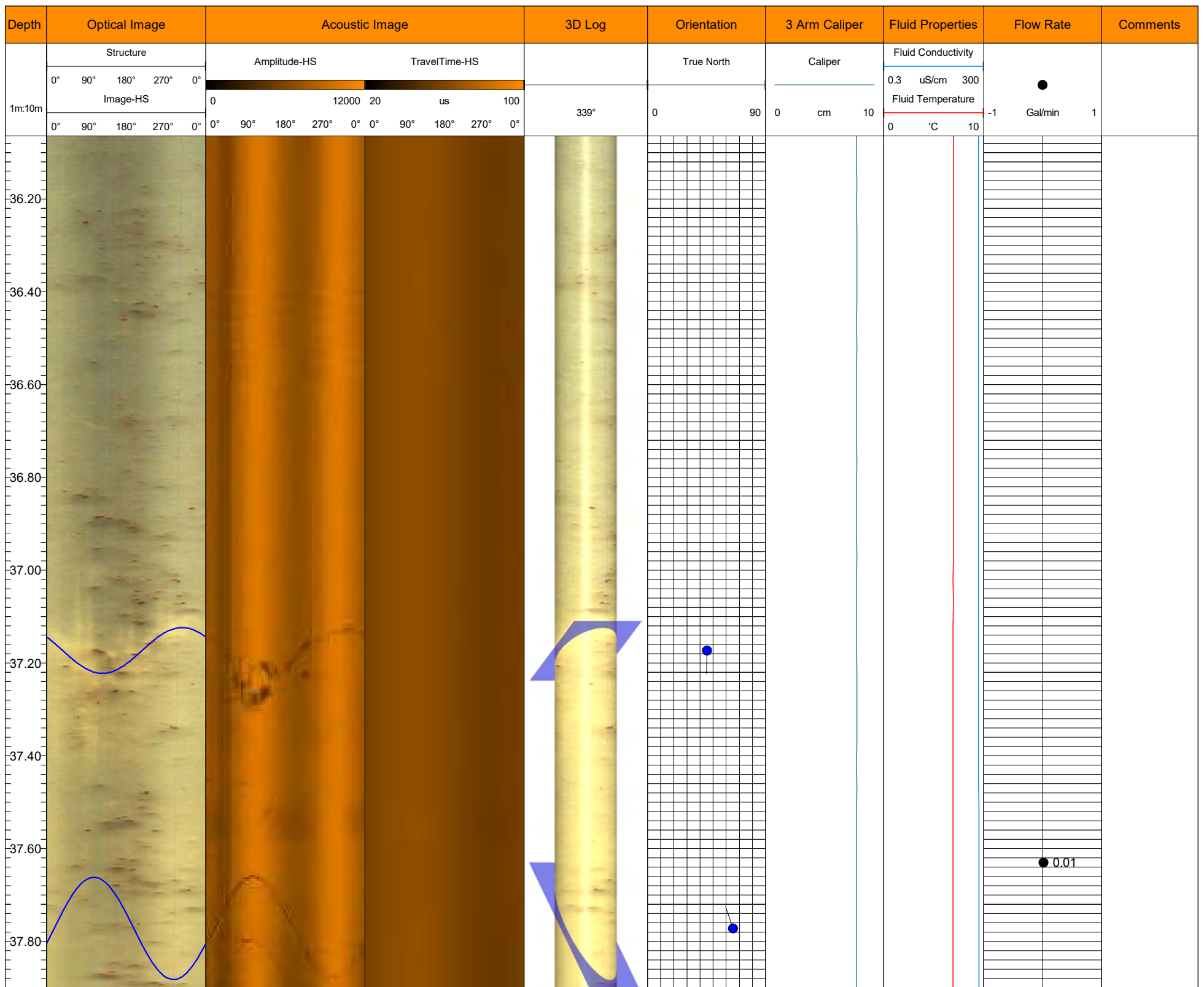








Depth	Optical Image					Acoustic Image								3D Log	Orientation		3 Arm Caliper		Fluid Properties			Flow Rate		Comments			
	Structure					Amplitude-HS				TravelTime-HS				339°	True North		Caliper		Fluid Conductivity			Gal/min					
	0°	90°	180°	270°	0°	Image-HS				0	12000	20	us		100	0	90	0	cm	10	0.3		uS/cm		300		
1m:10m	0°	90°	180°	270°	0°	0°	90°	180°	270°	0°	0°	90°	180°	270°	0°	339°	0	90	0	cm	10	0	°C	10	-1	Gal/min	1
32.20																											
32.40																											
32.60																											
32.80																											
33.00																											
33.20																											
33.40																											
33.60																											
33.80																											
34.00																											
34.20																											
34.40																											
34.60																											
34.80																											
35.00																											
35.20																											
35.40																											
35.60																											
35.80																											
36.00																											



Heat Pulse Flow Meter Data Summary With Comments

Borehole_ID	Depth_of Shot_m	Num_of Shots ¹	Evidence_of Flow ²	Average_Flow_Rate Gal_per_minute hots ³	Confidence_In_Raw Data ⁵	Comments
BH21-01	1.73	3	N			Shots show little to no evidence of flow.
BH21-01	6.04	3	Y	-0.323	High	Repeatable flow rates on all shots.
BH21-01	11.07	3	Y	-0.328	High	Repeatable flow rates on all shots.
BH21-01	16.01	3	Y	-0.300	High	Repeatable flow rates on all shots.
BH21-01	21.04	3	Y	-0.042	High	Repeatable flow rates on all shots.
BH21-01	26.05	3	Y	-0.041	High	Repeatable flow rates on all shots.
BH21-01	31.03	3	Y	-0.040	High	Repeatable flow rates on all shots.
BH21-01	36.02	2	Y	-0.041	High	Repeatable flow rates on all shots.
BH21-01	41.04	2	Y	-0.037	High	Repeatable flow rates on all shots.
BH21-02	15.00	3	N			Shots show little to no evidence of flow. Noisy data. Audible flow heard in borehole, flows maybe too high for tool detector
BH21-02	15.11	2	N			Shots show little to no evidence of flow. Noisy data. Audible flow heard in borehole, flows maybe too high for tool detector
BH21-02	17.99	3	N			Shots show little to no evidence of flow. Noisy data. Audible flow heard in borehole, flows maybe too high for tool detector
BH21-02	21.07	2	N			Shots show little to no evidence of flow. Noisy data. Audible flow heard in borehole, flows maybe too high for tool detector
BH21-02	24.12	3	N			Shots show little to no evidence of flow. Noisy data. Audible flow heard in borehole, flows maybe too high for tool detector
BH21-02	26.05	2	N			Shots show little to no evidence of flow. Noisy data. Audible flow heard in borehole, flows maybe too high for tool detector
BH21-02	30.01	2	N			Shots show little to no evidence of flow. Audible flow heard in borehole, flows maybe too high for tool detection.
BH21-02	31.03	2	N			Shots show little to no evidence of flow. Noisy data. Audible flow heard in borehole, flows maybe too high for tool detector
BH21-02	36.08	2	N			Shots show little to no evidence of flow. Noisy data. Audible flow heard in borehole, flows maybe too high for tool detector
BH21-02	38.72	2	N			Shots show little to no evidence of flow. Audible flow heard in borehole, flows maybe too high for tool detection.
BH21-02	41.03	3	N			Shots show little to no evidence of flow. Noisy data. Audible flow heard in borehole, flows maybe too high for tool detector
BH21-02	44.75	3	N			Shots show little to no evidence of flow. Noisy data. Audible flow heard in borehole, flows maybe too high for tool detector
BH21-02	46.03	2	Y	NR ⁴	Low	Noisy data. Possible flow exceeding 1 gallon per minute.
BH21-02	51.04	3	Y	-0.717	High	Repeatable flow rates. Flow rate near maximum of tool.
BH21-02	56.09	3	Y	-0.094	Med	
BH21-02	59.01	3	N			Shots show little to no evidence of flow.
BH21-03	8.52	3	N			Shots show little to no evidence of flow.
BH21-03	11.98	3	N			Shots show little to no evidence of flow.
BH21-03	13.48	5	Y	-0.012	Low	Noisy data. 2 of 5 shots appear to display low flow.
BH21-03	18.62	3	Y	-0.023	Med	Slight variability in flow within 2 shots. 1 shot removed as Noise.
BH21-03	23.53	3	Y	-0.016	Med	Slight variability in flow within 2 shots. 1 shot removed as Noise.
BH21-03	28.63	3	Y	-0.015	High	Repeatable flow rates on all shots.
BH21-03	29.92	3	Y	-0.014	High	Repeatable flow rates on all shots.
BH21-03	33.52	5	Y	-0.017	Med	3 of 5 shots show slight variation in flow.
BH21-03	38.58	4	Y	-0.017	Low	1 of 4 shots show low flow. Others show potential of very low flow near the end of the capture window.
BH21-03	43.56	3	Y	-0.014	High	Repeatable flow rates on all shots.
BH21-03	48.62	3	Y	-0.013	High	Repeatable flow rates on all shots.
BH21-03	53.55	3	Y	-0.013	High	Repeatable flow rates on all shots.
BH21-03	58.5	3	Y	-0.013	High	Repeatable flow rates on all shots.
BH21-03	63.56	3	Y	-0.011	Med	Slight variation in flows over 3 shots.
BH21-03	68.5	3	Y	-0.010	Med	Very low flow rate over 3 shots. Possible flows slightly less than reported, limits of capture window.
BH21-03	73.54	3	Y	-0.010	High	Repeatable flow rates on all shots.
BH21-03	77	3	Y	-0.012	Low	1 of 3 shots show flow. 2 shots appear to show very slow flow outside capture window.
BH21-03	78.54	5	Y	-0.011	Low	1 of 5 shots show flow. 4 shots appear to show very slow flow outside capture window.
BH21-03	83.51	5	Y	NR ⁴	Low	4 of 5 shots appear to show very slow flow outside capture window.
BH21-03	88.63	3	Y	NR ⁴	Low	3 of 3 shots appear to show very slow flow outside capture window.
BH21-03	90.47	4	Y	NR ⁴	Low	4 of 4 shots appear to show very slow flow outside capture window.
BH21-03	93.52	5	Y	NR ⁴	Low	5 of 5 shots appear to show very slow flow outside capture window.
BH21-03	98.52	6	Y	0.025	Low	4 of 6 shots appear to show slight upwards flow. Noisy data.
BH21-03	99.95	4	Y	0.022	Low	2 of 4 shots appear to show slight upwards flow. Noisy data.
BH21-03	103.58	4	Y	NR ⁴	Low	Noisy Data, 4 of 4 shots appear to show very slow flow outside capture window.
BH21-03	108.85	5	Y	0.016	Low	2 of 5 shots appear to show slight upwards flow. Noisy data.
BH21-03	113.47	6	Y	-0.023	Low	2 of 6 shots appear to show low flows, flows variable. 4 shots appear to show little to no flow.

Borehole_ID	Depth_of Shot_m	Num_of Shots ¹	Evidence_of Flow ²	Average_Flow_Rate Gal_per_minute hots ³	Confidence_In_Raw Data ⁵	Comments
BH21-03	119.1	2	N			Shots show little to no evidence of flow.
BH21-04	1.73	3	N			Shots show little to no evidence of flow. Noisy data.
BH21-04	5	3	Y	-0.015	Med	3 of 3 shots appear to show low flow, 2 shots with similar flows.
BH21-04	10.01	3	Y	-0.014	Med	Slight variation in flow between 3 shots.
BH21-04	15.01	3	Y	-0.014	High	Repeatable flow rates on all shots.
BH21-04	20.02	3	Y	-0.013	High	Repeatable flow rates on all shots.
BH21-04	25.01	3	Y	-0.012	High	Repeatable flow rates on all shots.
BH21-04	30.15	3	Y	-0.010	Low	2 of 3 shots appear to show low flow, 1 of 3 shots appear to show very low flow outside capture window.
BH21-04	35.02	3	Y	NR ⁴	Low	3 of 3 shots appear to show very slow flow outside capture window.
BH21-04	40.02	3	N			3 of 3 shots show little to no evidence of flow.
BH21-04	45.14	3	N			3 of 3 shots show little to no evidence of flow.
BH21-04	50.03	3	N			3 of 3 shots show little to no evidence of flow.
BH21-04	55.09	3	N			3 of 3 shots show little to no evidence of flow.
BH21-04	58.01	3	N			3 of 3 shots show little to no evidence of flow.
BH21-05	5.12	3	N			3 of 3 shots show little to no evidence of flow. Slightly noisy data.
BH21-05	11.02	3	N			3 of 3 shots show little to no evidence of flow. Slightly noisy data.
BH21-05	16.05	3	N			3 of 3 shots show little to no evidence of flow. Slightly noisy data.
BH21-05	21.01	3	N			3 of 3 shots show little to no evidence of flow. Slightly noisy data.
BH21-05	26.09	3	N			3 of 3 shots show little to no evidence of flow. Slightly noisy data.
BH21-05	31.01	3	N			3 of 3 shots show little to no evidence of flow. Slightly noisy data.
BH21-05	36.08	3	N			3 of 3 shots show little to no evidence of flow. Slightly noisy data.
BH21-05	41.27	3	N			3 of 3 shots show little to no evidence of flow. Slightly noisy data.
BH21-05	46.02	3	N			3 of 3 shots show little to no evidence of flow. Slightly noisy data.
BH21-05	51.07	3	N			3 of 3 shots show little to no evidence of flow. Slightly noisy data.
BH21-05	55.01	4	N			4 of 4 shots show little to no evidence of flow. Slightly noisy data.
BH21-09	22.5	3	N			3 of 3 shots show little to no evidence of flow.
BH21-09	27.5	5	N			5 of 5 shots show little to no evidence of flow.
BH21-09	32.52	3	N			3 of 3 shots show little to no evidence of flow.
BH21-09	37.57	3	N			3 of 3 shots show little to no evidence of flow.
BH21-09	42.54	3	N			3 of 3 shots show little to no evidence of flow.
BH21-09	47.82	3	N			3 of 3 shots show little to no evidence of flow.
BH21-09	52.54	3	N			3 of 3 shots show little to no evidence of flow.
BH21-09	54.17	3	N			3 of 3 shots show little to no evidence of flow.
BH21-10	1.73	1	N			1 of 1 shots show little to no evidence of flow. Slightly noisy data.
BH21-10	1.74	2	N			2 of 2 shots show little to no evidence of flow. Slightly noisy data.
BH21-10	6.8	3	Y	-0.048	Med	Slight variability in flow rates.
BH21-10	11.82	3	Y	-0.052	High	Repeatable flow rates on all shots.
BH21-10	16.87	3	Y	-0.051	High	Repeatable flow rates on all shots.
BH21-10	22.06	3	Y	-0.048	High	Repeatable flow rates on all shots.
BH21-10	27.52	3	Y	-0.038	High	Repeatable flow rates on all shots.
BH21-10	32.74	4	Y	-0.019	Med	3 of 4 shots appear to show low flow. 1 shot shows no evidence of flow.
BH21-10	37.52	3	Y	-0.015	Med	2 of 3 shots appear to show low flow. 1 shot shows no evidence of flow.
BH21-10	42.57	3	N			3 of 3 shots show little to no evidence of flow.
BH21-10	47.52	3	N			3 of 3 shots show little to no evidence of flow.
BH21-10	52.53	3	N			3 of 3 shots show little to no evidence of flow.
BH21-10	58.02	3	N			3 of 3 shots show little to no evidence of flow.
BH21-10	60	3	N			3 of 3 shots show little to no evidence of flow.
BH21-11	1.73	3	N			3 of 3 shots show little to no evidence of flow.
BH21-11	5.01	3	N			3 of 3 shots show little to no evidence of flow.
BH21-11	10.05	3	N			3 of 3 shots show little to no evidence of flow.
BH21-11	15	3	N			3 of 3 shots show little to no evidence of flow.
BH21-11	20	3	N			3 of 3 shots show little to no evidence of flow.
BH21-11	25.02	3	N			3 of 3 shots show little to no evidence of flow. Noisy data.
BH21-11	30	3	N			3 of 3 shots show little to no evidence of flow. Noisy data.

Borehole_ID	Depth_of Shot_m	Num_of Shots ¹	Evidence_of Flow ²	Average_Flow_Rate Gal_per_minute hots ³	Confidence_In_Raw Data ⁵	Comments
BH21-11	35.01	3	N			3 of 3 shots show little to no evidence of flow. Noisy data.
BH21-11	40.02	3	N			3 of 3 shots show little to no evidence of flow. Noisy data.
BH21-11	44.99	3	N			3 of 3 shots show little to no evidence of flow.
BH21-11	50.02	3	N			3 of 3 shots show little to no evidence of flow.
BH21-11	55.02	4	Y?	0.076	Low	1 of 4 shots show slight up flow. Noisy data.
BH21-11	58.06	3	N			3 of 3 shots show little to no evidence of flow.
BH21-12	2.5	3	N			3 of 3 shots show little to no evidence of flow. Noisy data.
BH21-12	7.58	3	Y	-0.047	High	Repeatable flow rates on all shots.
BH21-12	8.97	3	Y	-0.053	High	Repeatable flow rates on all shots.
BH21-12	12.58	3	Y	-0.027	Med	Slight variability in flow within 3 shots.
BH21-12	17.48	3	N			3 of 3 shots show little to no evidence of flow.
BH21-12	22.54	3	N			3 of 3 shots show little to no evidence of flow.
BH21-12	27.52	5	N			5 of 5 shots show little to no evidence of flow.
BH21-12	27.94	3	N			3 of 3 shots show little to no evidence of flow.
BH21-12	32.57	3	N			3 of 3 shots show little to no evidence of flow.
BH21-12	37.63	4	Y	0.012	Low	Appears to have variable upflow on 3 of the 4 shots. Noisy data.
BH21-12	39.94	3	N			3 of 3 shots show little to no evidence of flow. Noisy data.
BH21-12	40.24	3	N			3 of 3 shots show little to no evidence of flow. Noisy data.

Notes 1. # of Shots = The number of times pulse was fired at depth.

2. N = Little to no evidence of flow. This maybe due to: no flow, or flow which is outside the range in which the tool can detect, or noisy data

Y = Evidence of flow within the tools working range (Typically less than 1 gallon per minute, Ideal working range 0.03 to 1.0 gallons per minute, data outside working range may be noisy).

3. The average flow rate has been approximated (negative = downflow, positive = upflow) from the raw data based on tool calibration values (as provided by the manufacturer) at the depth of each shot. Flow rate Interpretation (from MatrixHeat™) is subject to user bias and may vary depending on the interpreter. As per the proposal, Stantec is responsible for the final interpretation of the borehole fluid flows.

4. NR = Possible appearance of flow but unable to determine flow rate. Refer to comments.

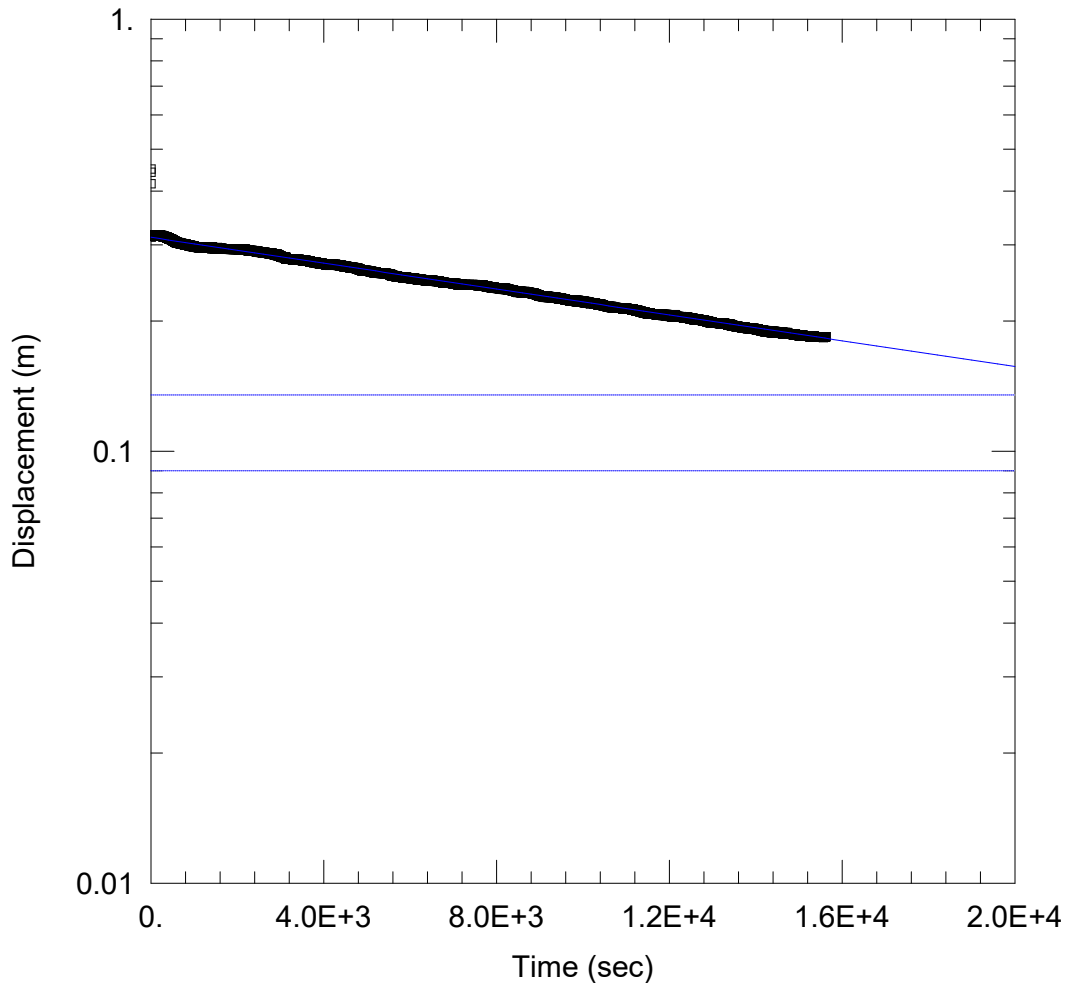
5. High = High confidence in raw data, repeatable data.

Med = Moderate confidence in raw data. Slight variation in raw data / consistent raw data with noise.

Low = Low confidence in raw data. Inconsistent noisy data. Not reliable results.

C.6 DOWNHOLE GEOPHYSICAL SURVEY REPORT





WELL TEST ANALYSIS

Data Set: C:\Users\jamine\Desktop\Projects\Atlantic Gold\00000\Slug Tests\In-Pit\HT-04.aqt
 Date: 03/10/22 Time: 10:55:19

PROJECT INFORMATION

Company: Stantec Consulting Ltd.
 Client: Atlantic Mining NS Inc.
 Project: 121619250
 Location: Touquoy In-Pit Disposal
 Test Well: HT-04
 Test Date: 27-01-2022

AQUIFER DATA

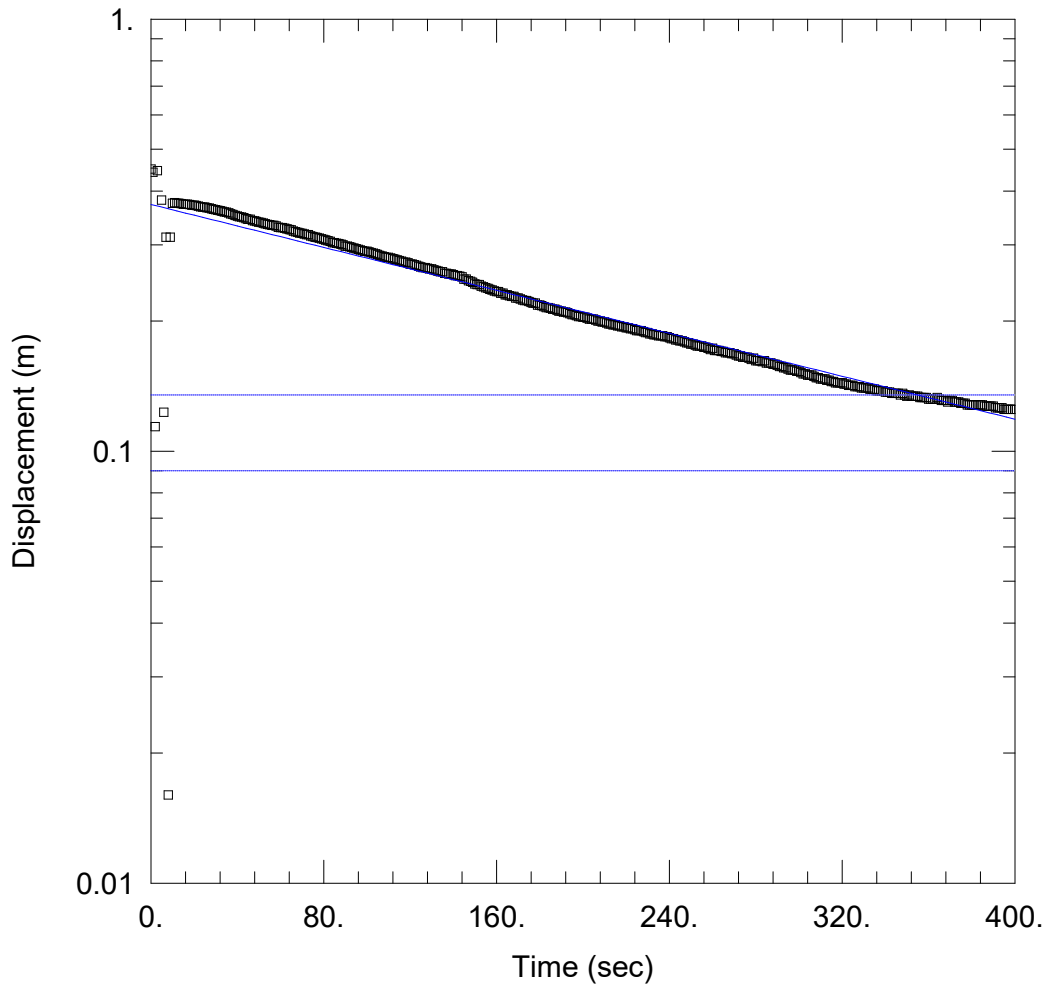
Saturated Thickness: 1.08 m Anisotropy Ratio (Kz/Kr): 0.1

WELL DATA (HT-04)

Initial Displacement: 0.45 m Static Water Column Height: 0.12 m
 Total Well Penetration Depth: 5.76 m Screen Length: 4.57 m
 Casing Radius: 0.025 m Well Radius: 0.075 m

SOLUTION

Aquifer Model: Unconfined Solution Method: Bower-Rice
 K = 2.8E-8 m/sec y0 = 0.3125 m



WELL TEST ANALYSIS

Data Set: C:\Users\jamine\Desktop\Projects\Atlantic Gold\00000\Slug Tests\In-Pit\HT-05.aqt
 Date: 03/10/22 Time: 10:52:58

PROJECT INFORMATION

Company: Stantec Consulting Ltd.
 Client: Atlantic Mining NS Inc.
 Project: 121619250
 Location: Touquoy In-Pit Disposal
 Test Well: HT-05
 Test Date: 27-01-2022

AQUIFER DATA

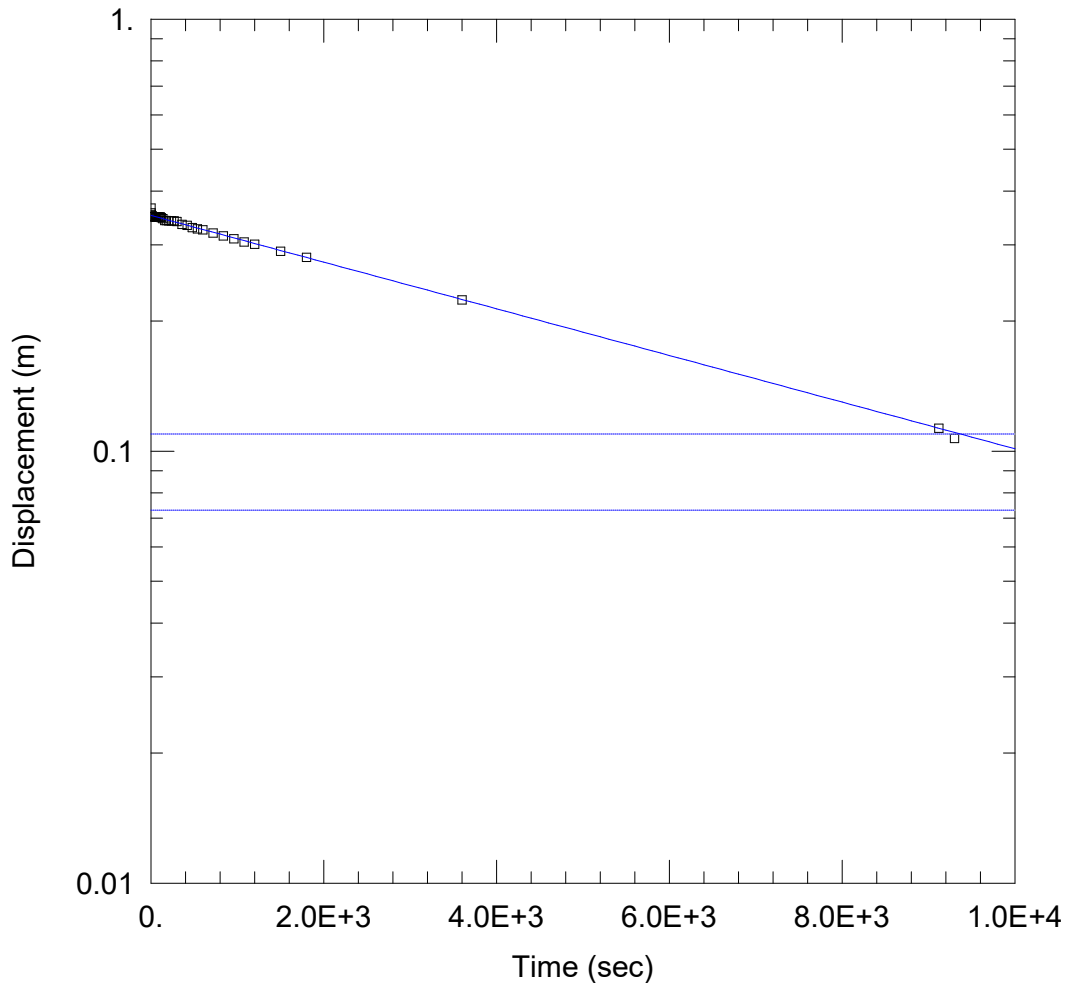
Saturated Thickness: 3.55 m Anisotropy Ratio (Kz/Kr): 0.1

WELL DATA (HT-5)

Initial Displacement: 0.45 m Static Water Column Height: 3.55 m
 Total Well Penetration Depth: 6.15 m Screen Length: 4.57 m
 Casing Radius: 0.025 m Well Radius: 0.075 m

SOLUTION

Aquifer Model: Unconfined Solution Method: Bower-Rice
 K = 8.3E-7 m/sec y0 = 0.3723 m



WELL TEST ANALYSIS

Data Set: C:\Users\jamine\Desktop\Projects\Atlantic Gold\00000\Slug Tests\In-Pit\HT-6_Test01.aqt
 Date: 03/10/22 Time: 10:51:58

PROJECT INFORMATION

Company: Stantec Consulting Ltd.
 Client: Atlantic Mining NS Inc.
 Project: 121619250
 Location: Touquoy In-Pit Disposal
 Test Well: HT-6
 Test Date: 26-01-2022

AQUIFER DATA

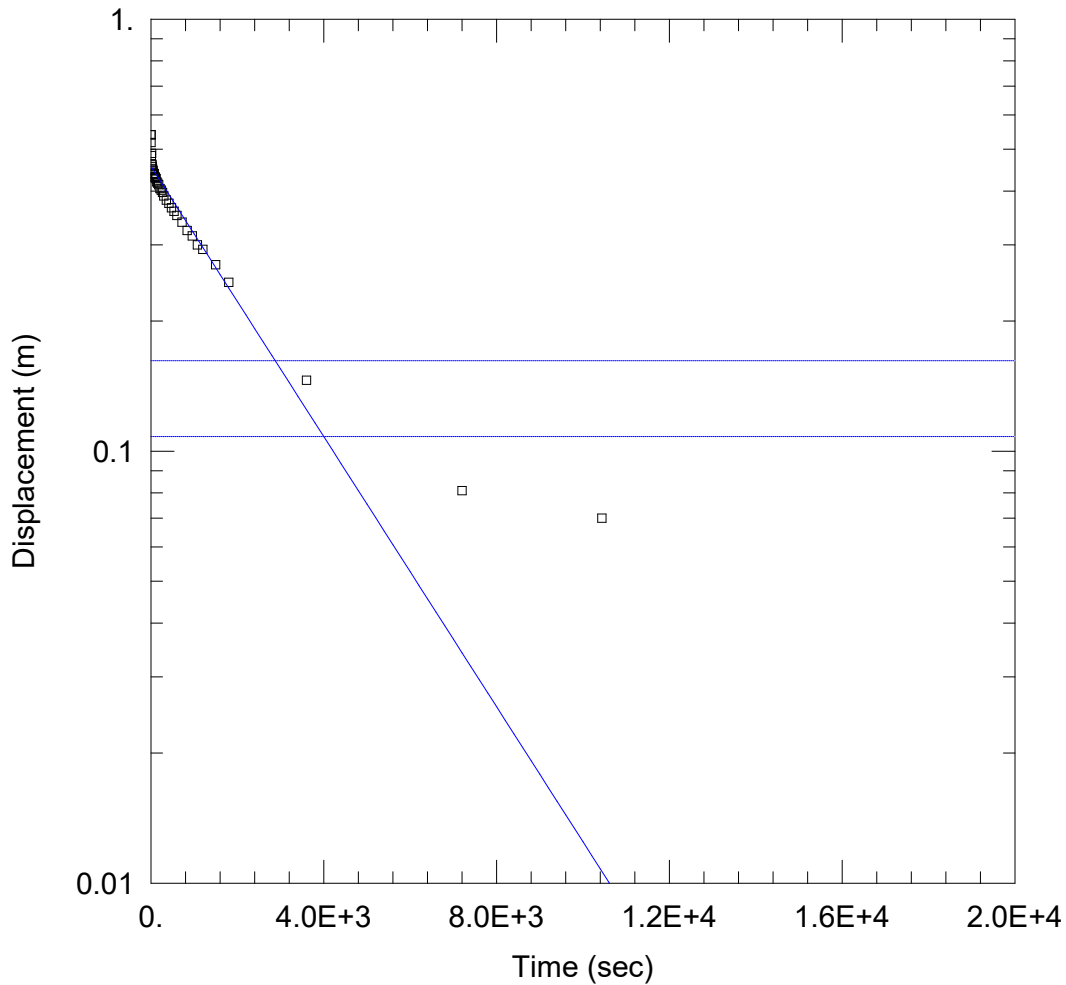
Saturated Thickness: 3.33 m Anisotropy Ratio (Kz/Kr): 0.1

WELL DATA (HT-6)

Initial Displacement: 0.365 m Static Water Column Height: 3.33 m
 Total Well Penetration Depth: 5.9 m Screen Length: 4.57 m
 Casing Radius: 0.025 m Well Radius: 0.075 m

SOLUTION

Aquifer Model: Unconfined Solution Method: Bower-Rice
 K = 3.8E-8 m/sec y0 = 0.3511 m



WELL TEST ANALYSIS

Data Set: C:\Users\jamine\Desktop\Projects\Atlantic Gold\00000\Slug Tests\In-Pit\HT-6_Test02.aqt
 Date: 03/10/22 Time: 10:56:59

PROJECT INFORMATION

Company: Stantec Consulting Ltd.
 Client: Atlantic Mining NS Inc.
 Project: 121619250
 Location: Touquoy In-Pit Disposal
 Test Well: HT-6
 Test Date: 26-01-2022

AQUIFER DATA

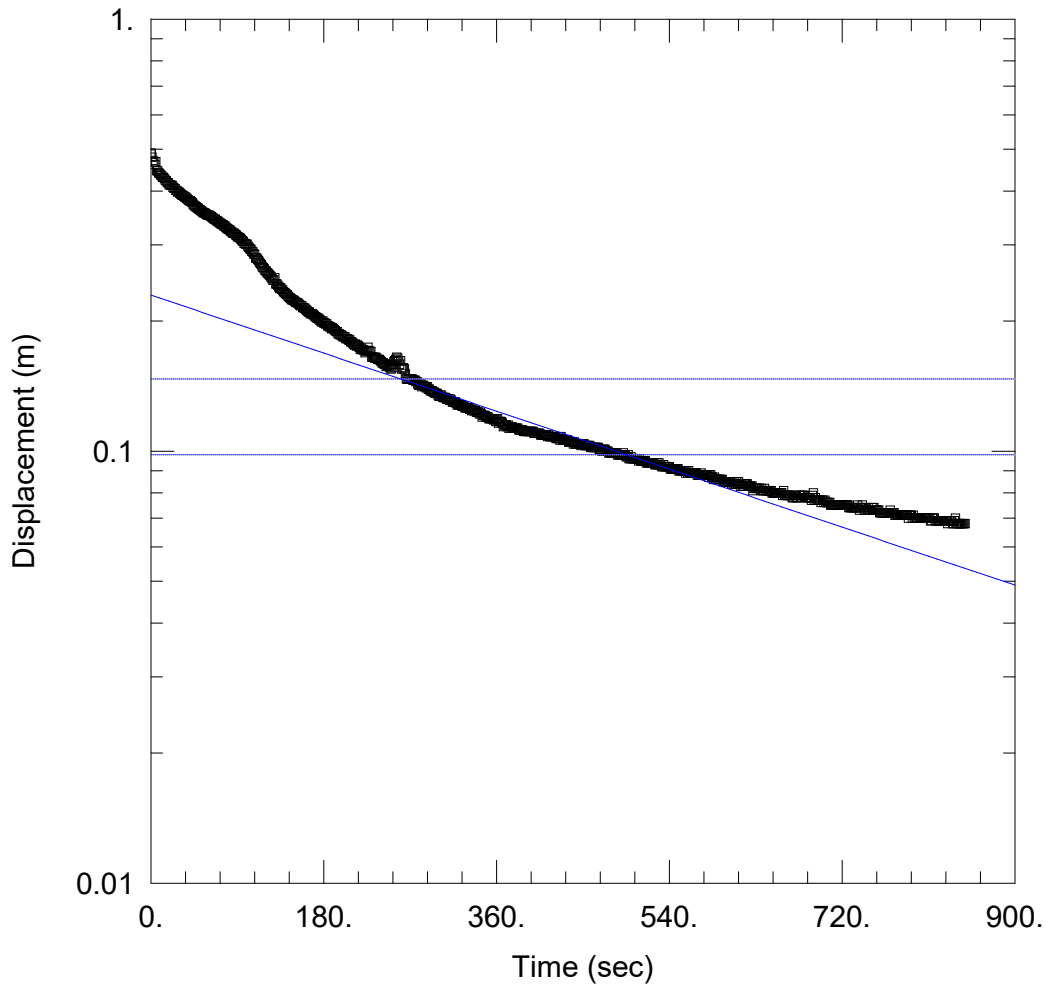
Saturated Thickness: 3.33 m Anisotropy Ratio (Kz/Kr): 0.1

WELL DATA (HT-6)

Initial Displacement: 0.54 m Static Water Column Height: 3.33 m
 Total Well Penetration Depth: 5.9 m Screen Length: 4.57 m
 Casing Radius: 0.025 m Well Radius: 0.075 m

SOLUTION

Aquifer Model: Unconfined Solution Method: Bower-Rice
 K = 1.1E-7 m/sec y0 = 0.4559 m



WELL TEST ANALYSIS

Data Set: C:\Users\jamine\Desktop\Projects\Atlantic Gold\00000\Slug Tests\In-Pit\HT-07.aqt
 Date: 03/10/22 Time: 10:45:28

PROJECT INFORMATION

Company: Stantec Consulting Ltd.
 Client: Atlantic Mining NS Inc.
 Project: 121619250
 Location: Touquoy In-Pit Disposal
 Test Well: HT-7
 Test Date: 26-01-2022

AQUIFER DATA

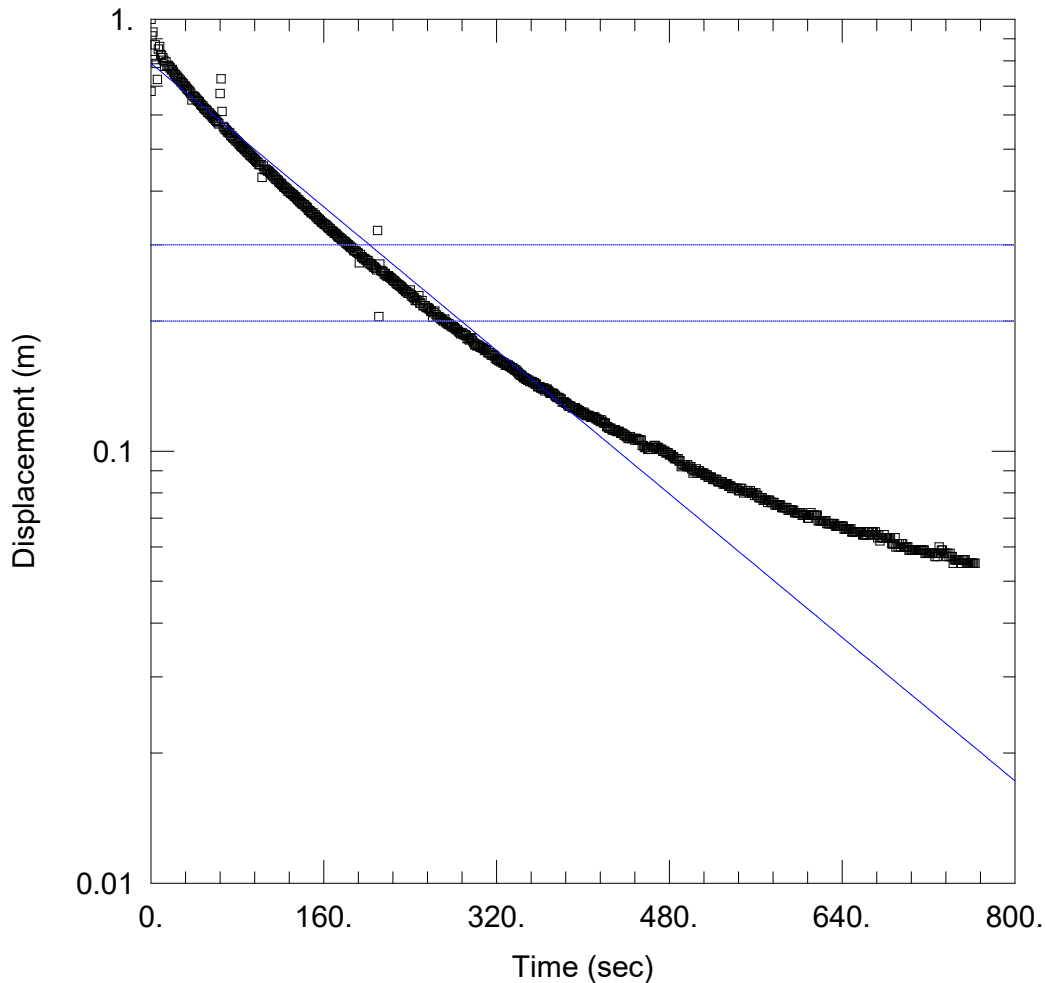
Saturated Thickness: 4. m Anisotropy Ratio (Kz/Kr): 0.1

WELL DATA (HT-07)

Initial Displacement: 0.49 m Static Water Column Height: 4.035 m
 Total Well Penetration Depth: 5.77 m Screen Length: 4.57 m
 Casing Radius: 0.025 m Well Radius: 0.075 m

SOLUTION

Aquifer Model: Unconfined Solution Method: Bower-Rice
 K = 4.4E-7 m/sec $y_0 =$ 0.2296 m



WELL TEST ANALYSIS

Data Set: C:\Users\jamine\Desktop\Projects\Atlantic Gold\00000\Slug Tests\In-Pit\HT-08.aqt
 Date: 03/10/22 Time: 10:58:26

PROJECT INFORMATION

Company: Stantec Consulting Ltd.
 Client: Atlantic Mining NS Inc.
 Project: 121619250
 Location: Touquoy In-Pit Disposal
 Test Well: HT-08
 Test Date: 27-01-2022

AQUIFER DATA

Saturated Thickness: 8.4 m Anisotropy Ratio (Kz/Kr): 0.1

WELL DATA (HT-08)

Initial Displacement: 1. m Static Water Column Height: 8.4 m
 Total Well Penetration Depth: 8.94 m Screen Length: 7.62 m
 Casing Radius: 0.025 m Well Radius: 0.075 m

SOLUTION

Aquifer Model: Unconfined Solution Method: Bower-Rice
 K = 9.2E-7 m/sec y0 = 0.7898 m

C.7 GPR SURVEY REPORT





TOUQUOY OPEN-PIT MINE: DETECTION OF UNDERGROUND MINE WORKINGS USING GROUND-PENETRATING RADAR

Stantec Consulting Ltd.

St. John's, NL

January 2022

D-ANALYTICS



Document Title: Touquoy Open-Pit Mine: Detection of Underground Mine Workings Using Ground-Penetrating Radar

Client: Stantec Consulting Ltd.
St. John's, NL

Project Identifier: STC-2022-01



Project Field Crew: Sean McOuat (Stantec) and Adam Gogacz (d-Analytics)

Client Representative: Paul Deering

Project Manager: Adam Gogacz

Report written by: Adam Gogacz

Proofread by: Heather O'Brien

d-Analytics Services Inc.

19 Falkland Street
St. John's, NL
A1B 1V8
Canada

Tel: +1 709 763 4014
Email: agogacz@d-analytics.com

www.d-analytics.com

CONTENTS

1	Introduction.....	5
2	Data Collection	7
2.1	Recording and System Parameters	7
2.2	Survey Geometry.....	7
2.3	Surface Conditions	8
2.4	Equipment	10
2.4.1	Ground-Penetrating Radar	10
2.4.2	Global Navigation Satellite System.....	10
3	Data Processing	11
3.1	Geometry: Metadata Compilation and Assignment.....	11
3.2	First-break Flattening and Offset Correction	12
3.3	Dewow Filter.....	12
3.4	Bandpass	12
3.5	Local Background Removal (Multi-trace Running Average Removal).....	12
3.6	Normalization (Exponential Time-Gain)	12
3.7	Automatic Gain Control.....	13
3.8	Velocity Analysis (Migration).....	13
3.9	Migration.....	13
3.10	Envelope Extraction.....	13
3.11	Time to Depth Transformation	13
3.12	Final Datum Shift	13
4	Interpretation	14
4.1	Identified Features.....	14
4.1.1	Fault I.....	16
4.1.2	Fault II.....	20
4.1.3	Fault III.....	23
4.1.4	Zone of Interest I	25
4.1.5	Zone of Interest II.....	27
4.1.6	Zone of Interest III.....	29
4.1.7	Zone of Interest IV.....	31
4.1.8	Zone of Interest V.....	34
4.1.9	Zone of Interest VI.....	36
4.1.10	Zone of Interest VII	38
4.1.11	Zone of Interest VIII	40

4.1.12	Zone of Interest IX.....	43
4.1.13	Zone of Interest X.....	46
4.1.14	Region of Interest I.....	48
5	Summary	51

1 INTRODUCTION

Further to the request of *Stantec Consulting Ltd.* and correspondence with Mr. Paul Deering P.Eng., P.Geo., *d-Analytics* has conducted a ground-penetrating radar (GPR) survey at the Touquoy Open-Pit mine, NS, to support identification and delineation of historical underground mine workings in the upper 50 to 60 metres.

While prior work, archival and open-pit mining, revealed locations of historical mine workings within the pit area (see Figure 1), uncertainty about the extension of these workings beyond the pit's rim persisted. This project focused on a patch in the southwestern region immediately outside of the pit (see Figure 2).

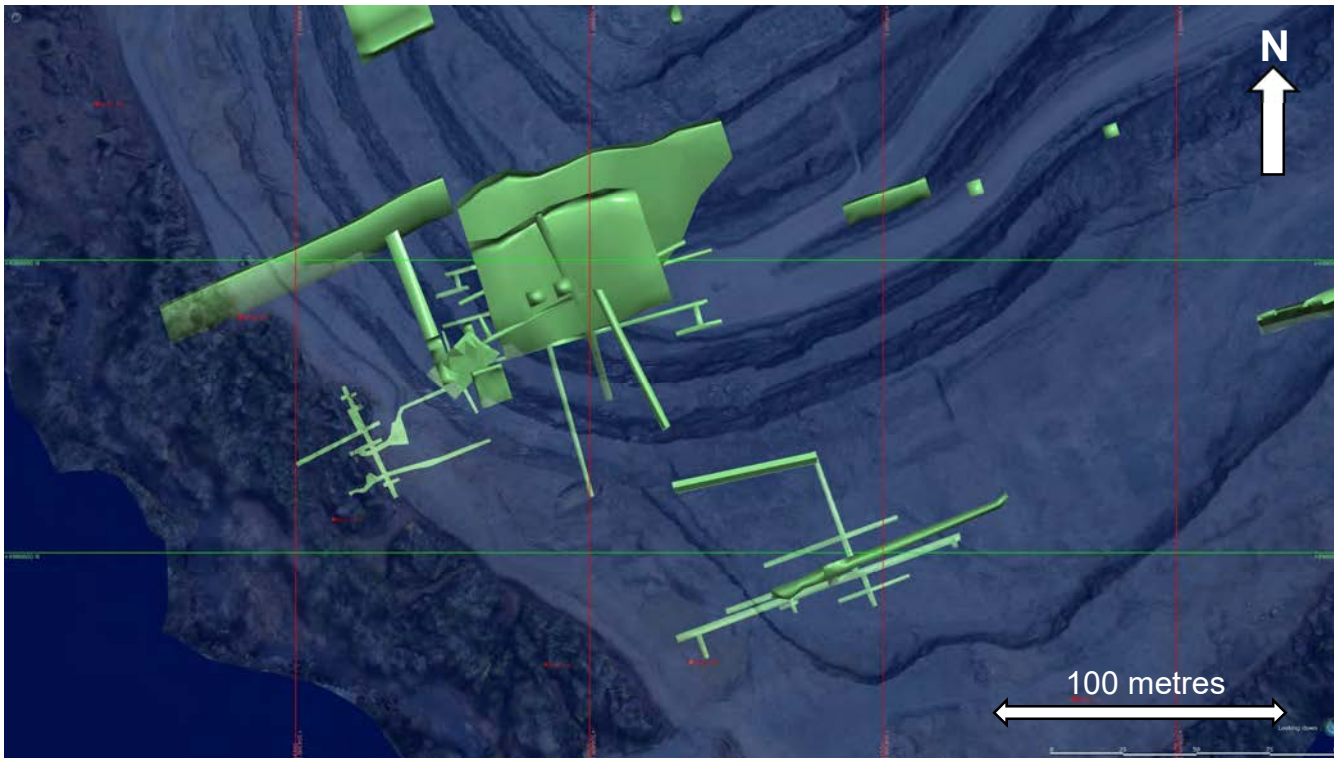


Figure 1. Model of underground mine workings (courtesy of Stantec).

The physically and archivally identified underground workings (personal communications) comprised tubular or sheet-like, subhorizontal or subvertical openings, presently collapsed and/or filled with underground water. The GPR technology was selected for the project as it best met all the constraints and objectives. In particular, a rough-terrain antenna (RTA) GPR system was selected for its optimal deployment suitability in physically constrained environments (e.g. forests or dense brush).

The data were processed with *d-Analytics'* proprietary software (*d-PULSE*), and interpretation of the processed data was carried out on *dGB Earth Sciences* software *OpendTect*. The complexity of the varying surface conditions and the nature of the targets required a compilation of a custom-tailored processing workflow. The workflow was established through an iterative scheme both in the parametrization and selection of each constituting processing block/function. The interpretation of the processed data was primarily guided by the expectation of continuity of inferred zone of interest across proximal and subparallel lines.

The remainder of this report details data collection, data processing, and interpretation of the processed data, all with the singular aim to identify zones where underground mine workings may be inferred from the data.



Figure 2. Tracks of the GPR lines (red lines to the southwest) within the greater Touquoy open-pit mine; labelled lines are shown in Figure 3.

2 DATA COLLECTION

The fieldwork commenced on January 18th, 2022 and concluded on January 26th, 2022, with mobilization and demobilization days, respectively, before and after. The pertinent aspects of data collection are detailed in the following sections.

2.1 Recording and System Parameters

	MALÅ RTA 25 MHz	MALÅ RTA 100 MHz
Central frequency:	25 MHz	100 MHz
Sampling frequency:	719.368530 MHz	1000.097778 MHz
Samples per trace:	872 samples	624 samples
Station interval:	~ 0.5 metres	~ 0.5 metres
GNSS to Rx-Tx midpoint:	8.585 metres (ahead)	4.94 metres (ahead)
Rx-Tx offset:	6.2 metres	2.2 metres

2.2 Survey Geometry

The survey was designed to comprise a series of parallel lines running perpendicular to the expected orientation of the underground mine workings and with line separation adequate to intersect any feature of interest with three or more lines. The actual line geometry (see postplots Figure 3) was largely established as an optimum between an ideal grid and environmental constraints, all the while still meeting the imaging objectives.

Each line was extended as far south and north as the surface conditions allowed; roads and other clearings were used as much as possible. In the end, the survey was concluded with 15 lines; some lines were made up of two segments; each segment or line made up a separate data collection effort/task.

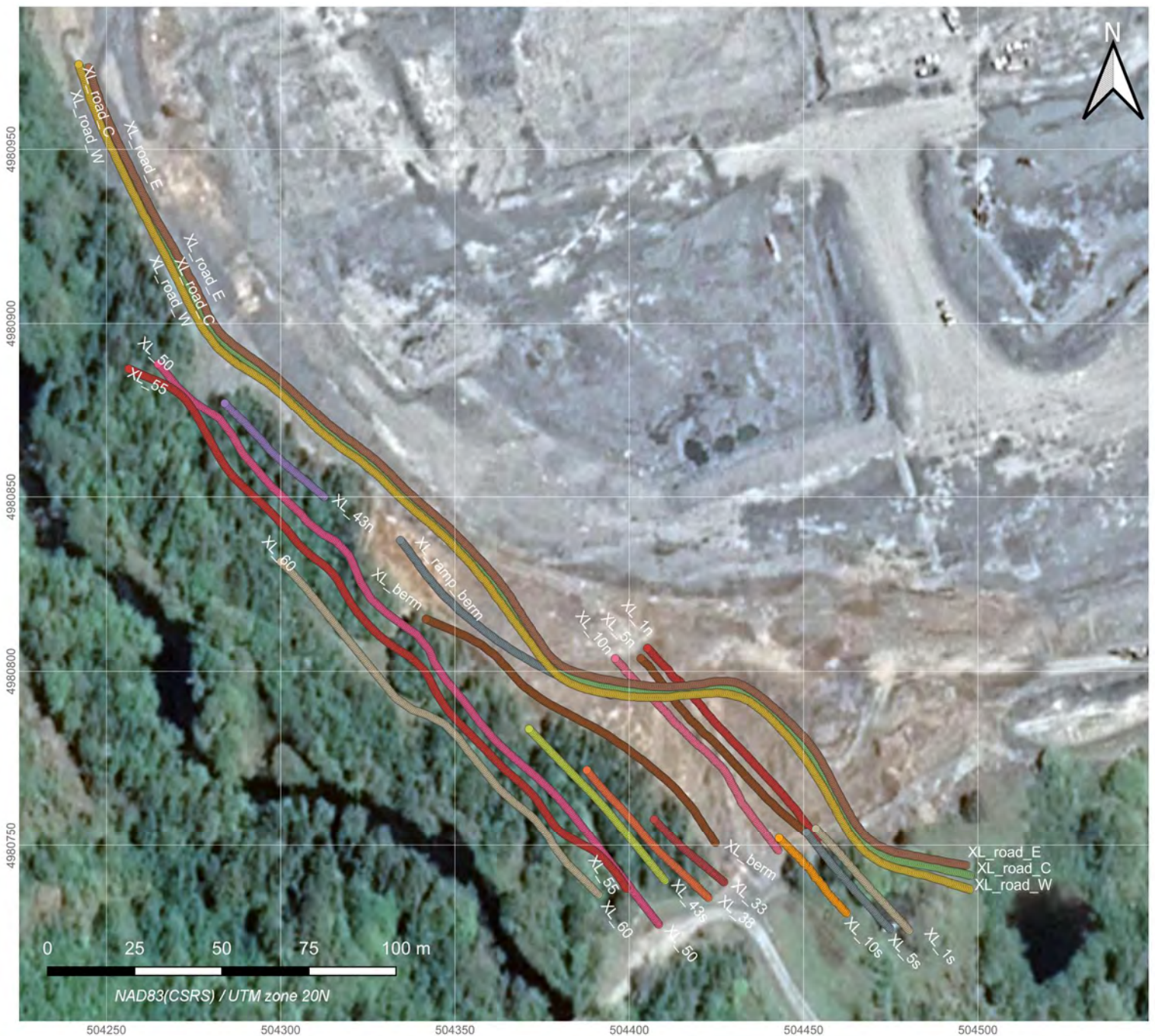


Figure 3. Postplots (actual) of data collection lines.

2.3 Surface Conditions

The surface conditions within the survey boundary varied from gravel roads to a gravel-soil berm to dense vegetation. Accessibility and ease of data collection along the berm or the roads (see Figure 4) were offset by dense vegetation and numerous rapid elevation changes to the west of the berm and the roads.

While environmental restrictions prohibited cutting down live trees, recent and older treefalls were cleared from paths to make up lines as close as possible to the initial design. The vegetation and its associated root network contributed to the attenuation of the transmitted signals. However, the vegetation is relatively small; hence the scattering from roots for low-frequency systems was minimized.

The gravel roads were constructed for light-truck traffic and were well packed from use. The thin veneer of road-gravel overlaid competent rock. The berm was made up of sand and rock fragments. The entire near-surface was frozen with little to no snow cover. At the time and prior to data collection, the temperatures during the day ranged between -15°C and -5°C.



Figure 4. Data collection in progress along a gravel road (courtesy of Sean McQuat, Stantec).



Figure 5. Example of a rapid elevation change along a line.



Figure 6. Example of typical conditions along lines to the west of the road.

2.4 Equipment

Apart from all ancillary instrumentations, tools, and other equipment, the two main data collection systems were the GPR and global navigation satellite system (GNSS). The GPR provides a “look” into the subsurface, and the GNSS tells where on the surface the data were collected.

2.4.1 Ground-Penetrating Radar

The GPR survey was carried out using two rough-terrain ground-penetrating radar antennas (RTA) shown in Figure 7; the datasets were collected sequentially. The first leg of the survey was carried out with MALÅ’s RTA 25 MHz system, and the second leg was completed with the 100 MHz RTA.

	MALÅ RTA 25 MHz	MALÅ RTA 100 MHz
Central frequency:	25 MHz	100 MHz
Antenna Length:	13 metres	6.5 metres
Tx-Rx offset:	6.2 metres	2.2 metres
Application:	deep < 50 metres	shallow < 15 metres

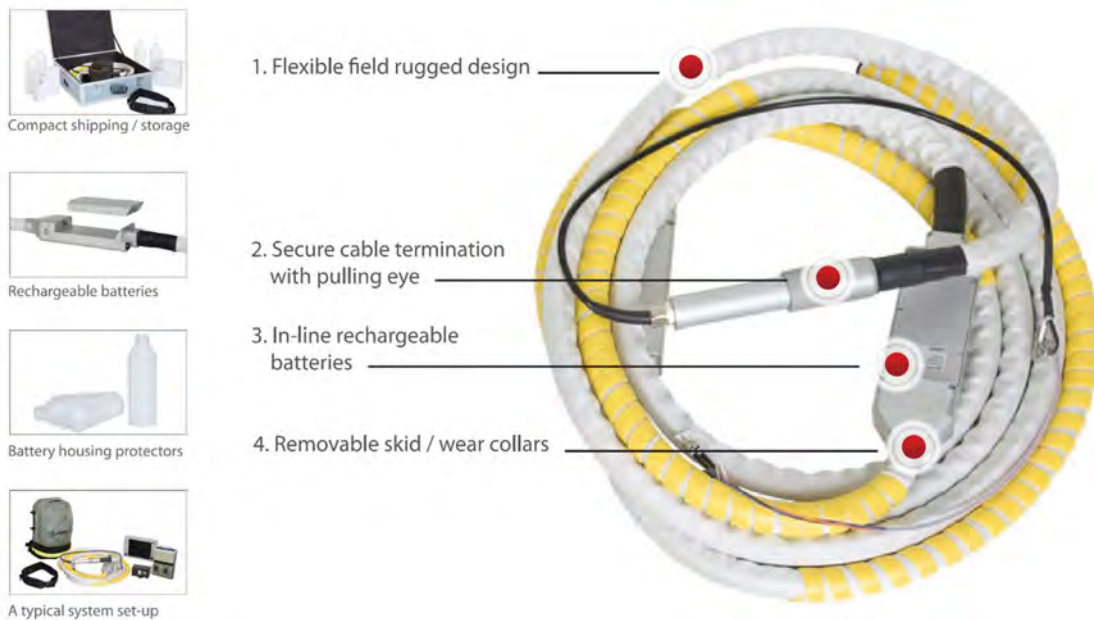


Figure 7. Components of MALÅ’s RTA.

2.4.2 Global Navigation Satellite System

The positions at each data collection station (a point where single sensor readings were collected) were acquired using Trimble’s TSC3 controller (see Figure 8) and two Spectra Geospatial’s SP80 receivers (see Figure 9) set up in a base-rover RTK configuration. The positional data was acquired with sub-5 cm accuracy. All positional data were reported in UTM [Zone 20N] / NAD83 coordinate reference system.



Figure 8. GNSS controller.



Figure 9. GNSS receiver.

3 DATA PROCESSING

The final purpose-designed processing workflow was constructed from industry-standard data processing techniques and practices using *d-PULSE*. The processing focused entirely on the accentuation and “extraction” of data features compatible with local reflections and scattering caused by underground mine workings. The final processing workflow is shown in Figure 10.

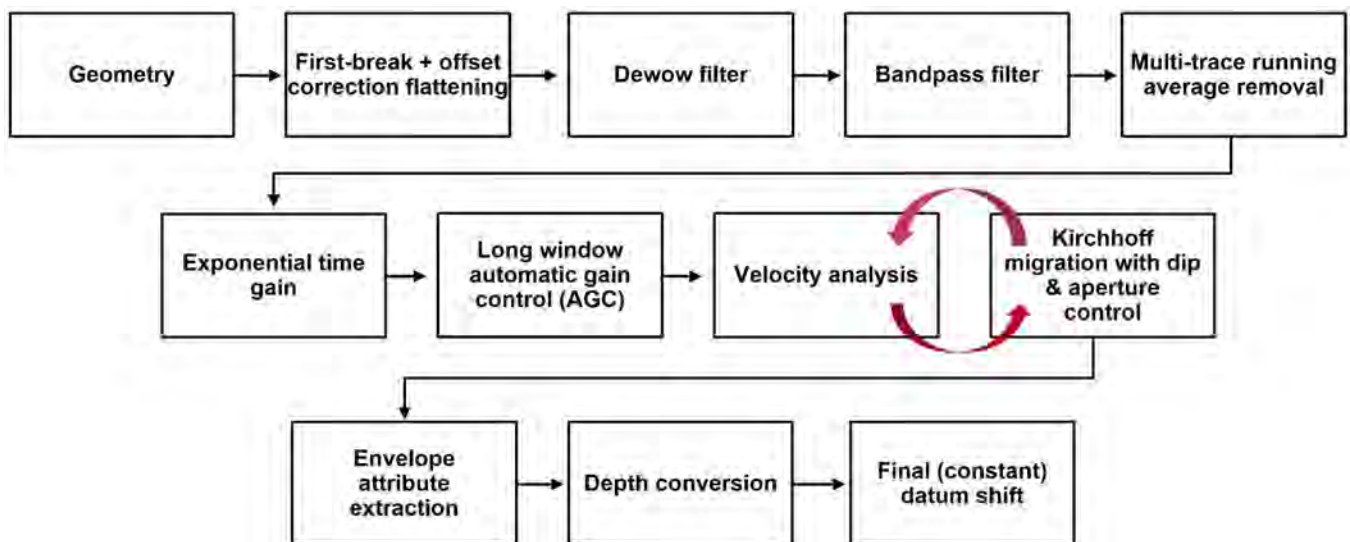


Figure 10. Processing workflow.

3.1 Geometry: Metadata Compilation and Assignment

The GNSS and the GPR data were harvested independently, concurrently, and position or time-synchronized. Weak satellite signals under the canopies of the trees did not allow for the RTK system to acquire fixed positions. As a result, in the open areas (e.g. road) and for each survey line, the GNSS and

GPR controllers were started simultaneously. The GNSS and the GPR controllers were set to collect a sample point once per second (i.e. 1 Hz sampling). After some interpolations and shifts accounting for the offset between the GNSS rover and the source (Tx) and receiver (Rx) positions, the GPR and the calculated positional (source and receiver x,y,z) datasets were merged.

In the canopied part of the survey, the GPR data were acquired using a “hip-wheel”¹ distance-based trigger. Following the GPR data collection, the GNSS rover was traced along the GPR data collection lines where control points along each line were collected; some locations required many seconds to get an RTK fix. As in the continuous-time GNSS dataset, this control point-based data was interpolated onto a path with a prescribed station-to-station interval (i.e. 0.5 metres) and shifted to account for the operator to GPR offset. The resulting positional dataset was then merged with the GPR dataset.

3.2 First-break Flattening and Offset Correction

Typically, the GPR recording data stream is set off before the transmission. Consequently, the recorded data contain spurious energy before the onset of the direct wave, which travels through the air. This extra data must be removed before running any time-depth or time-velocity processes. The removal and offset correction consisted of identifying first-breaks (arrival of the high-amplitude direct wave) and a cumulative removal of all samples before the onset, followed by the addition of samples, which account for travel time between the source and the receiver at the speed of propagation of electromagnetic waves through the air (~300 m/μs).

3.3 Dewow Filter

A multitude of complex phenomena may induce a low-frequency background “wow” signal, which (additively) biases the recorded traces; the recorded traces show a drift of the high-frequency reflections away from the expected local zero-mean trend. The dewow filter is implemented as a gated moving average subtraction filter. The filter length was set to 1.5 wavelengths and individually applied to each trace.

3.4 Bandpass

Further noise suppression was achieved through bandpass filtering. The applied bandpass filter was implemented in the frequency domain and was constructed from Butterworth windows with the following corner frequencies:

- 5 MHz – 10 MHz – 60 MHz – 85 MHz for the 25 MHz dataset
- 5 MHz – 10 MHz – 250 MHz – 300 MHz for the 100 MHz dataset

3.5 Local Background Removal (Multi-trace Running Average Removal)

The GPR antenna typically produces a ringing artifact resulting in horizontal banding frequently dominating the underlying signal of relevance. The ringing may be due to, for example, impedance contrast between the antenna and the ground or residual currents within the unit. On short lines, the banding is suppressed by subtraction of the average trace from the data. On longer lines, subtraction of the average trace (within a sliding window) from individual traces is preferable.

3.6 Normalization (Exponential Time-Gain)

Amplitude decay due to geometric spreading (frequency invariant) and absorptive phenomena (frequency-dependent) attenuate the relative reflective/scattering strength of surfaces at depth. The

¹ The hip-wheel unit is a calibrated distance measuring device attached to a fixed point on the ground and the instrumentation. Distance measurement is obtained from a thread spun around a wheel, where the wheel is turned as the unit is moving ahead.

exponential time-gain operator preferentially scales upward arrivals at later times according to the user-specified exponent constant.

3.7 Automatic Gain Control

In addition to the deterministic exponential time-gain scaling, the traces were individually scaled with (thresholded, RMS) automatic gain control (AGC) operator 300-nanosecond and 200-nanosecond long for the 25 MHz and 100 MHz datasets, respectively.

3.8 Velocity Analysis (Migration)

Typically, velocity analysis is carried out on multi-offset data. However, where diffracting subsurface features are present, migration velocity analysis may be carried on constant-offset data via focusing on the point or edge-like diffractions. For this project, numerous lines were constant-velocity migrated between 60 m/ μ s through 130 m/ μ s at 10 m/ μ s intervals. Focusing analysis showed that optimal focusing was obtained at 90 m/ μ s.

3.9 Migration

Migration of the data is a process whereby the horizontal reflectors are moved to their correct positions and whereby diffraction hyperbolas are collapsed to a single locus; the migrated data is nearly always preferable for interpretation than unmigrated data. The data were migrated with the Kirchhoff migration method. The Kirchhoff migration implementation in d-PULSE allows for the control of the maximum expected geological dip. The data were migrated with a maximum dip of 15°, a maximum aperture of 30°, a constant velocity of 90 m/ μ s, and common-offset weighting.

3.10 Envelope Extraction

Accentuation of space-limited features, such as subwavelength tubular channels, is further accentuated by the transformation of the reflection/scattering amplitudes to an “energy” attribute. The transformation was done via Hilbert transforms methods.

3.11 Time to Depth Transformation

The conversion of the data from the time-domain to the depth-domain was done using the final (constant velocity) migration value of 90 m/ μ s.

3.12 Final Datum Shift

While the migration processes accounted for the variable topography, the data were migrated to a floating datum (smoother version of the elevation curve/surface). The final datum shift “moves” the processed and migrated traces to a constant elevation level such that the onset of each trace follows the topography.

4 INTERPRETATION

The data interpretation primarily focused on identifying high-energy localized regions with lateral extent (line to line correlation). Fault and fractures, “visible” to the GPR at the associated wavelength, were targets of secondary interest; these geological features may be used for collocation and verification with field observations.

The GPR data were acquired with as much lateral redundancy as was possible and solely constrained by accessibility. The lateral line to line redundancy was exploited to minimize false-positive interpretations.

4.1 Identified Features

The identified features of interest were binned into three categories, namely,

- faults; zones with a substantial sub-vertical scattering
- zones of interest (Zoi); interpreted as probable underground mine workings
- region of interest (Rol); interpreted as complex networks of likely underground workings

The following subsections show the processed profiles and the individual identified features.

Figure Notes:

- each feature is presented in a separate subsection; the first figure shows the location (white outlined oval) of the feature on the map, while the remaining figures show the feature’s expression in the processed data;
- all low frequency processed data is scaled at $\frac{35}{8} : \frac{27}{2}$ (vertical to horizontal) and the high-frequency data is scaled at $\frac{45}{16} : \frac{27}{2}$ (vertical to horizontal);
- a schematic of the figure annotations is shown in Figure 11;
- the “*Confidence*” metric indicates the measure of interpretation of an event and its contrast against the background.

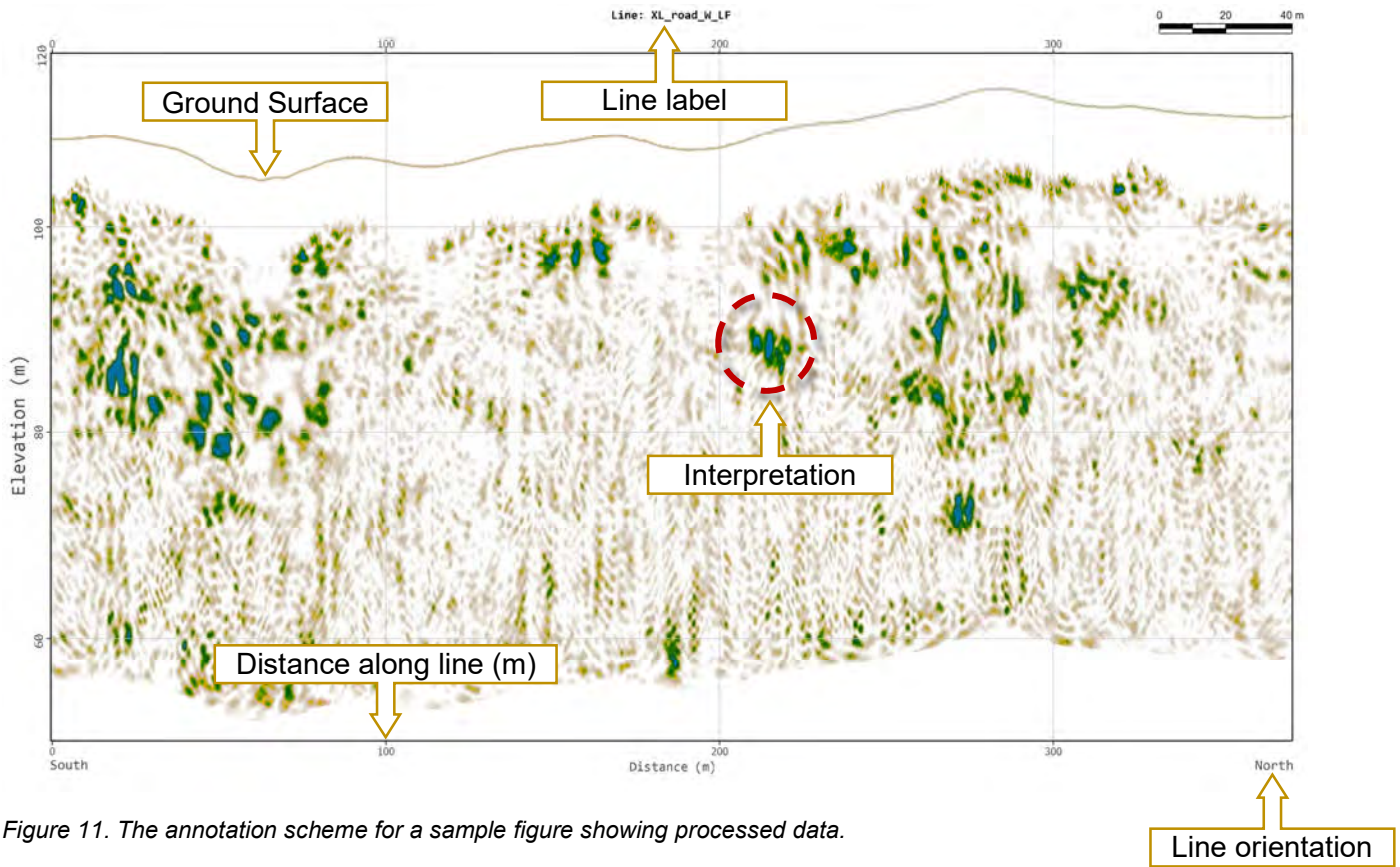


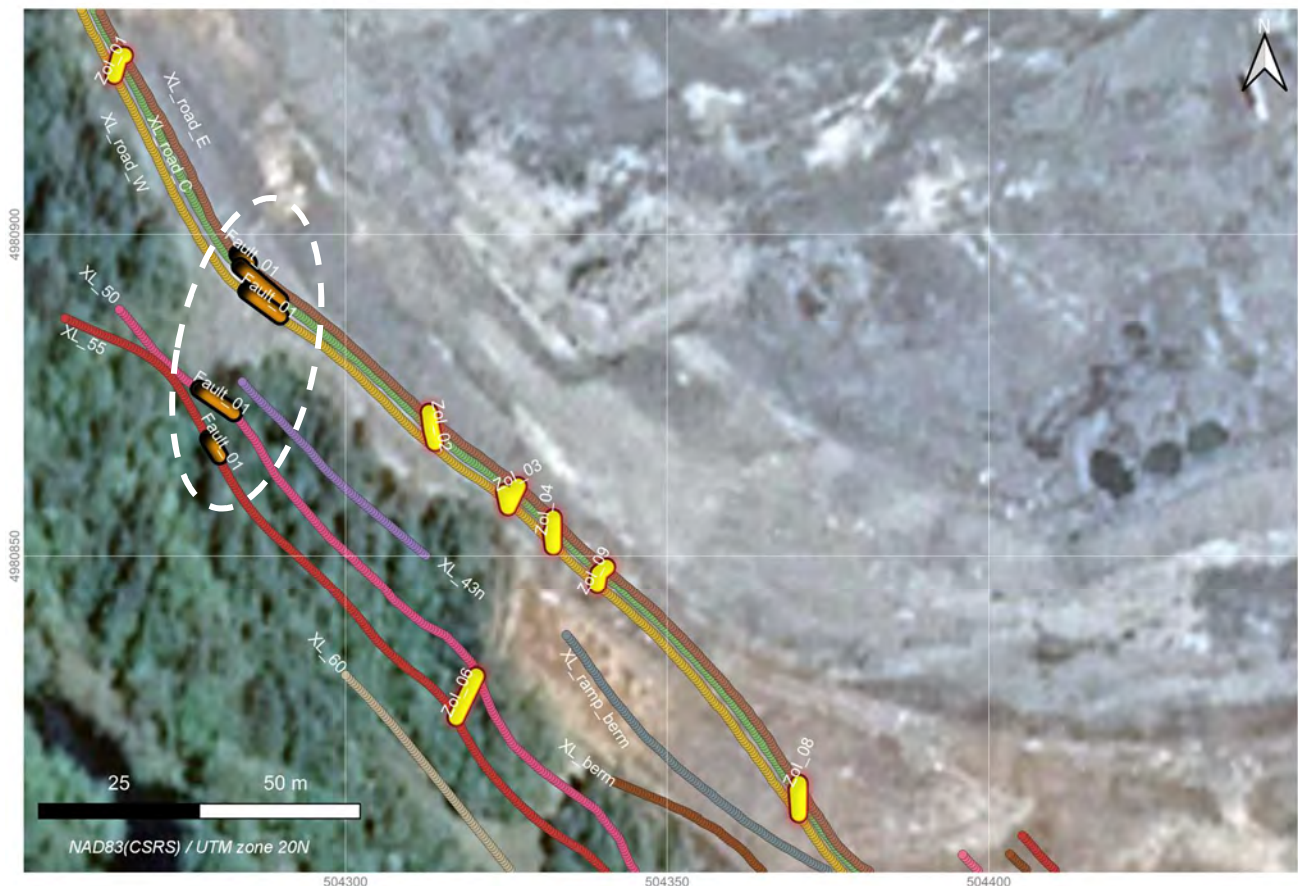
Figure 11. The annotation scheme for a sample figure showing processed data.

4.1.1 Fault I

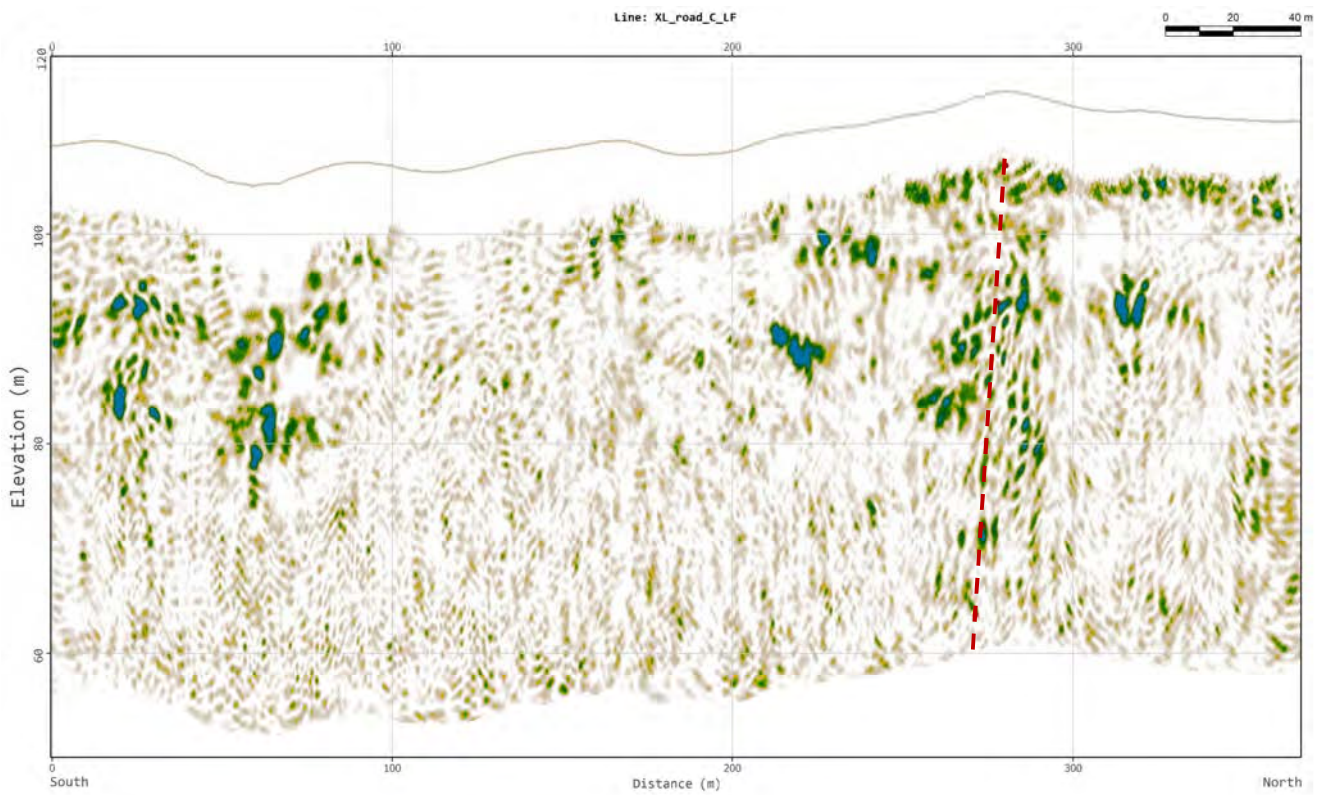
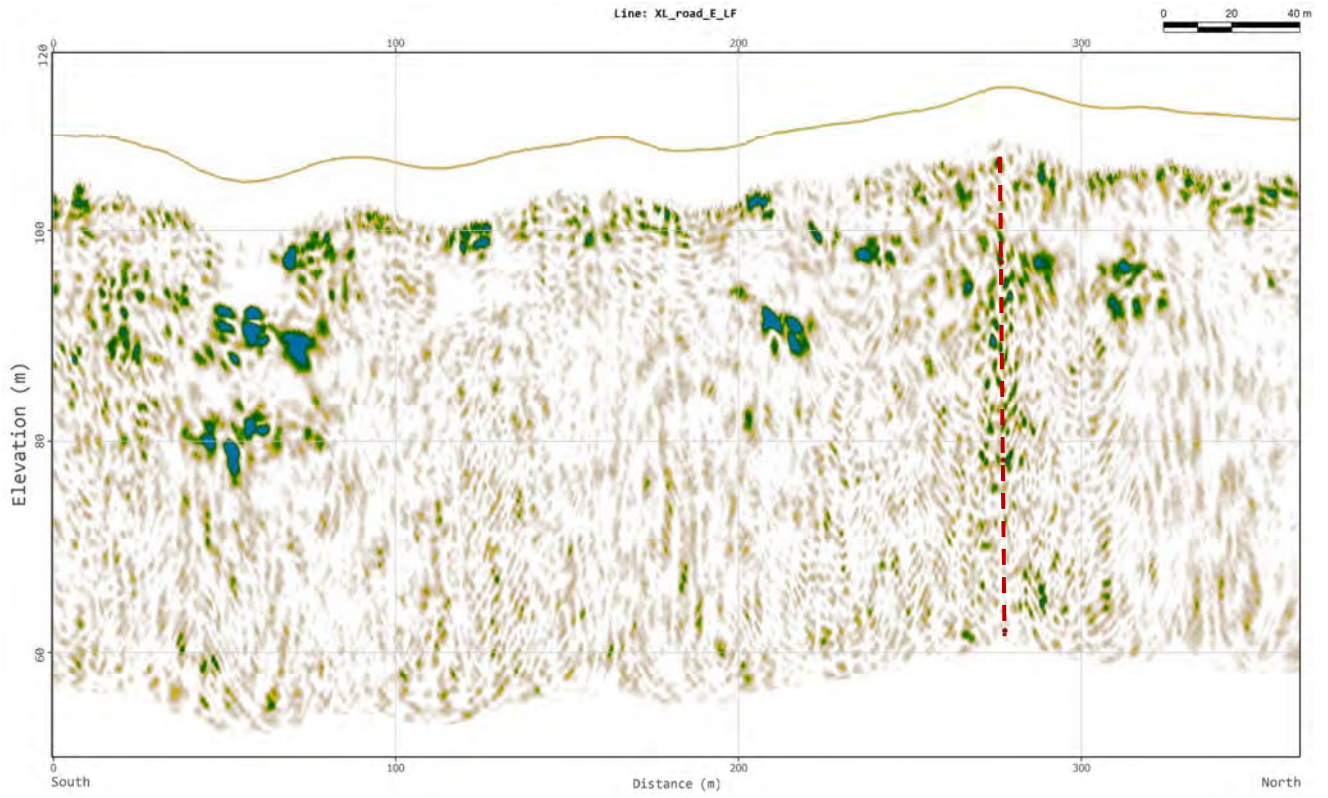
Confidence:	High
Characterization:	Sub-vertical feature with substantial scattering down the shown (red) curve.

COORDINATES OF THE FEATURE (NAD 83, UTM 20N)

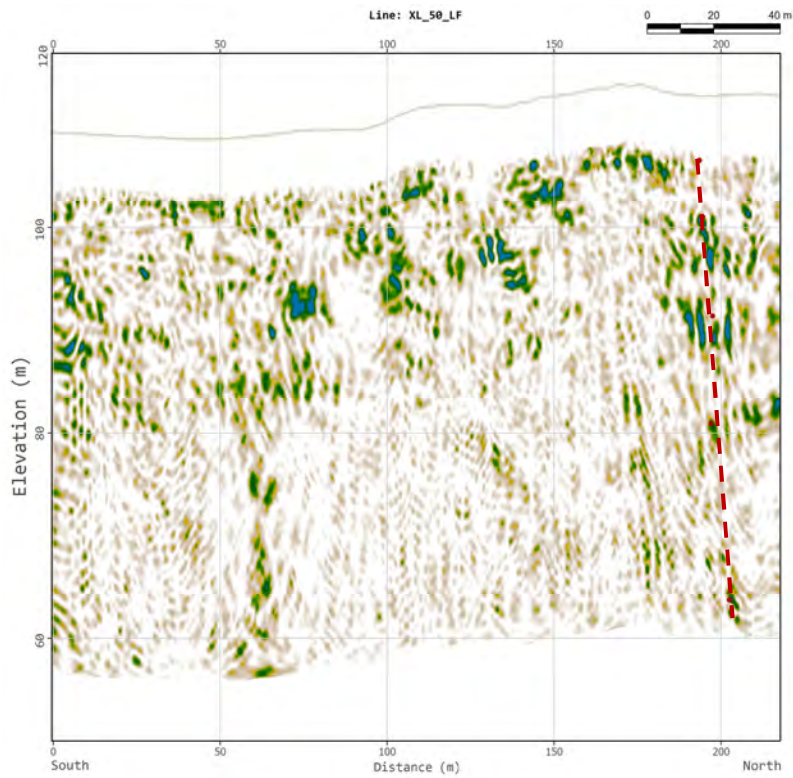
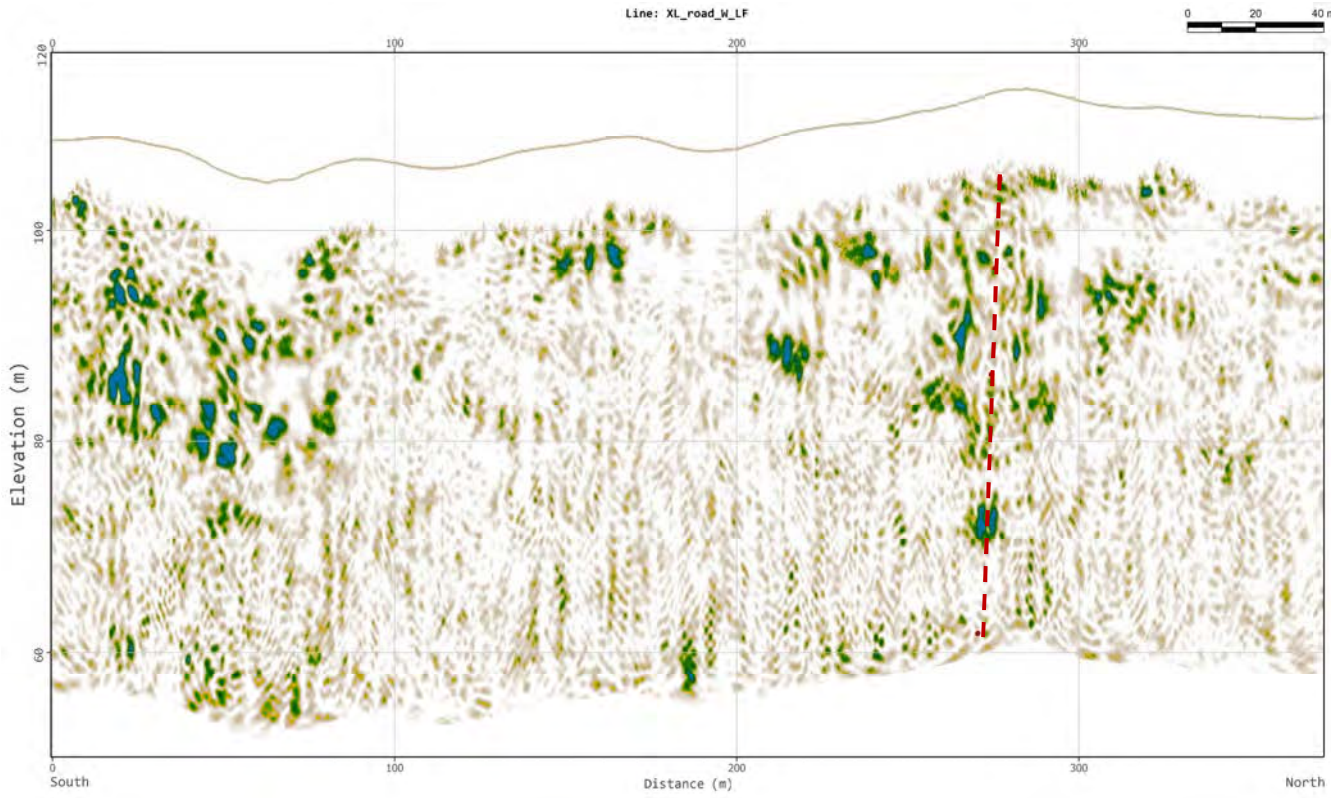
EASTING (m)	NORTHING (m)	ELEVATION (m)
504284.4	4980896	106.7
504284	4980896.3	97
504283.6	4980896.6	78.2
504283.2	4980896.9	62
504289	4980890.5	63.6
504287.7	4980891.6	72
504284.2	4980894.5	93.4
504282.2	4980896.3	106.5
504289.8	4980887.3	61.7
504286.6	4980889.7	86.3
504286.1	4980890.1	96.3
504284.6	4980891.2	104.9
504275.1	4980877.4	63.6
504279.5	4980874.4	80.9
504279.4	4980874.5	91.4
504281.8	4980872.8	101
504282.4	4980872.5	106.5
504280.1	4980866	62.5
504277.7	4980869.8	78.5
504279.5	4980867	98.2
504279.9	4980866.4	106.3

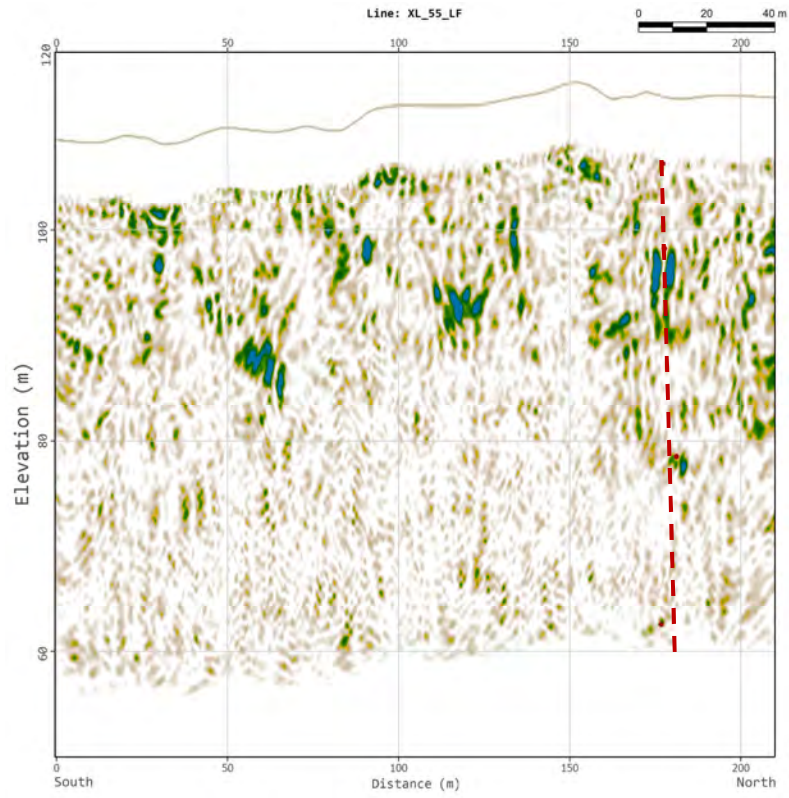


Touquoy Open-Pit Mine: Detection of Underground Mine Workings Using Ground-Penetrating Radar



Touquoy Open-Pit Mine: Detection of Underground Mine Workings Using Ground-Penetrating Radar

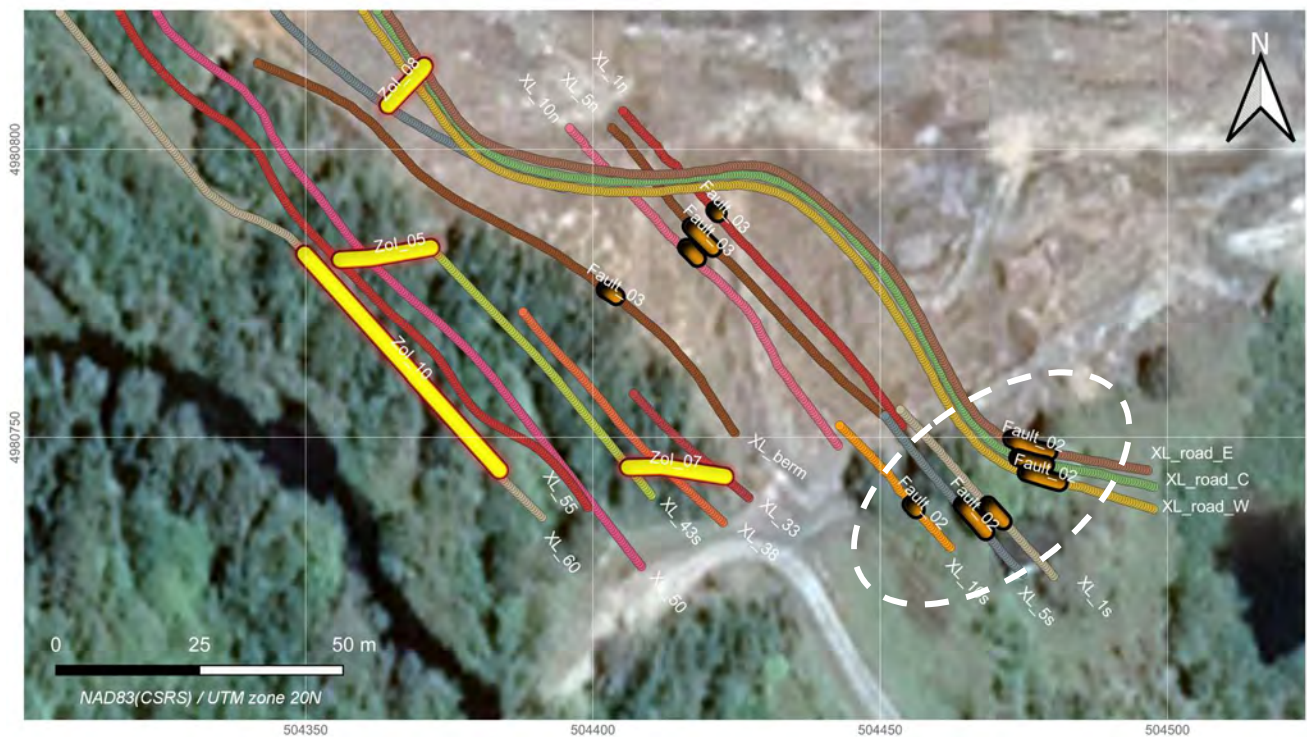




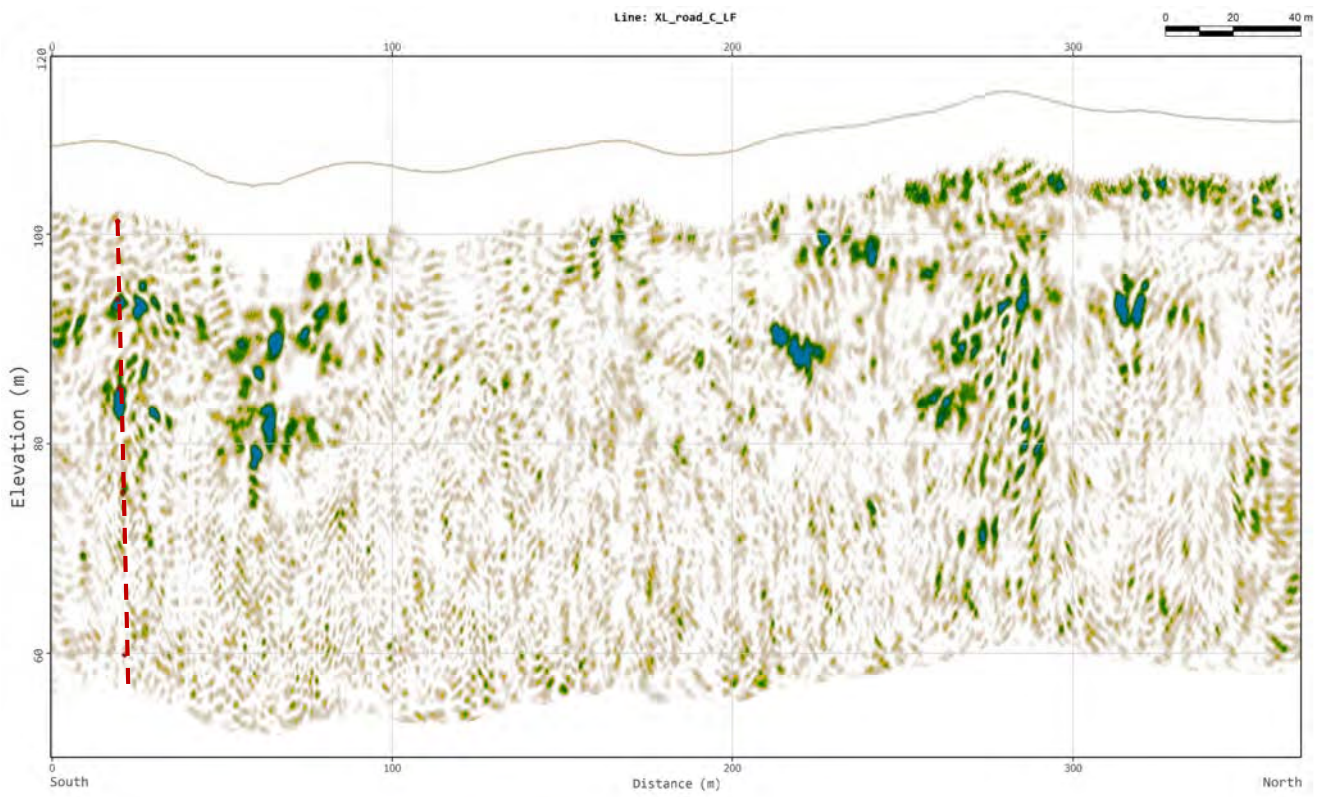
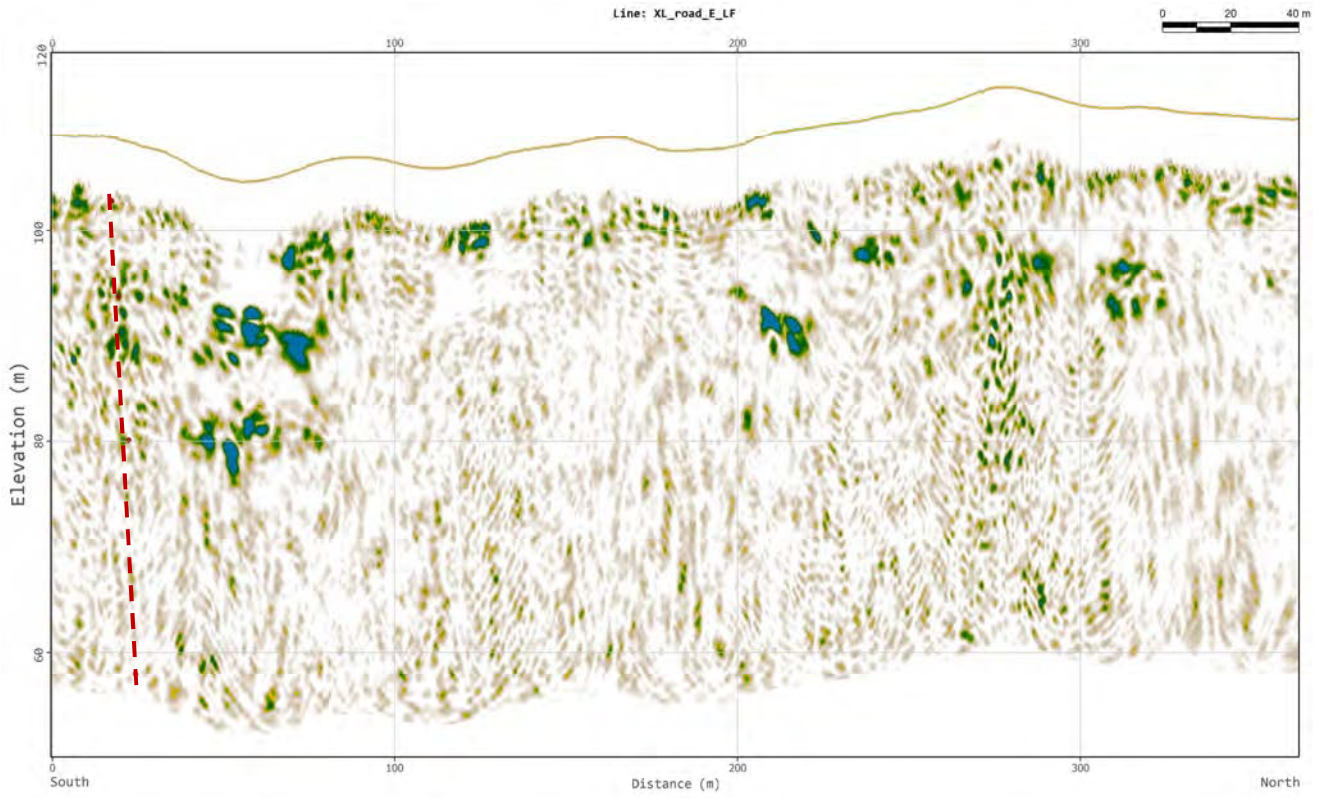
4.1.2 Fault II

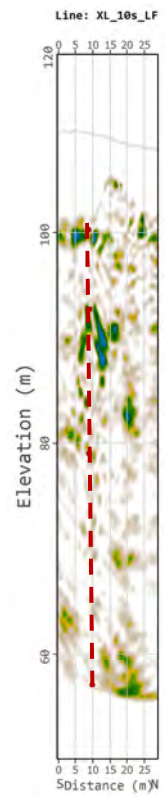
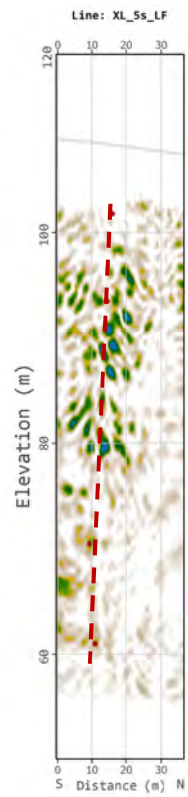
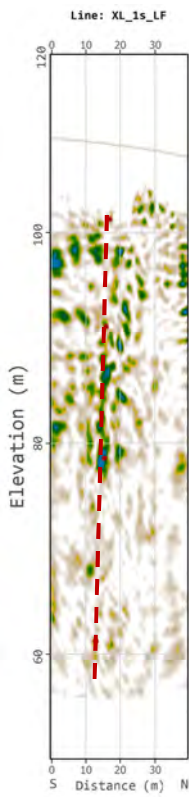
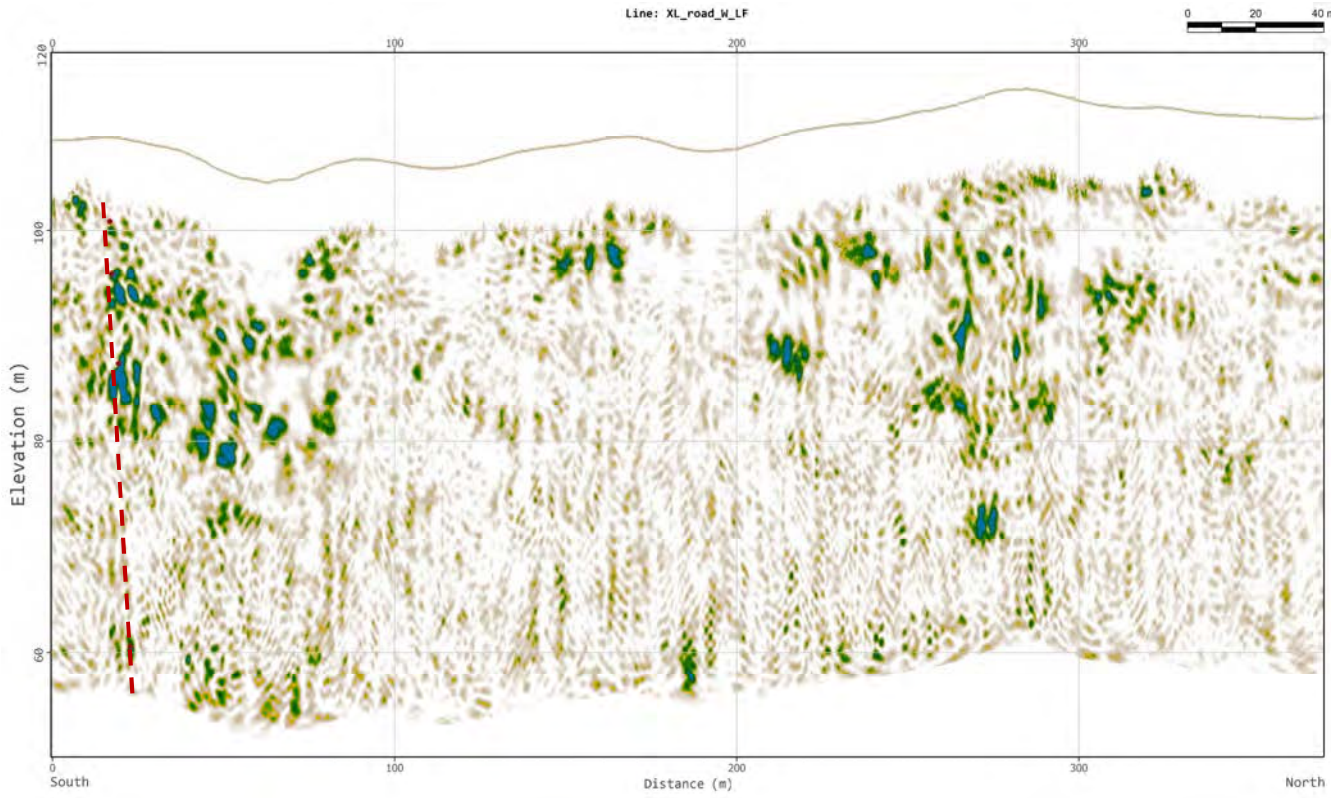
Confidence:	High
Characterization:	Sub-vertical feature with substantial scattering down the shown (red) curve.

COORDINATES OF THE FEATURE (NAD 83, UTM 20N)		
EASTING (m)	NORTHING (m)	ELEVATION (m)
504472.9	4980749.7	57.9
504474.5	4980748.8	80
504477.5	4980747.8	93.6
504479.3	4980747.4	102.8
504473.9	4980746.5	57
504476.8	4980745.6	59.8
504477.1	4980745.6	75.3
504478.2	4980745.4	85.3
504478.8	4980745.2	93.7
504478.6	4980745.3	101.2
504475.4	4980743.8	60.5
504478.9	4980742.7	87.4
504480.6	4980742.3	95.8
504481.1	4980742.1	100.8
504471.4	4980735.4	61.2
504469.7	4980737.2	78.5
504469.4	4980737.6	91
504468.8	4980738.2	101.2
504467.6	4980734.5	60.9
504468.4	4980733.6	70.4
504466.6	4980735.6	81
504465	4980737.4	93.5
504464.3	4980738.3	101.8
504455.4	4980738.3	57
504456.2	4980737.4	79
504455.8	4980737.8	92.7
504456.3	4980737.4	100.2



Touquoy Open-Pit Mine: Detection of Underground Mine Workings Using Ground-Penetrating Radar



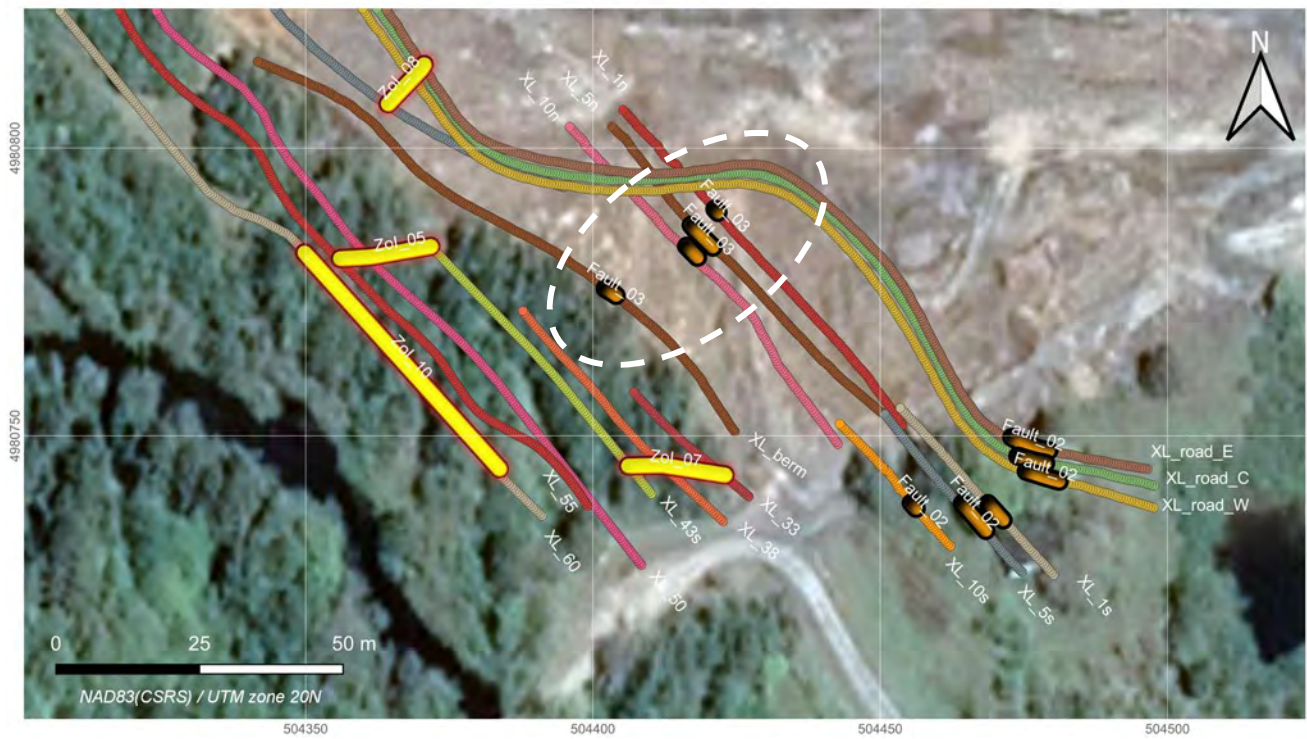


4.1.3 Fault III

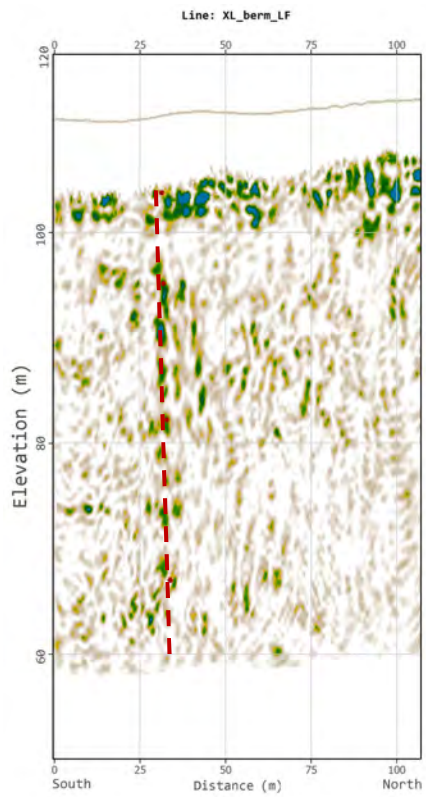
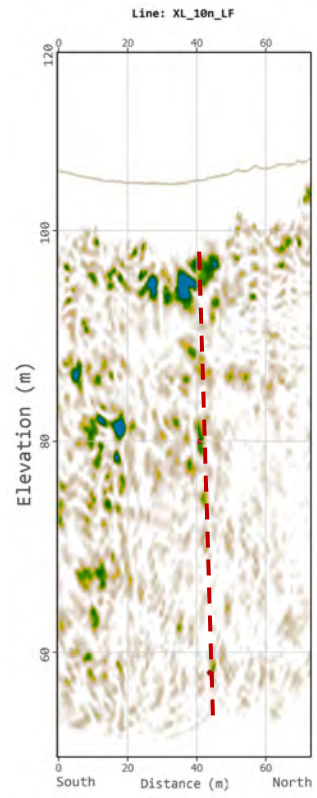
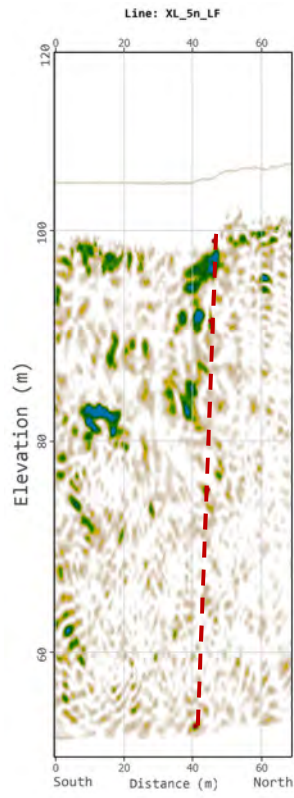
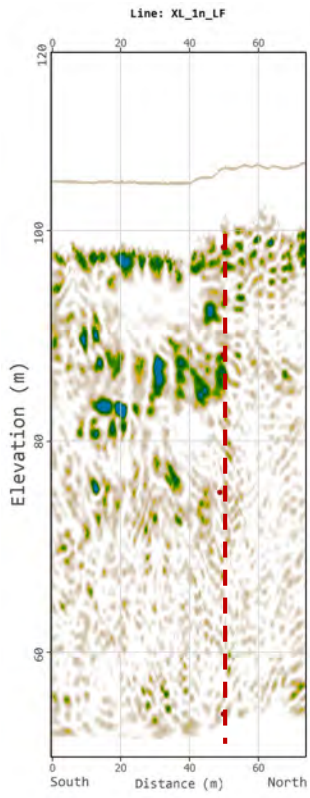
Confidence:	Medium to high
Characterization:	Sub-vertical feature with substantial scattering down the shown (red) curve.

COORDINATES OF THE FEATURE (NAD 83, UTM 20N)

EASTING (m)	NORTHING (m)	ELEVATION (m)
504402.1	4980775.6	67
504403.1	4980775	82.2
504403.6	4980774.7	95.1
504404	4980774.4	103.8
504418.1	4980781.1	79.9
504418.2	4980781	96.5
504416.3	4980782.9	58
504417.1	4980786.6	99
504417.7	4980785.8	91.4
504418.6	4980785	75.4
504420.9	4980782.8	52.9
504421.2	4980789.4	54.1
504421.7	4980788.8	75.1
504421.3	4980789.3	88.2
504421.3	4980789.3	98.4



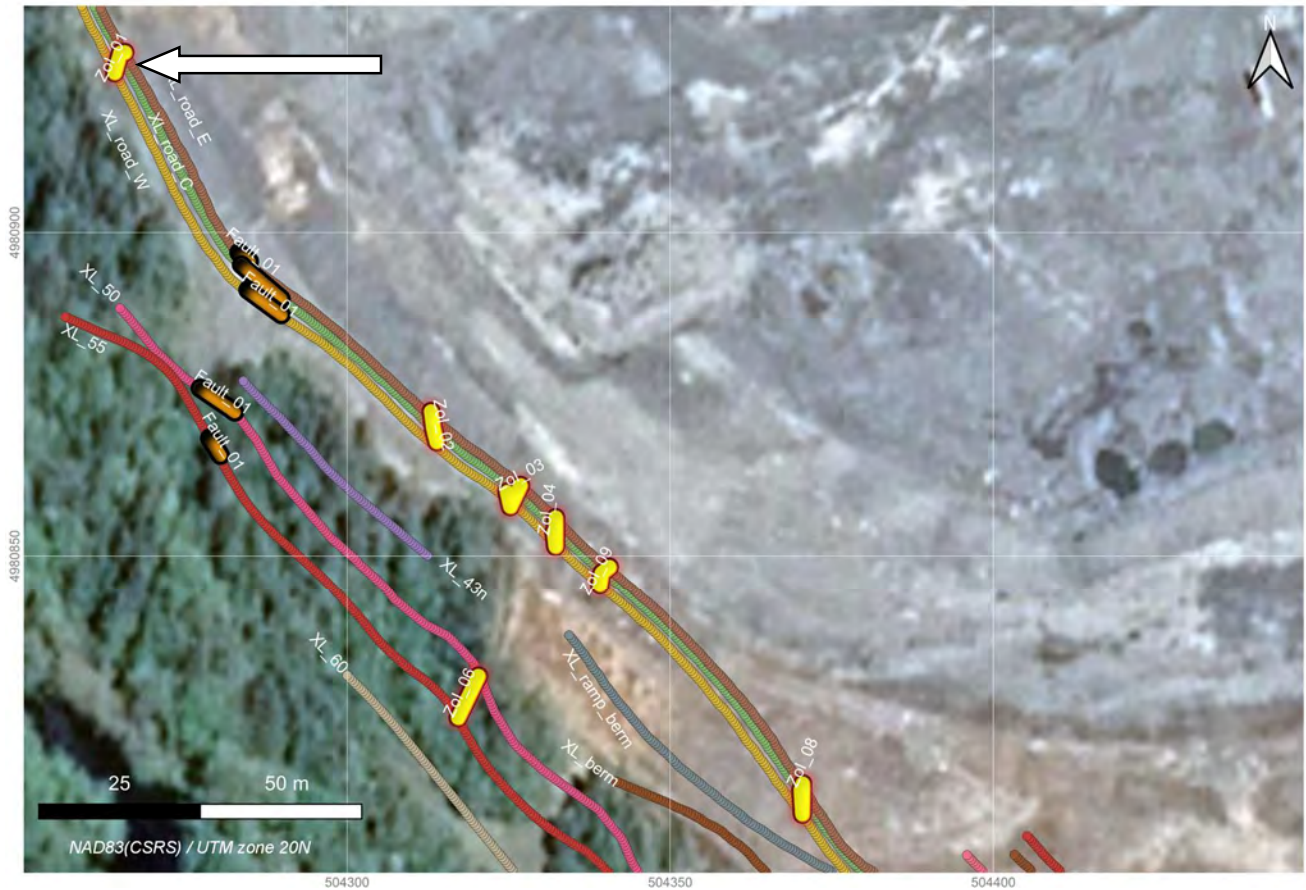
Touquoy Open-Pit Mine: Detection of Underground Mine Workings Using Ground-Penetrating Radar



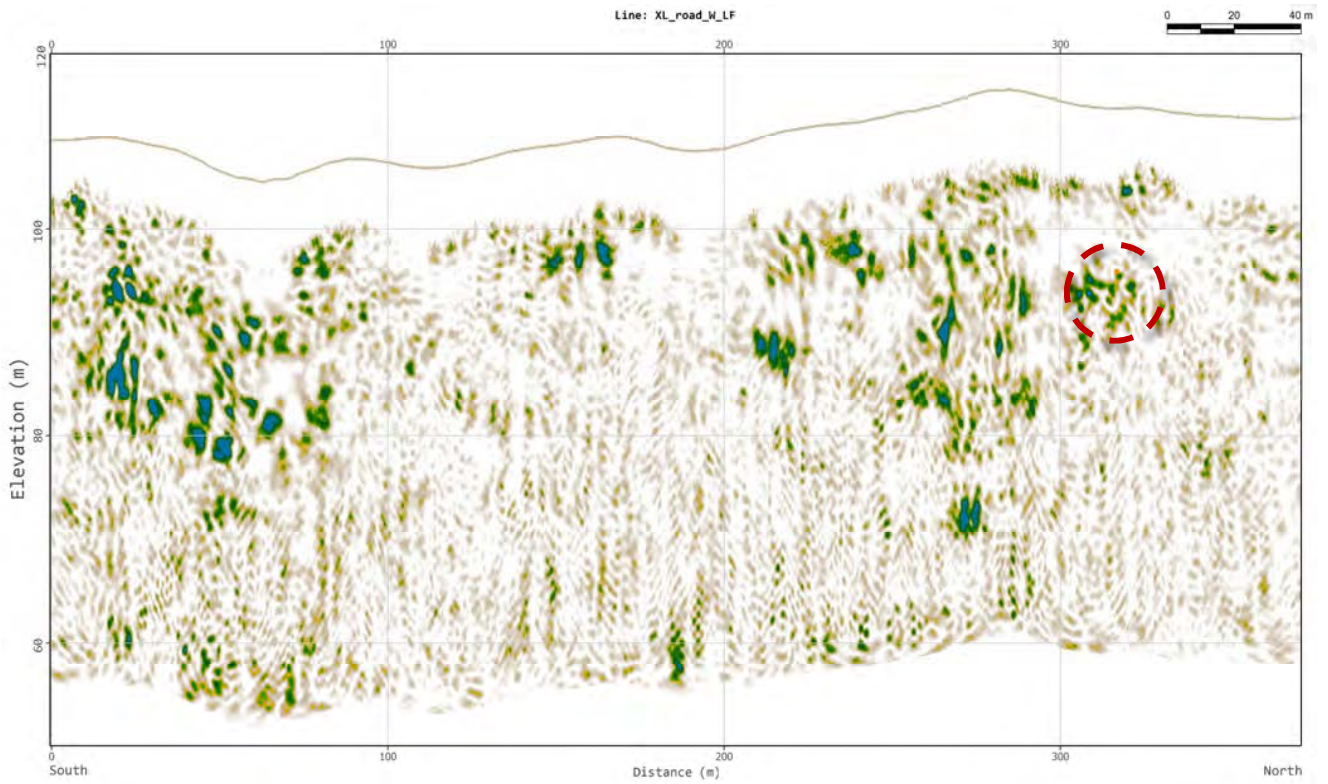
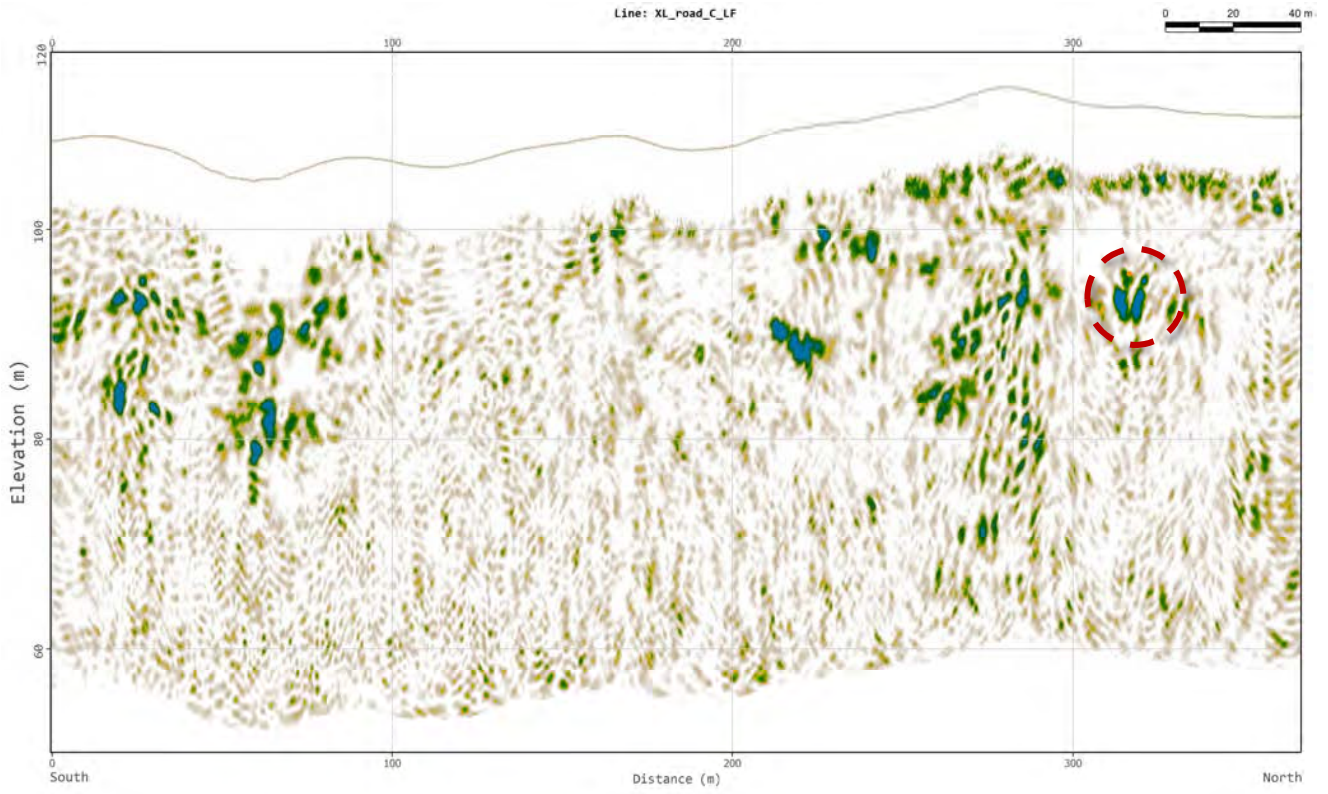
4.1.4 Zone of Interest I

Confidence:	High
Characterization:	Tubular, prominent and isolated, likely 2 metres in diameter or larger

COORDINATES OF THE FEATURE (NAD 83, UTM 20N)		
EASTING (m)	NORTHING (m)	ELEVATION (m)
504265.8	4980927.6	97.4
504264.9	4980927.8	95.7
504264	4980924.8	95.9



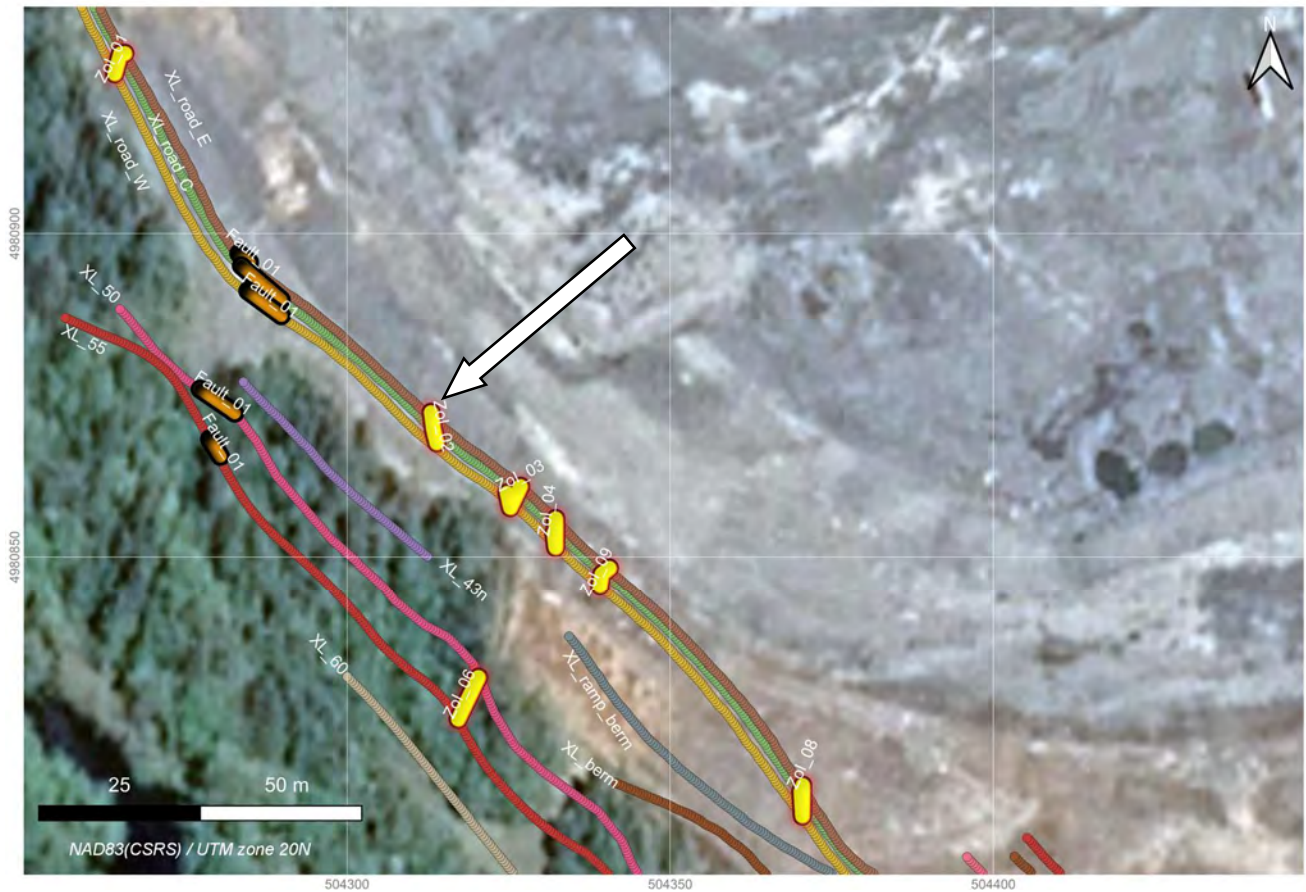
Touquoy Open-Pit Mine: Detection of Underground Mine Workings Using Ground-Penetrating Radar



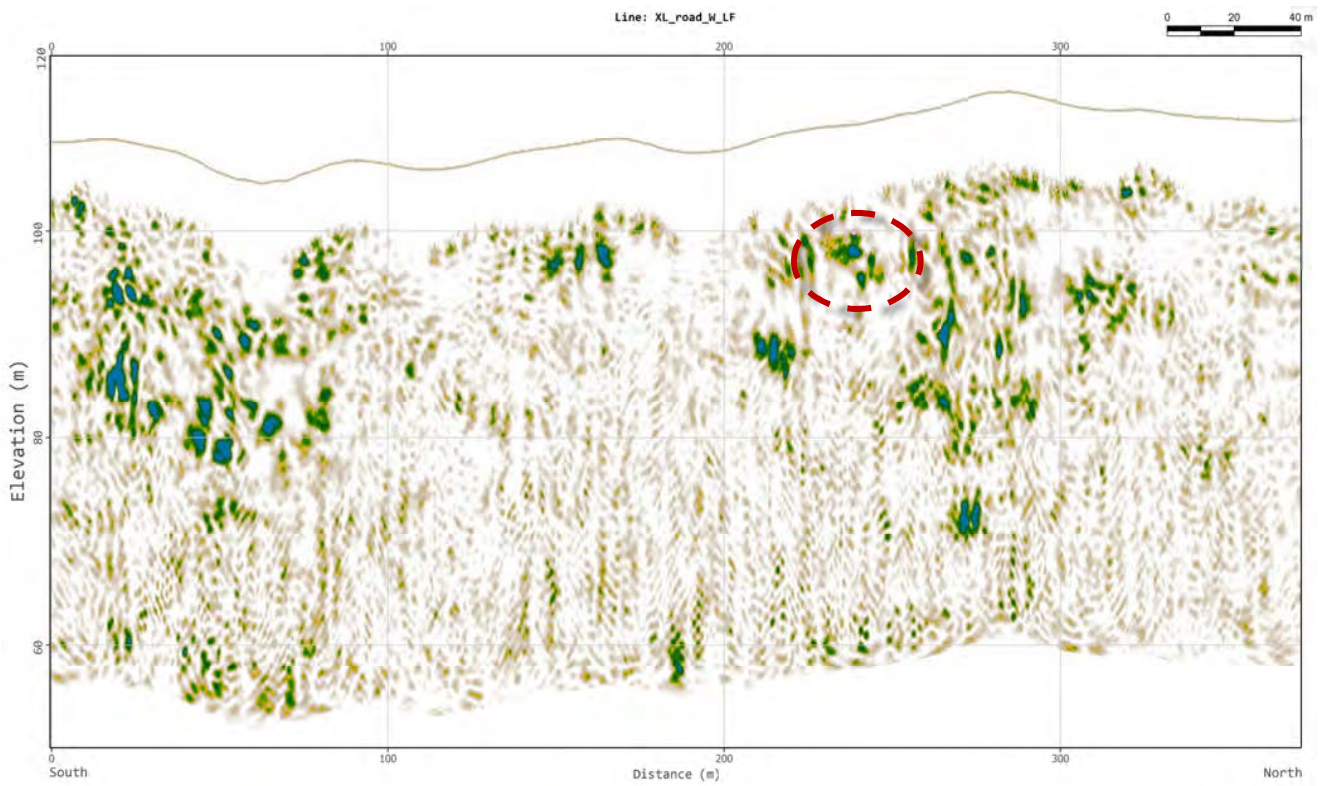
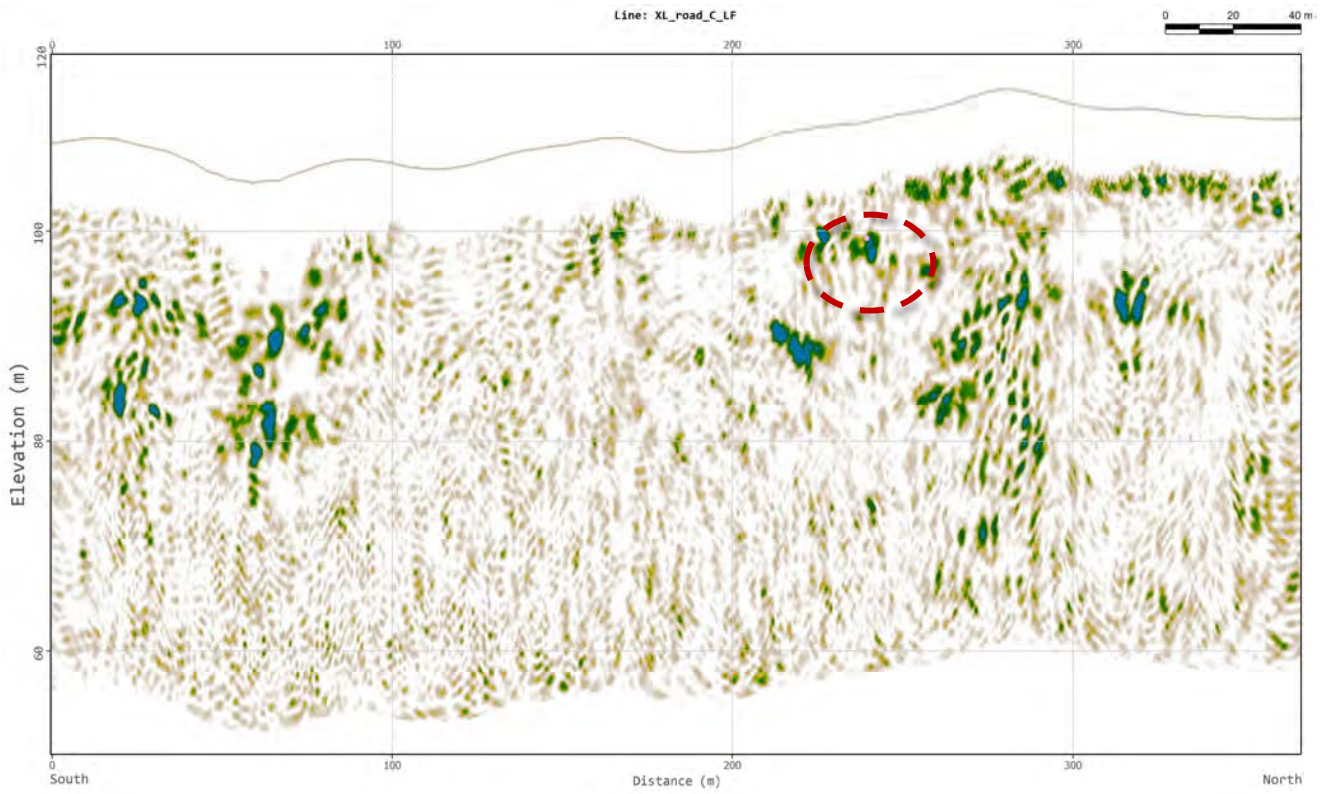
4.1.5 Zone of Interest II

Confidence:	High
Characterization:	Tubular and oval, prominent with lateral discontinuous extent, likely 3 metres in diameter or larger

COORDINATES OF THE FEATURE (NAD 83, UTM 20N)		
EASTING (m)	NORTHING (m)	ELEVATION (m)
504313	4980872.4	99.3
504313.4	4980869.6	99.3
504314.3	4980867.3	99.8



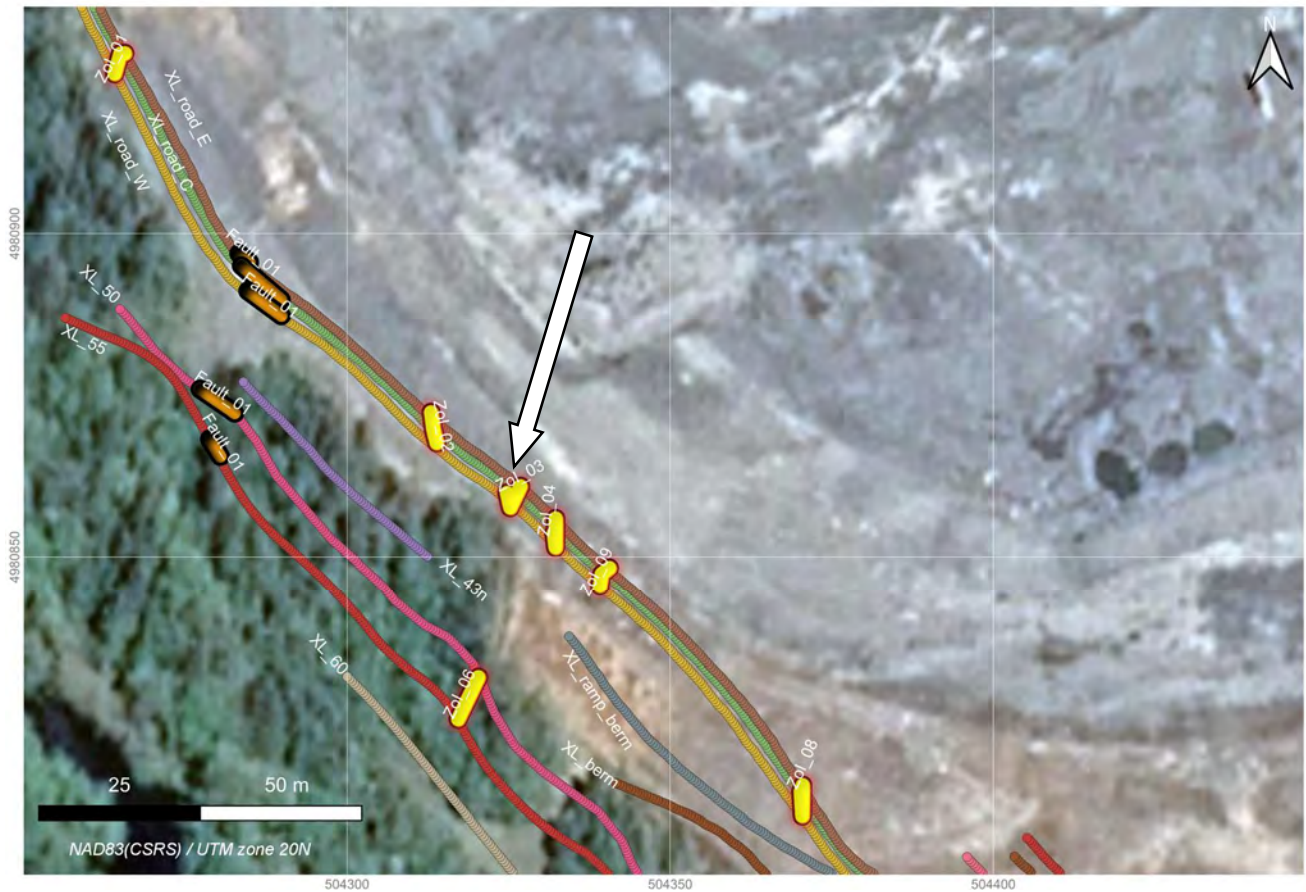
Touquoy Open-Pit Mine: Detection of Underground Mine Workings Using Ground-Penetrating Radar



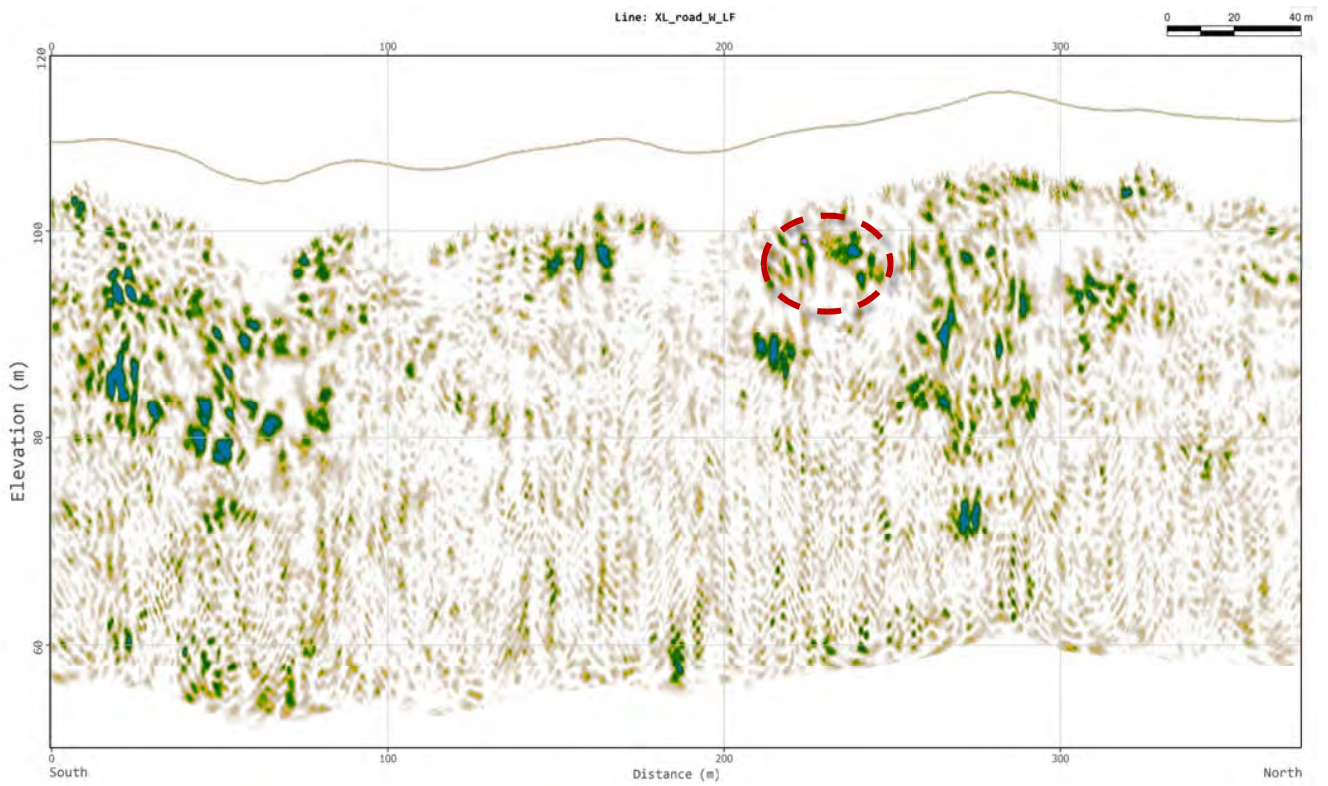
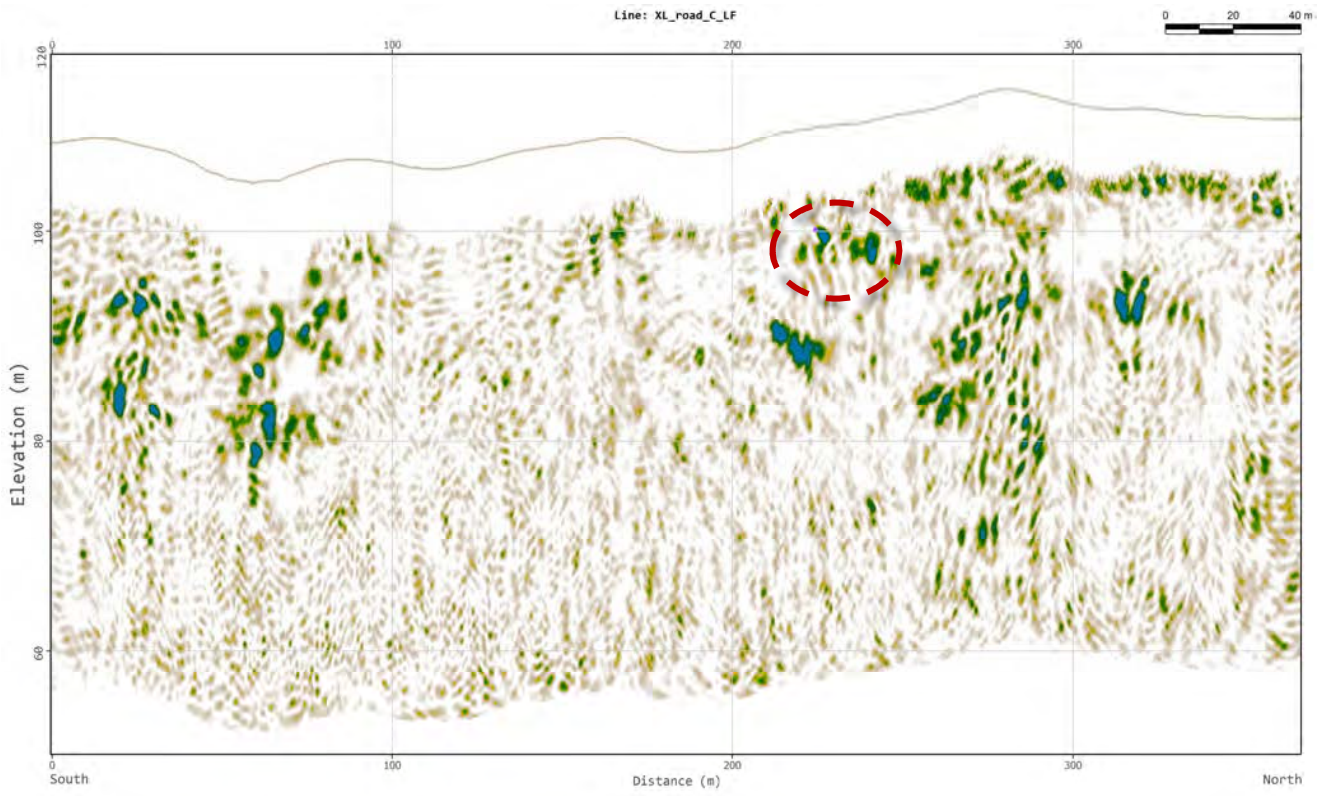
4.1.6 Zone of Interest III

Confidence:	High
Characterization:	Tabular, prominent with lateral discontinuous extent, likely 3 metres in diameter or larger, proximity to Zone of Interest II may imply the existence of an underground network structure

COORDINATES OF THE FEATURE (NAD 83, UTM 20N)		
EASTING (m)	NORTHING (m)	ELEVATION (m)
504326.7	4980861	100.8
504324.6	4980860	100.1
504325.3	4980857.6	98.9



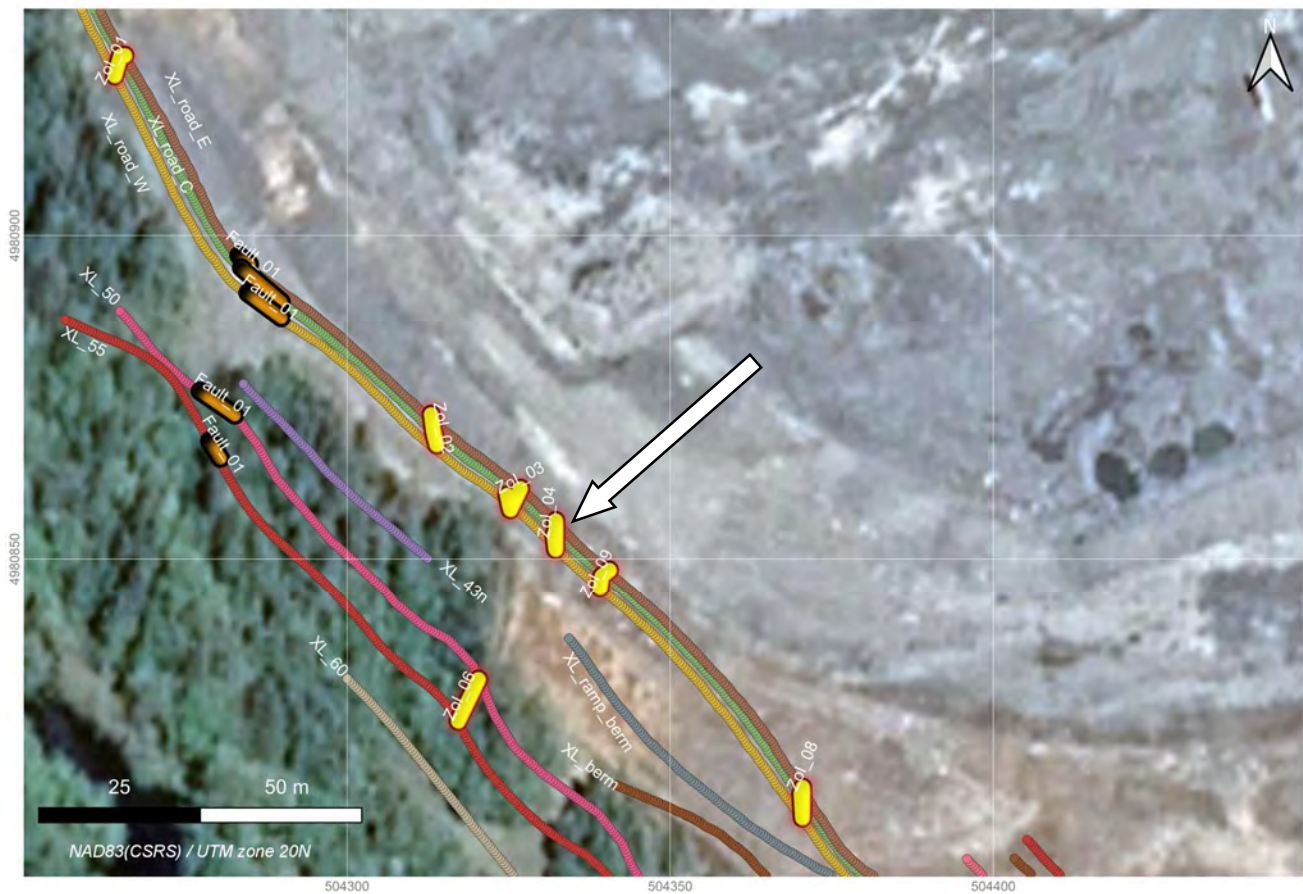
Touquoy Open-Pit Mine: Detection of Underground Mine Workings Using Ground-Penetrating Radar

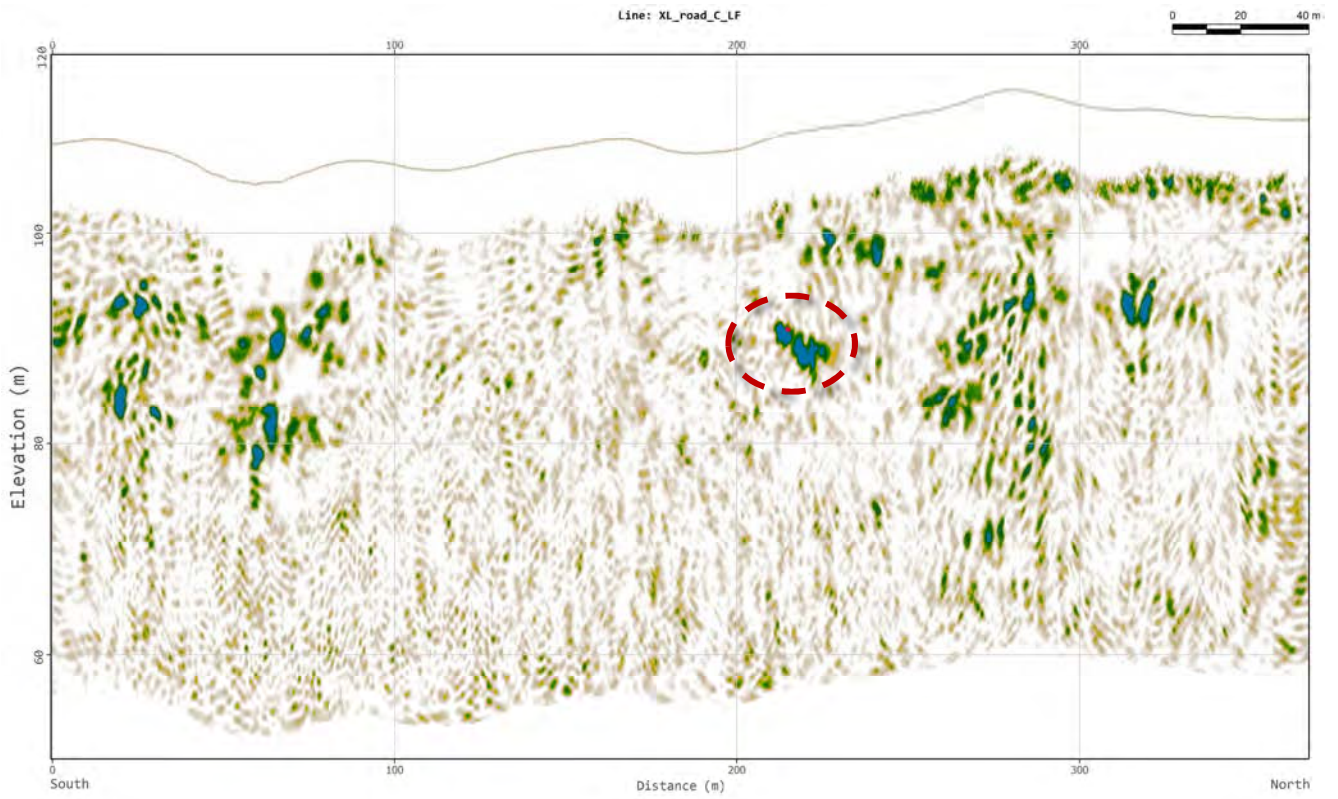
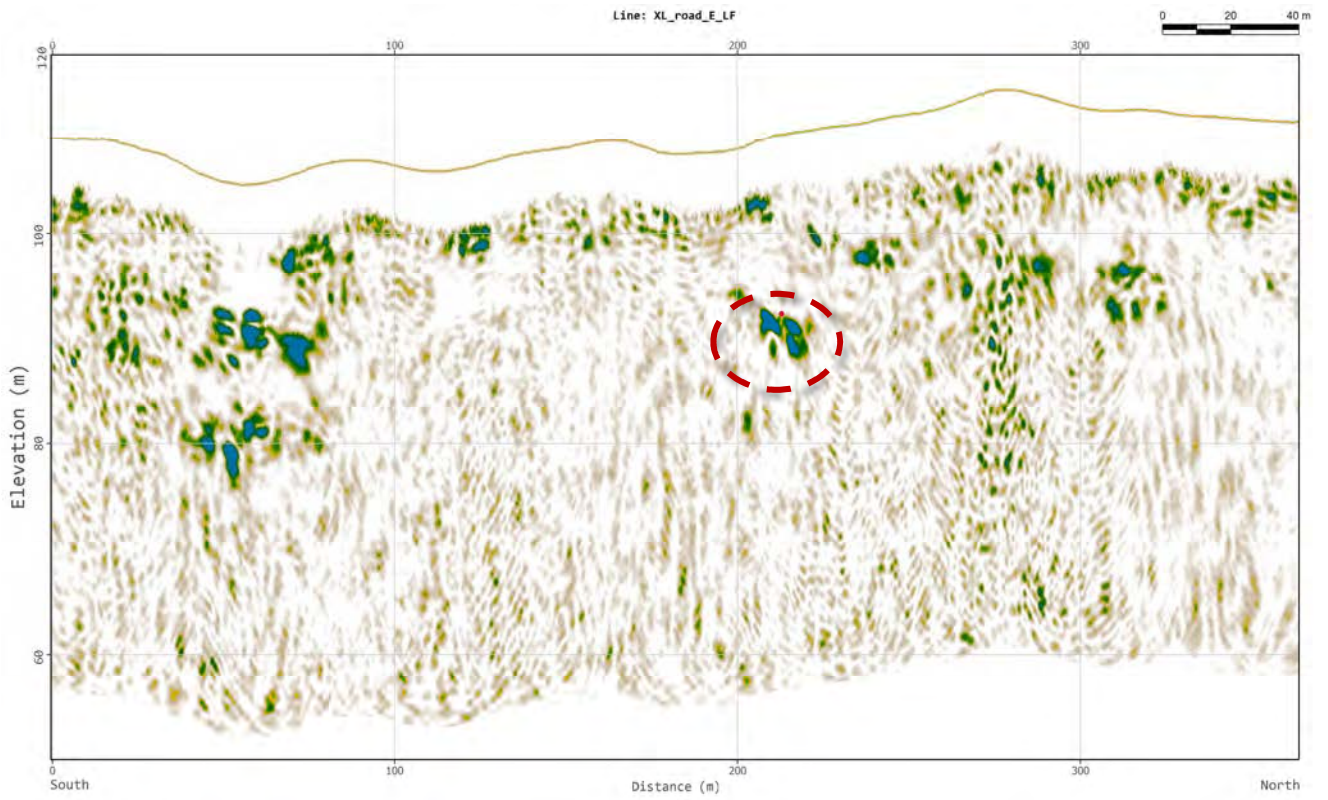


4.1.7 Zone of Interest IV

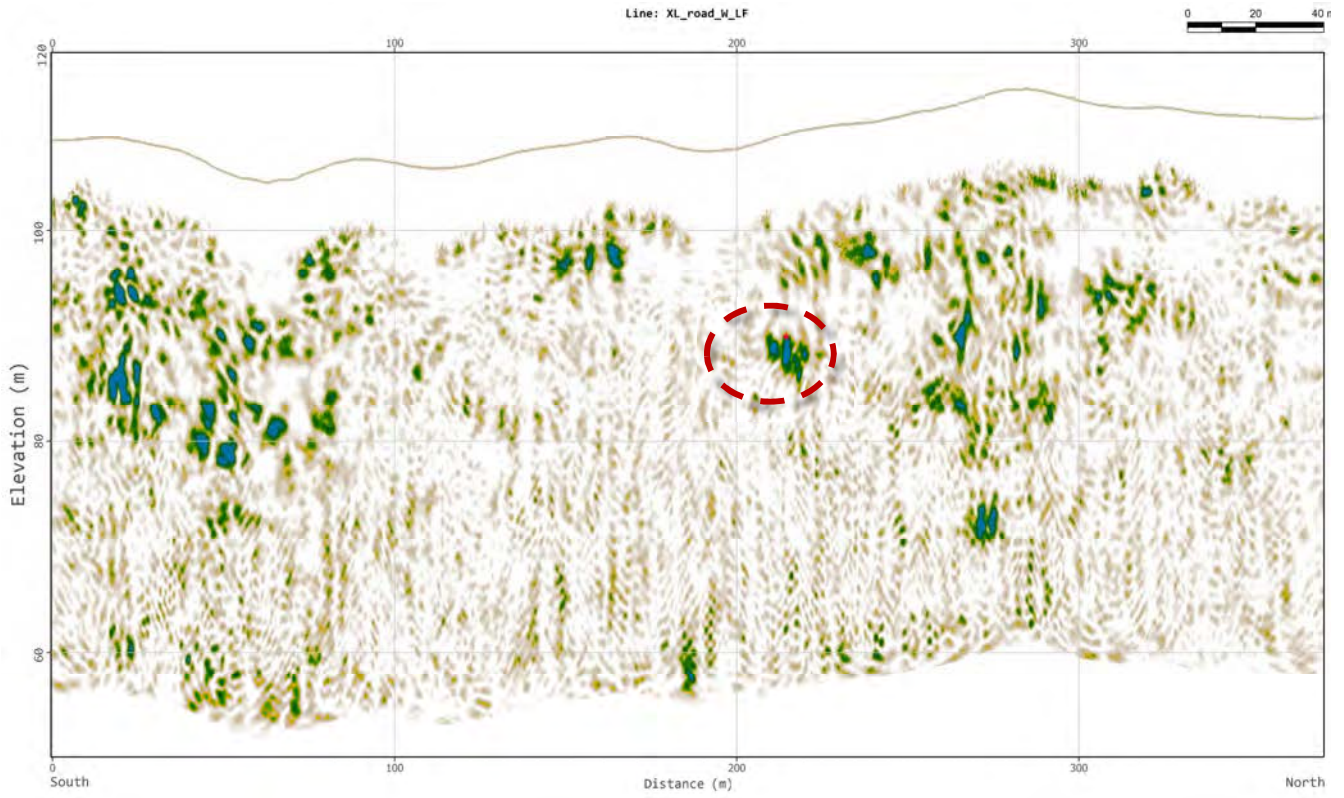
Confidence:	High
Characterization:	Tabular, prominent, well-defined, likely 6 metres or larger across horizontally, proximity to Zone of Interest II may imply the existence of an underground network structure

COORDINATES OF THE FEATURE (NAD 83, UTM 20N)		
EASTING (m)	NORTHING (m)	ELEVATION (m)
504332.7	4980855.6	92.2
504331.9	4980853.7	90.8
504332.4	4980851.4	89.9





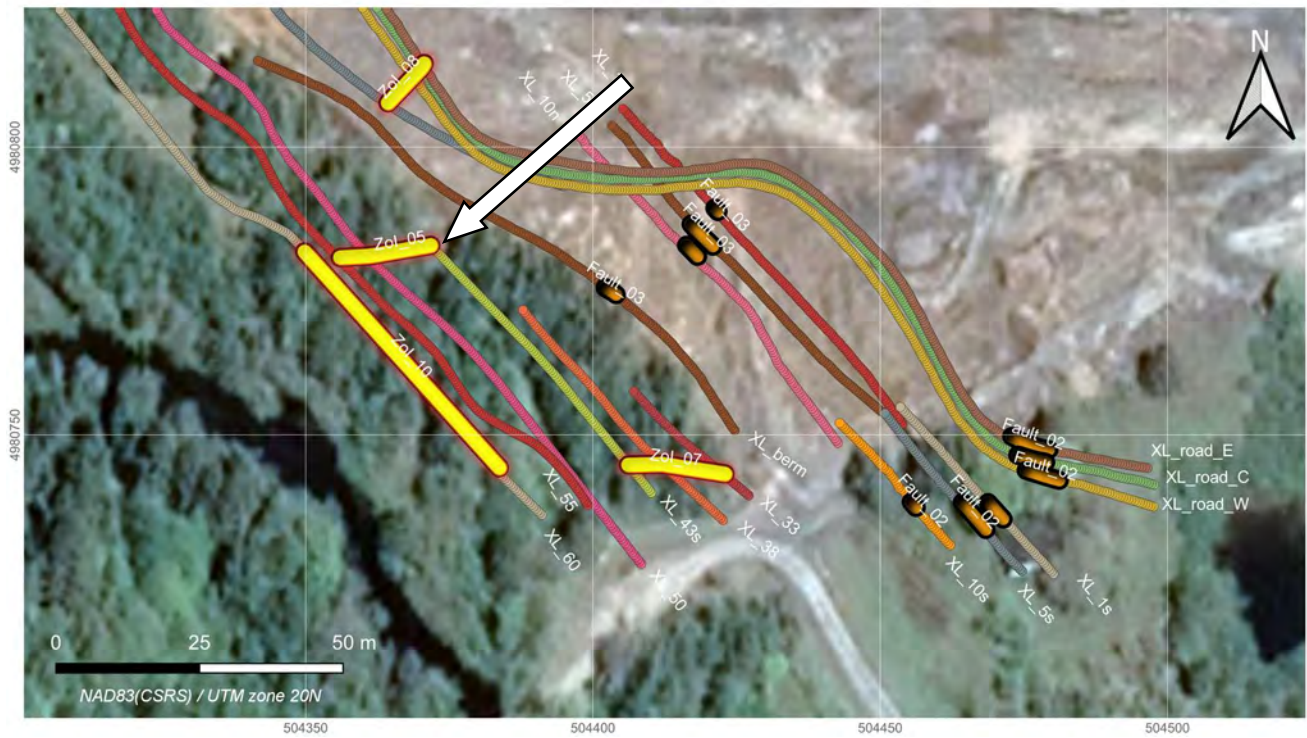
Touquoy Open-Pit Mine: Detection of Underground Mine Workings Using Ground-Penetrating Radar



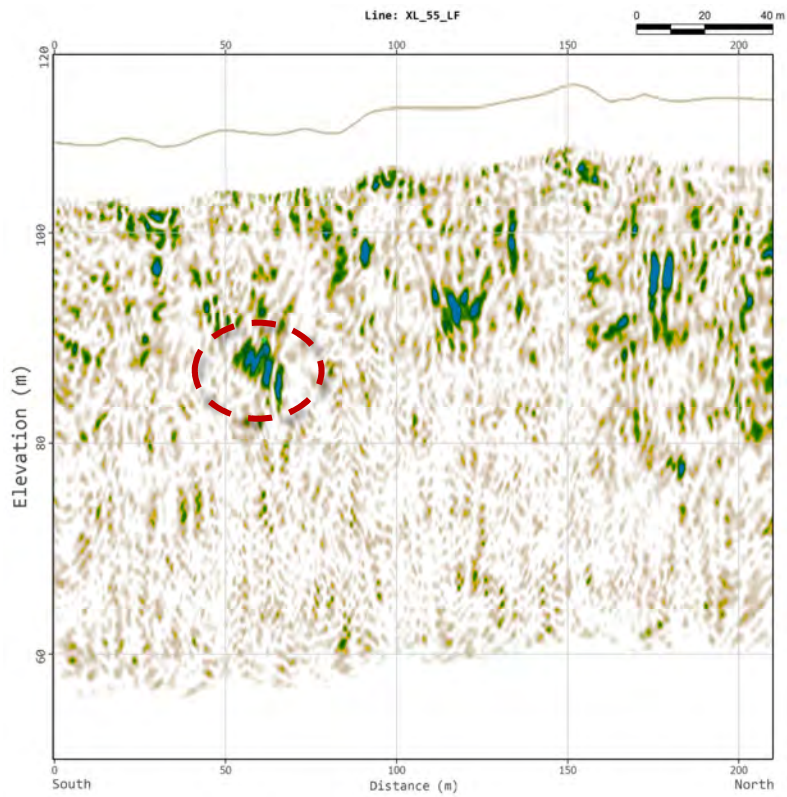
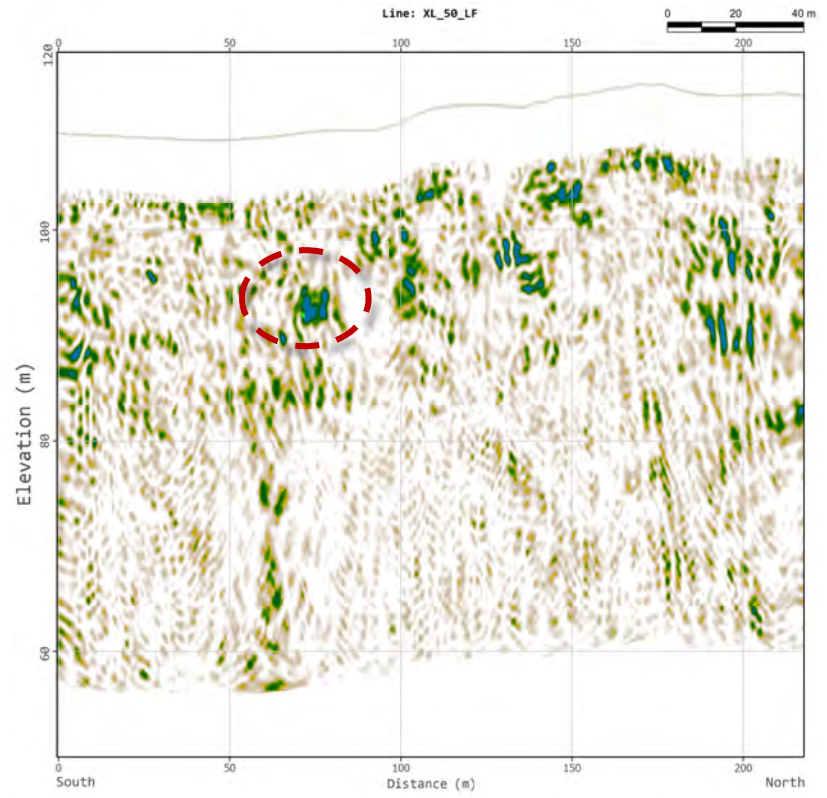
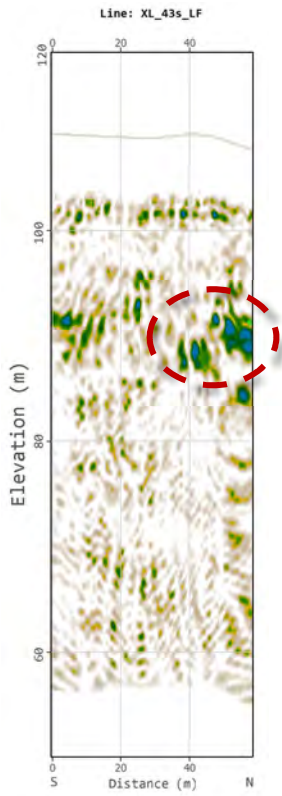
4.1.8 Zone of Interest V

Confidence:	High
Characterization:	Tabular, prominent, well-defined, likely 4 metres or larger across horizontally, likely connected to Zone of Interest X (detailed below)

COORDINATES OF THE FEATURE (NAD 83, UTM 20N)		
EASTING (m)	NORTHING (m)	ELEVATION (m)
504356	4980780.8	89.7
504371.8	4980782.9	91.2
504361.4	4980781.1	92



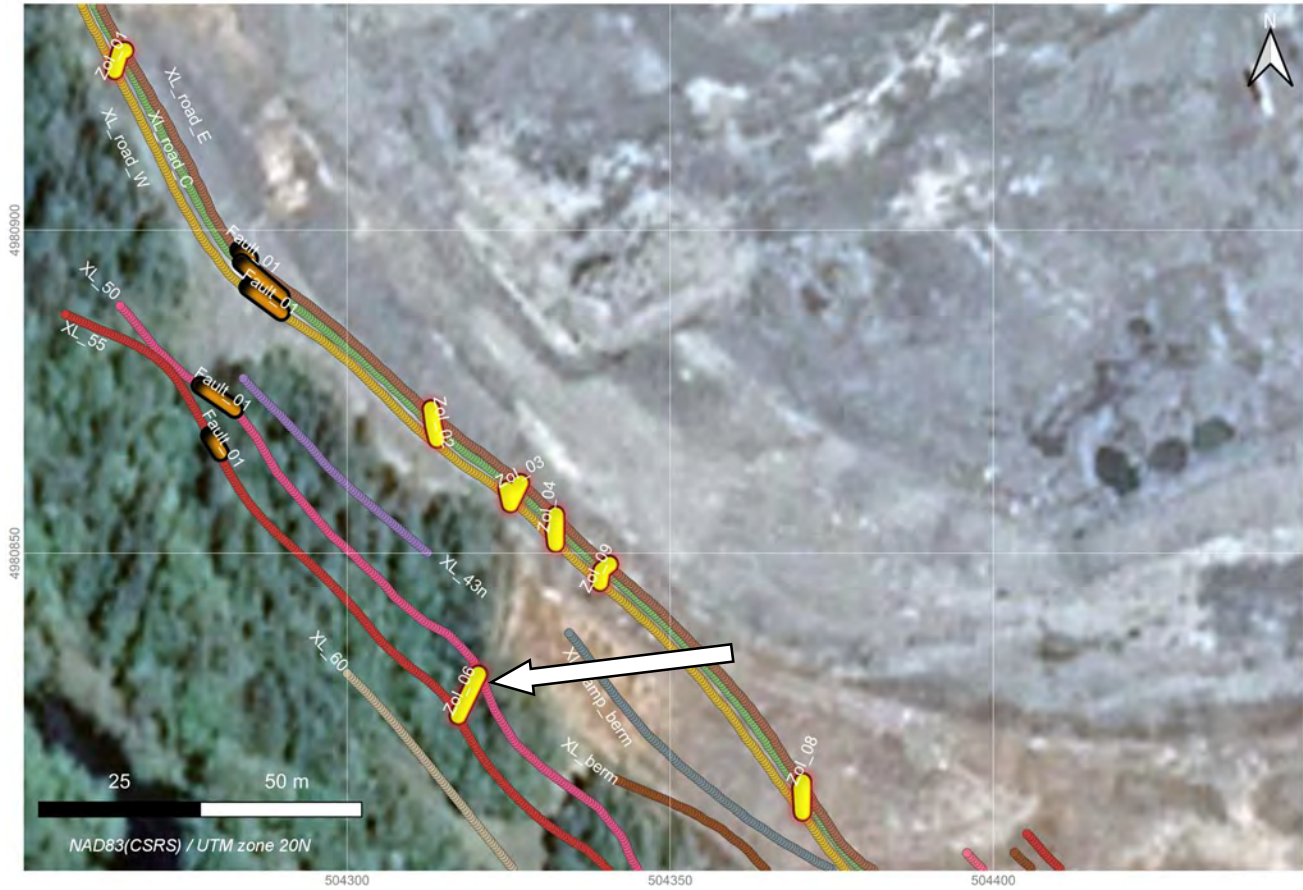
Touquoy Open-Pit Mine: Detection of Underground Mine Workings Using Ground-Penetrating Radar

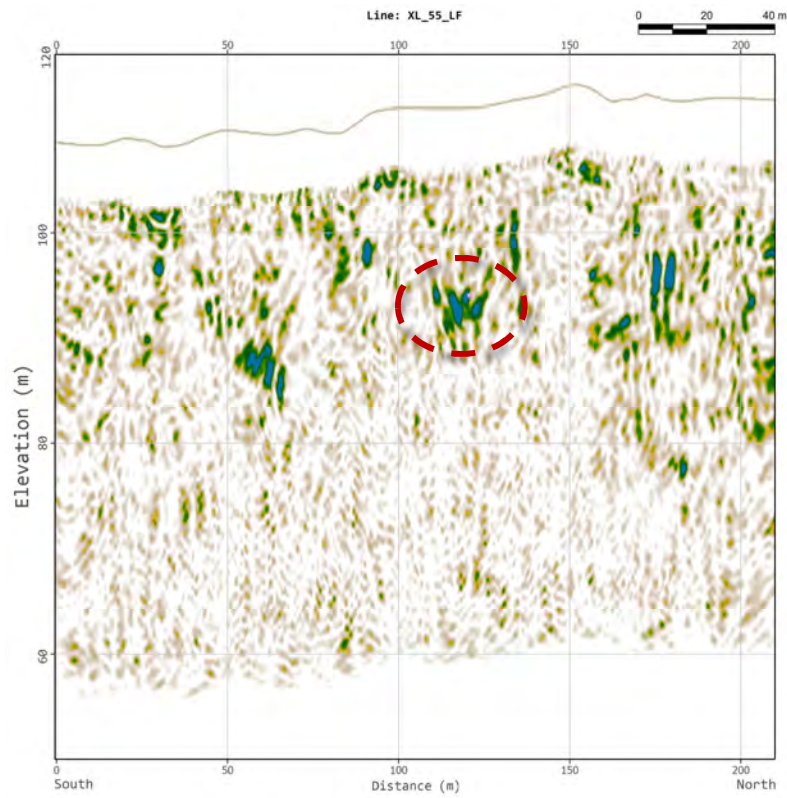
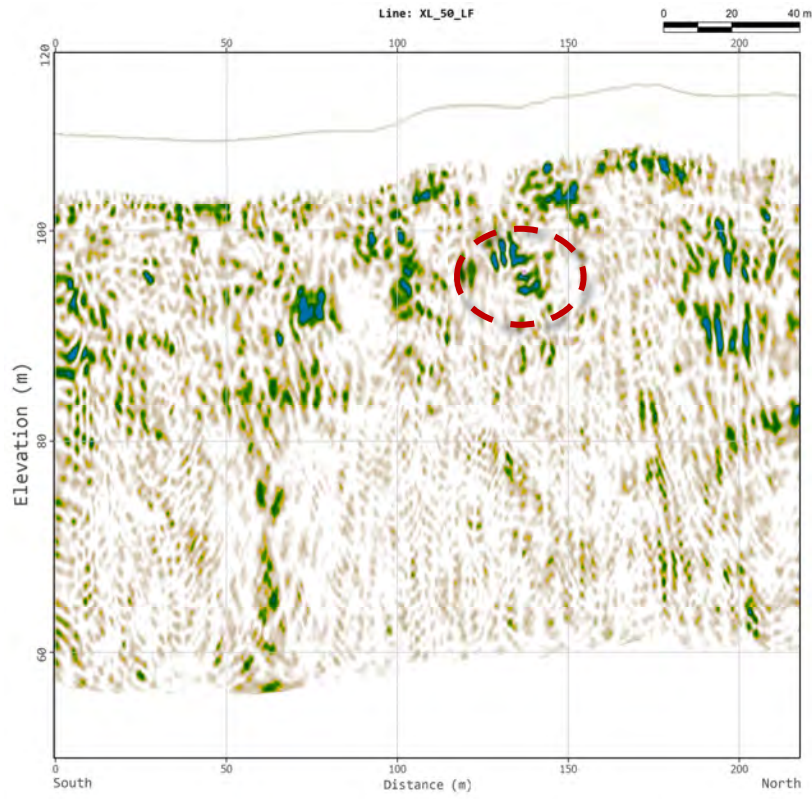


4.1.9 Zone of Interest VI

Confidence:	High
Characterization:	Tabular, prominent, well-defined and proximal to other features, likely 4 metres or larger across horizontally

COORDINATES OF THE FEATURE (NAD 83, UTM 20N)		
EASTING (m)	NORTHING (m)	ELEVATION (m)
504317.3	4980824.7	94
504320.3	4980831.4	96

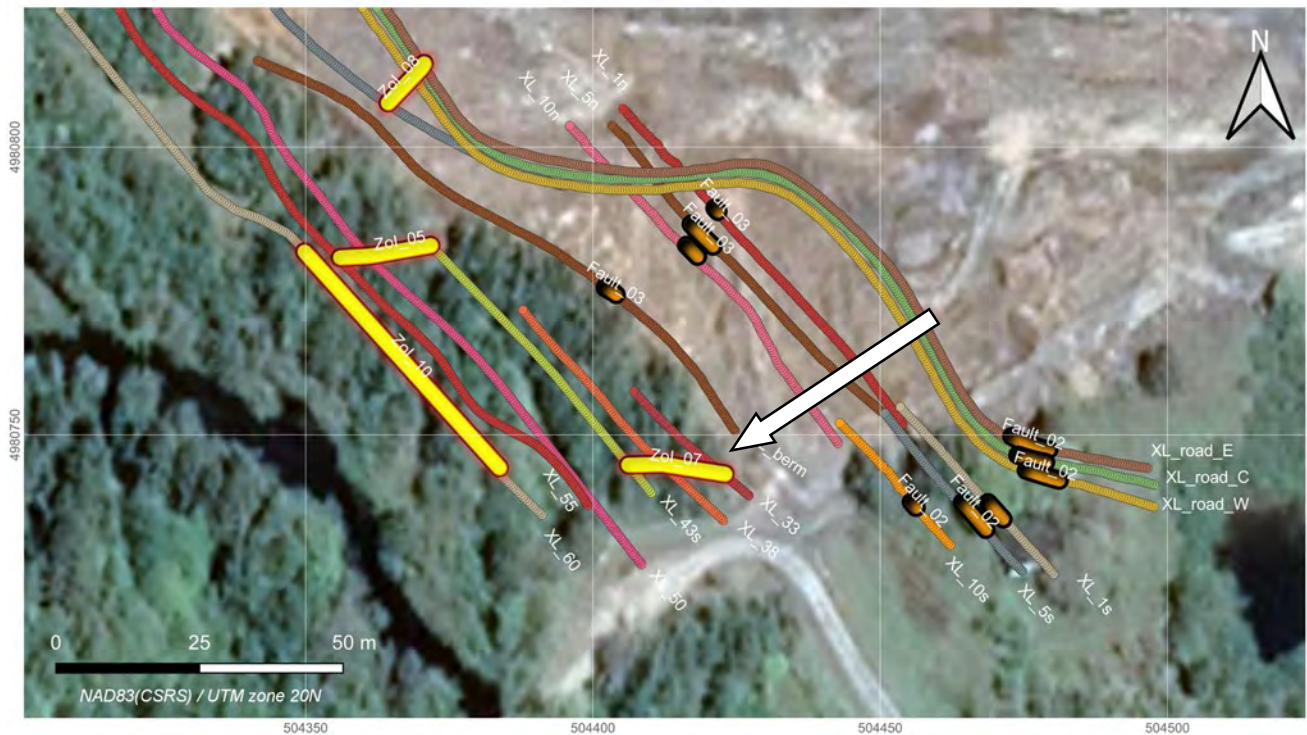




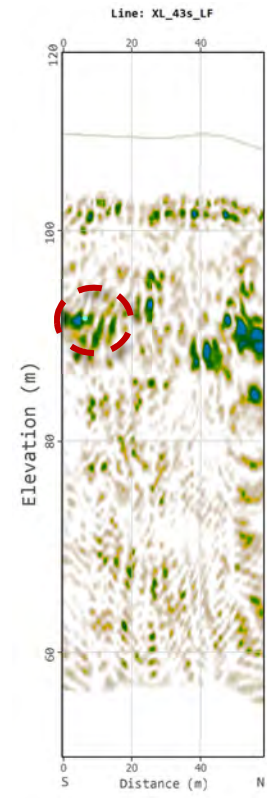
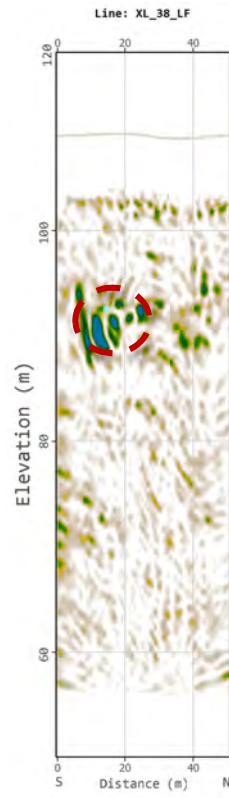
4.1.10 Zone of Interest VII

Confidence:	High
Characterization:	Tabular, prominent with lateral discontinuous extent, likely 10 metres or larger across horizontally

COORDINATES OF THE FEATURE (NAD 83, UTM 20N)		
EASTING (m)	NORTHING (m)	ELEVATION (m)
504412.1	4980744.9	92.5
504406.1	4980744.8	91.6
504423	4980743.2	93.9



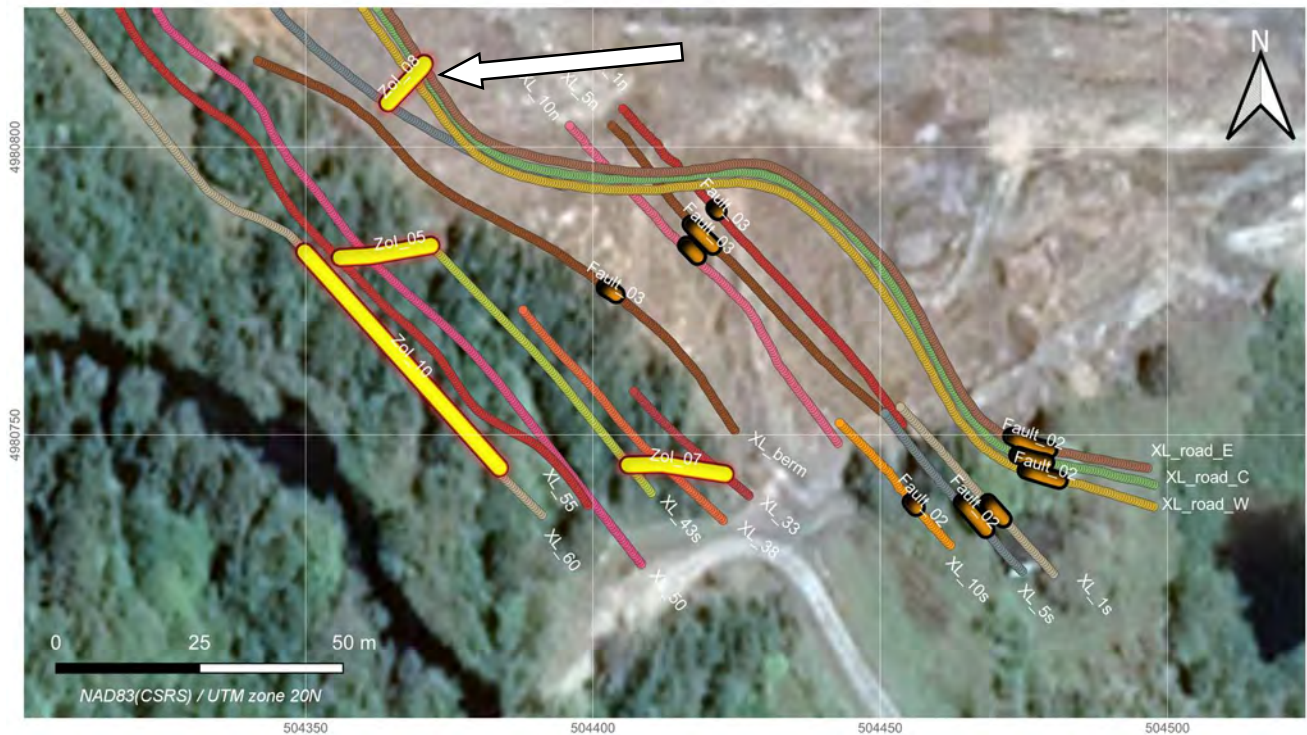
Touquoy Open-Pit Mine: Detection of Underground Mine Workings Using Ground-Penetrating Radar



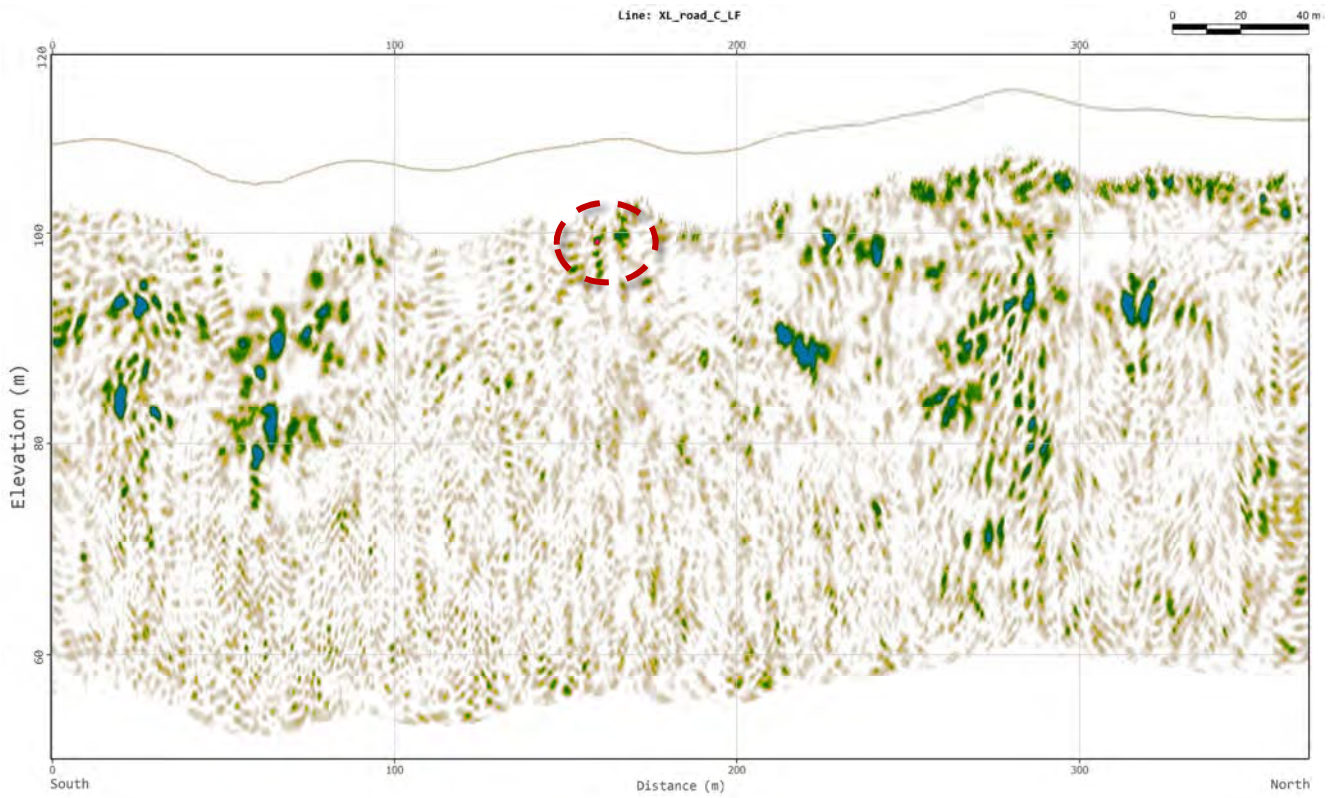
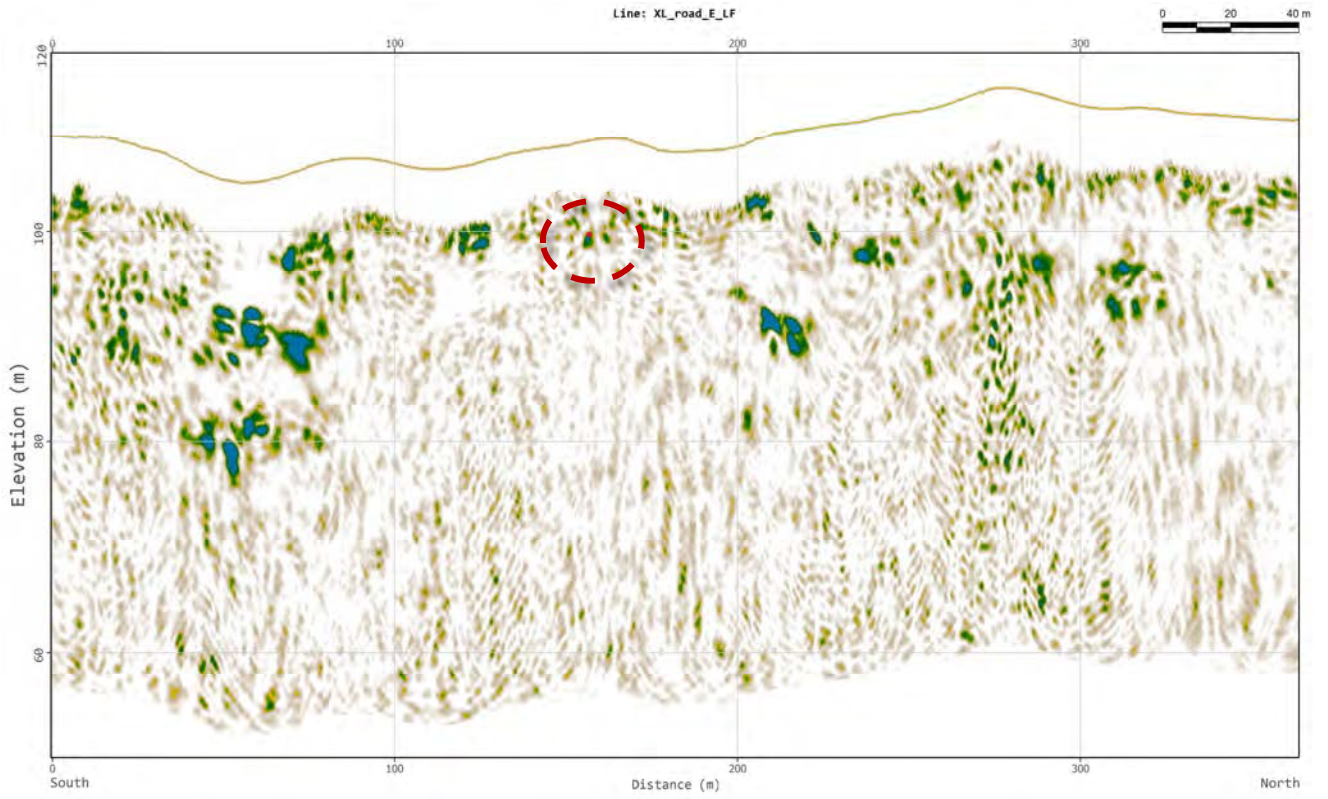
4.1.11 Zone of Interest VIII

Confidence:	High
Characterization:	Tabular, prominent with discontinuous lateral extensions, likely 10 metres or larger across horizontally

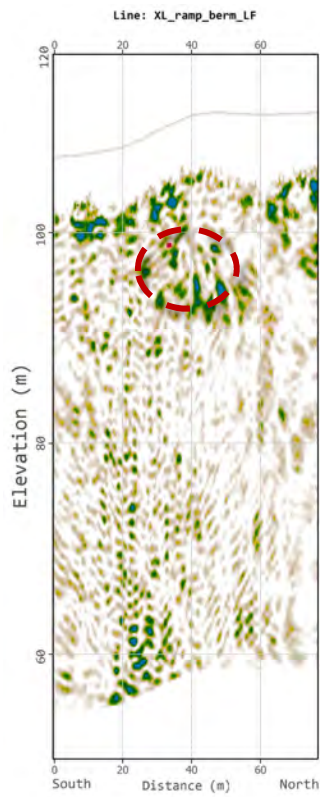
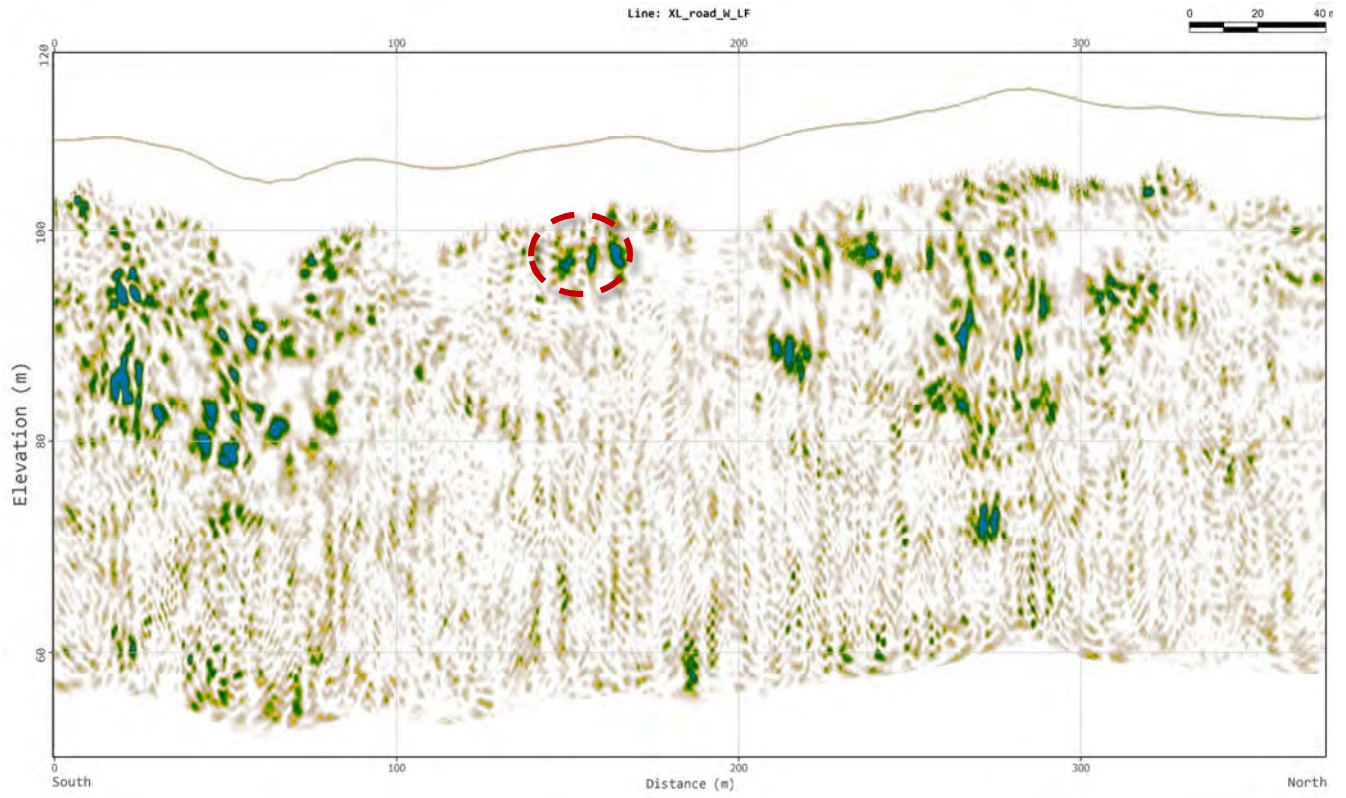
COORDINATES OF THE FEATURE (NAD 83, UTM 20N)		
EASTING (m)	NORTHING (m)	ELEVATION (m)
504370.6	4980814.5	99.6
504370.1	4980813.8	99.1
504364.3	4980807.7	98.8



Touquoy Open-Pit Mine: Detection of Underground Mine Workings Using Ground-Penetrating Radar



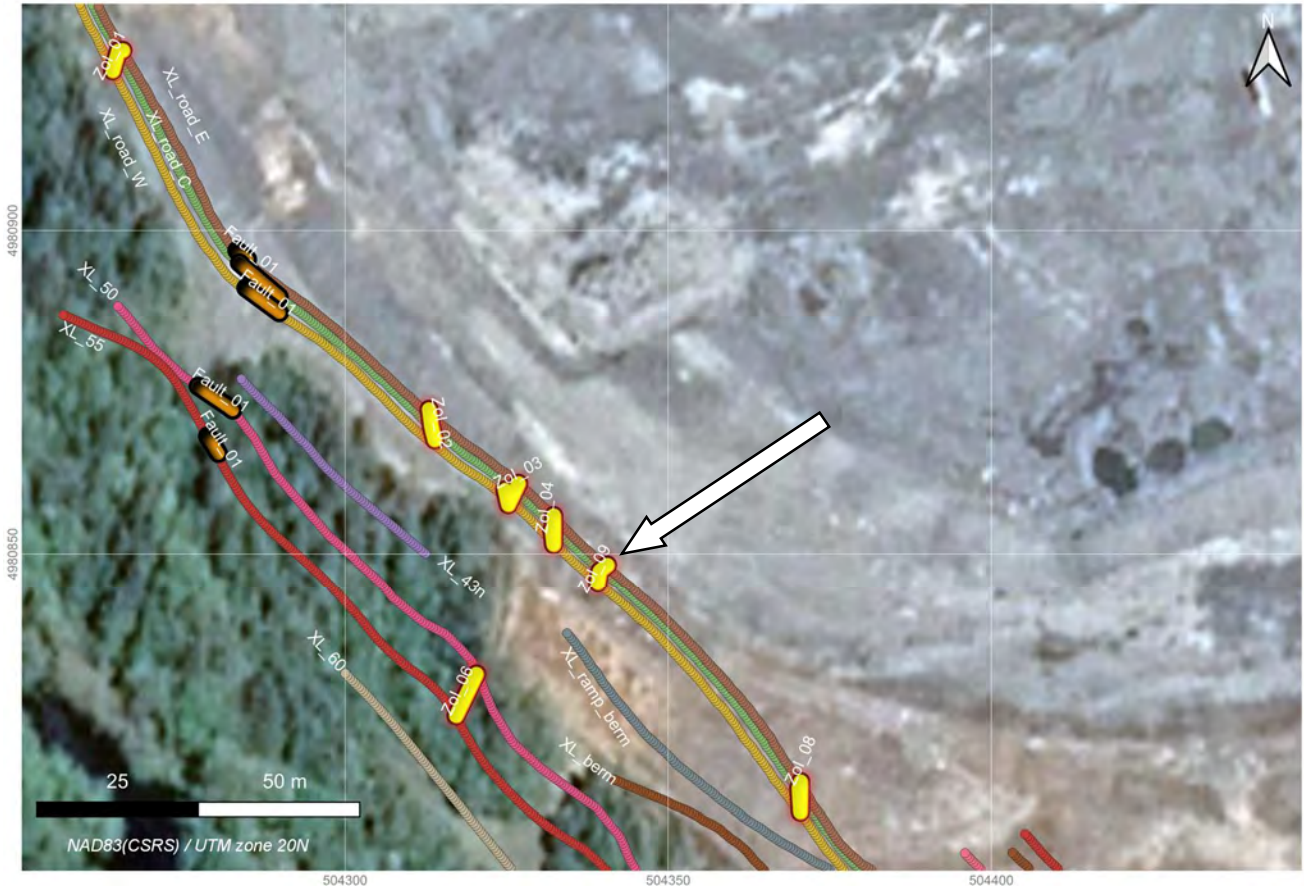
Touquoy Open-Pit Mine: Detection of Underground Mine Workings Using Ground-Penetrating Radar



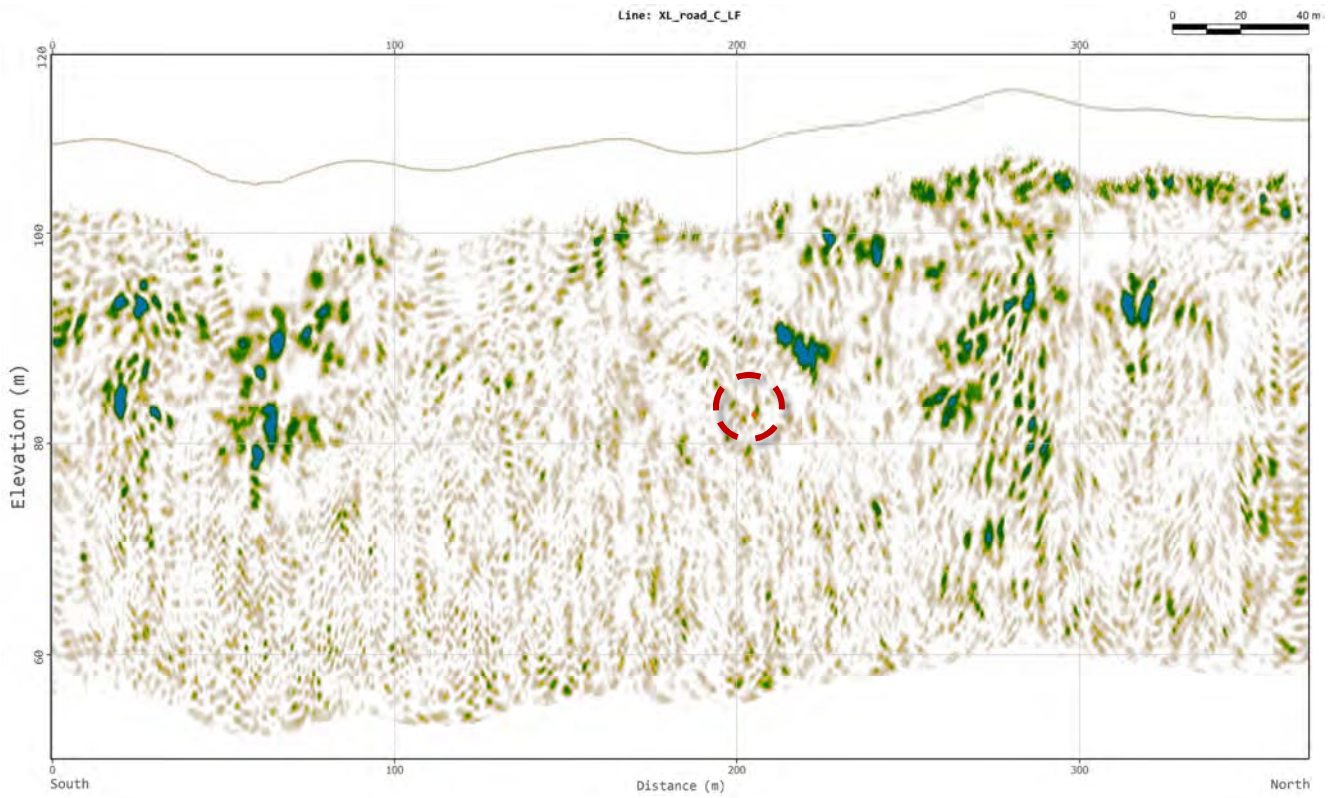
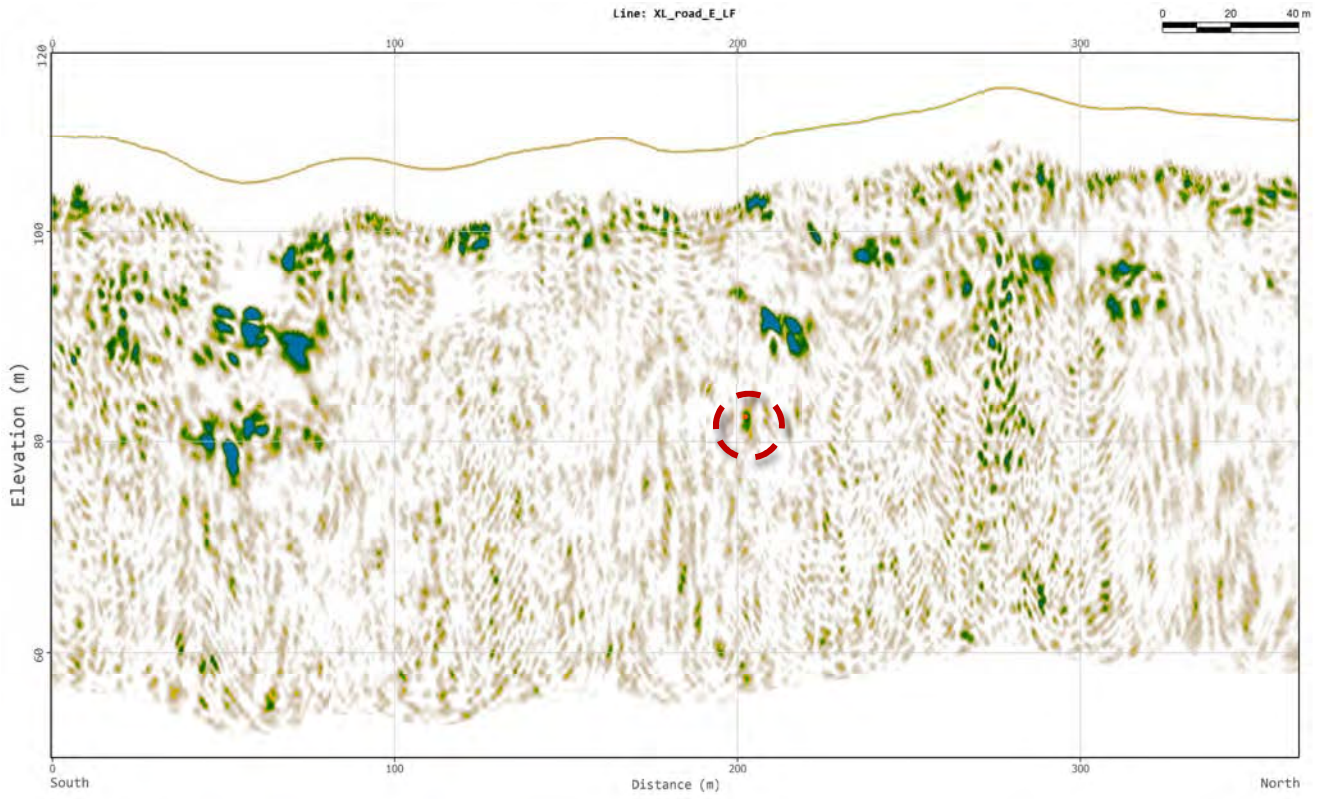
4.1.12 Zone of Interest IX

Confidence:	Medium
Characterization:	Tubular, isolated, high-energy, likely 2 metres or larger in diameter

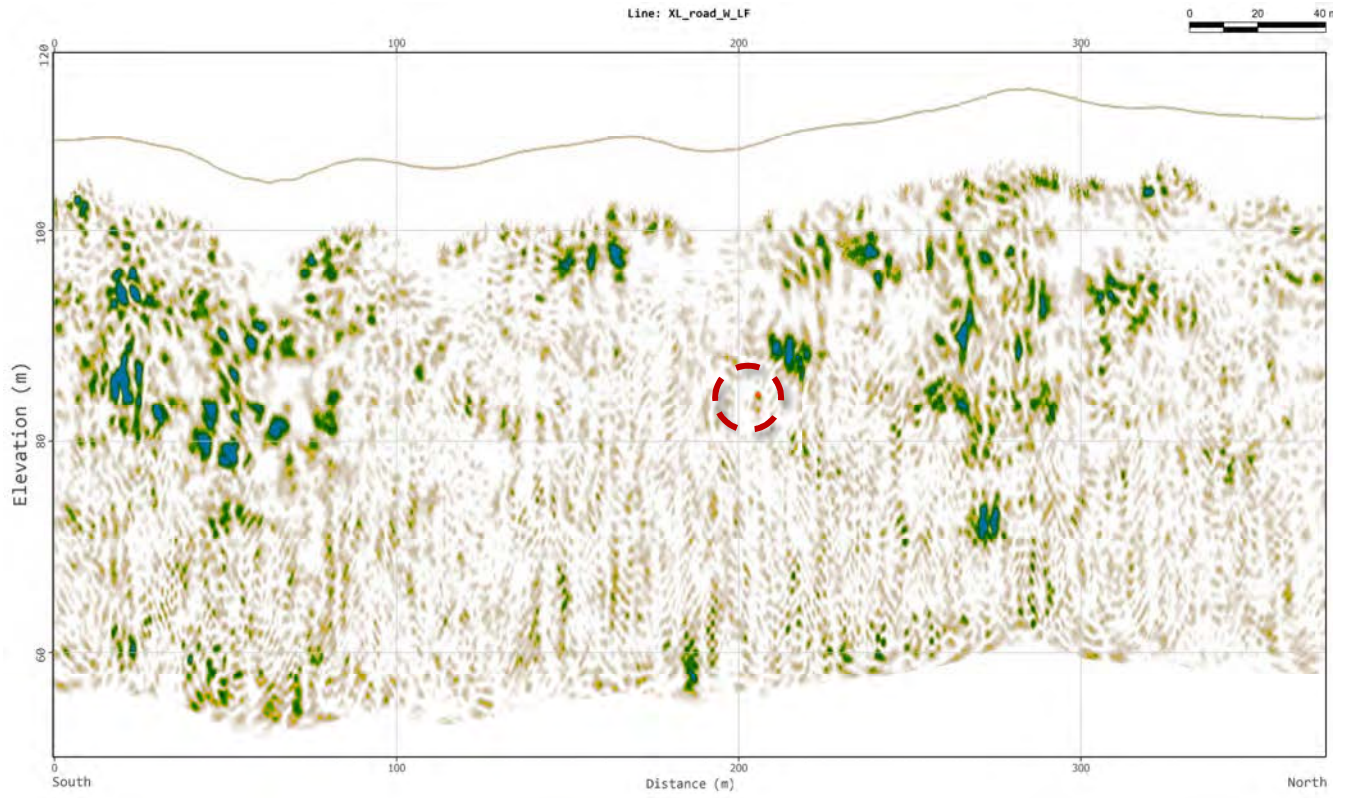
COORDINATES OF THE FEATURE (NAD 83, UTM 20N)		
EASTING (m)	NORTHING (m)	ELEVATION (m)
504340.1	4980848.7	82.3
504339.2	4980847.5	82.7
504339.2	4980845.4	84.3



Touquoy Open-Pit Mine: Detection of Underground Mine Workings Using Ground-Penetrating Radar



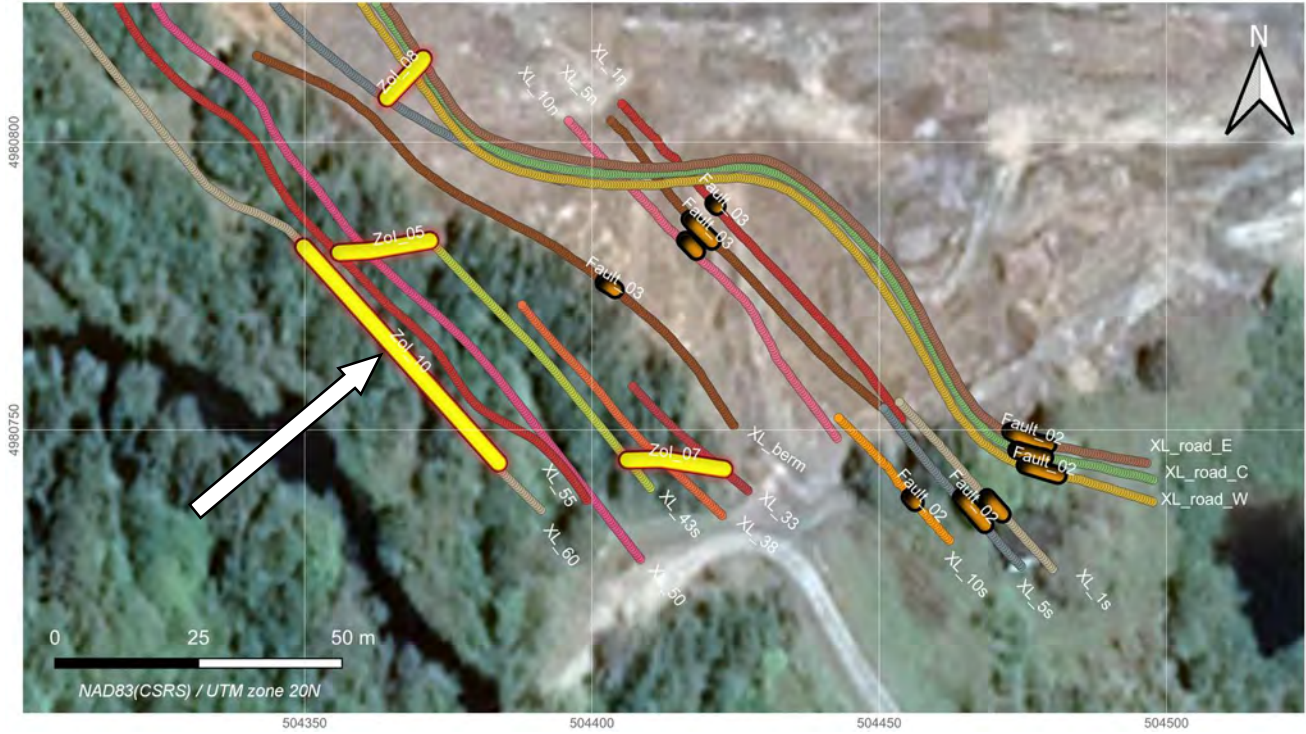
Touquoy Open-Pit Mine: Detection of Underground Mine Workings Using Ground-Penetrating Radar

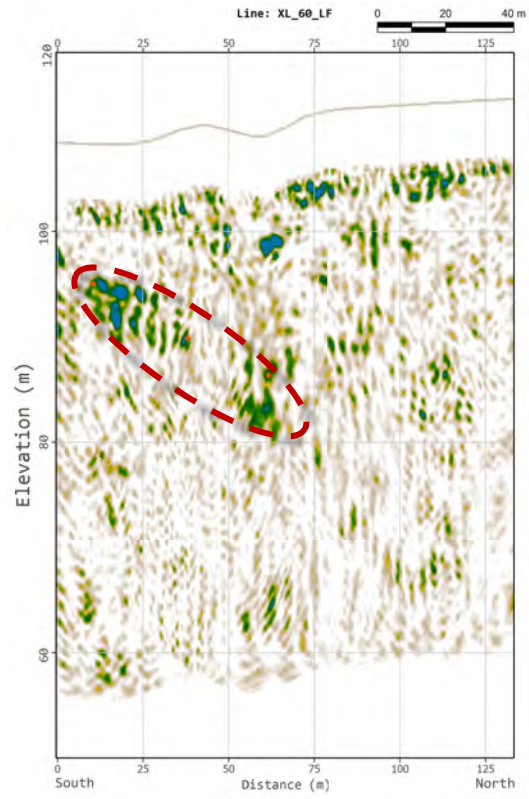


4.1.13 Zone of Interest X

Confidence:	High
Characterization:	Tabular, well-defined, dipping towards NW, high-energy, likely 2 metres or larger in diameter

COORDINATES OF THE FEATURE (NAD 83, UTM 20N)		
EASTING (m)	NORTHING (m)	ELEVATION (m)
504383.7	4980744.3	94.9
504365.5	4980764.5	89.8
504349.8	4980781.8	86.3

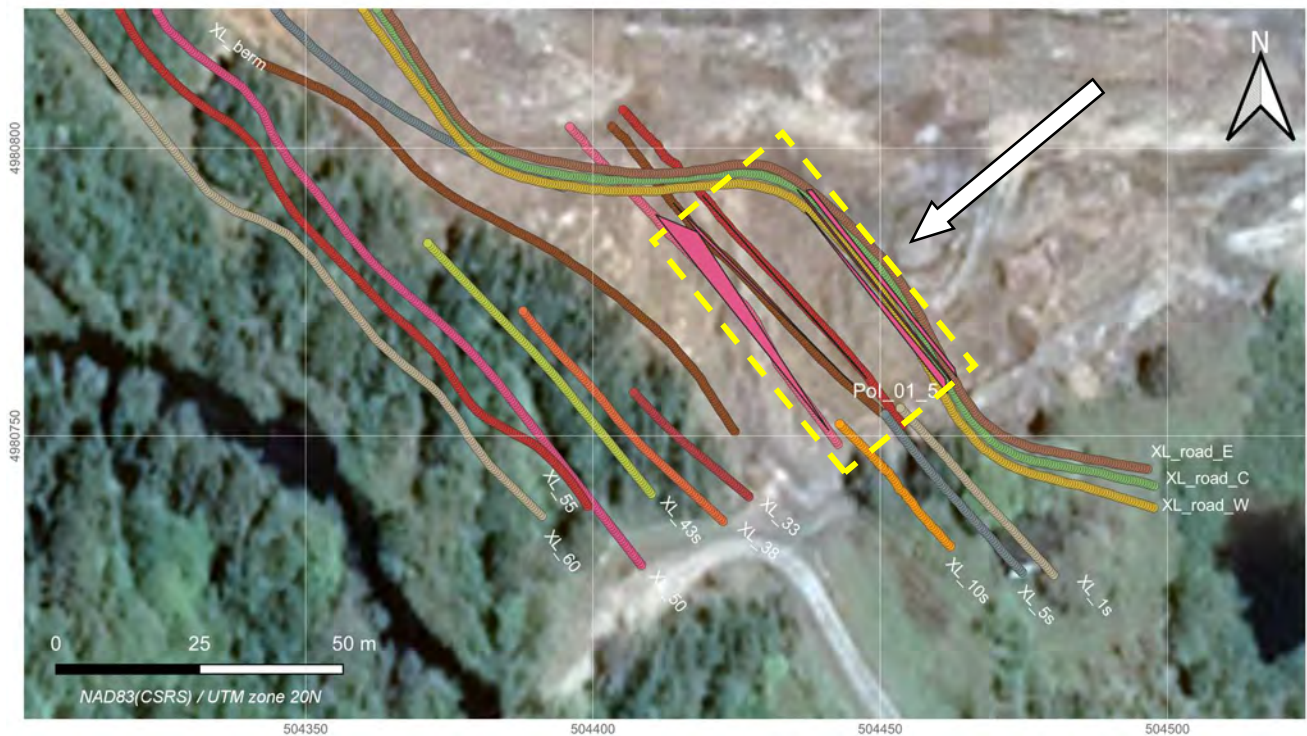


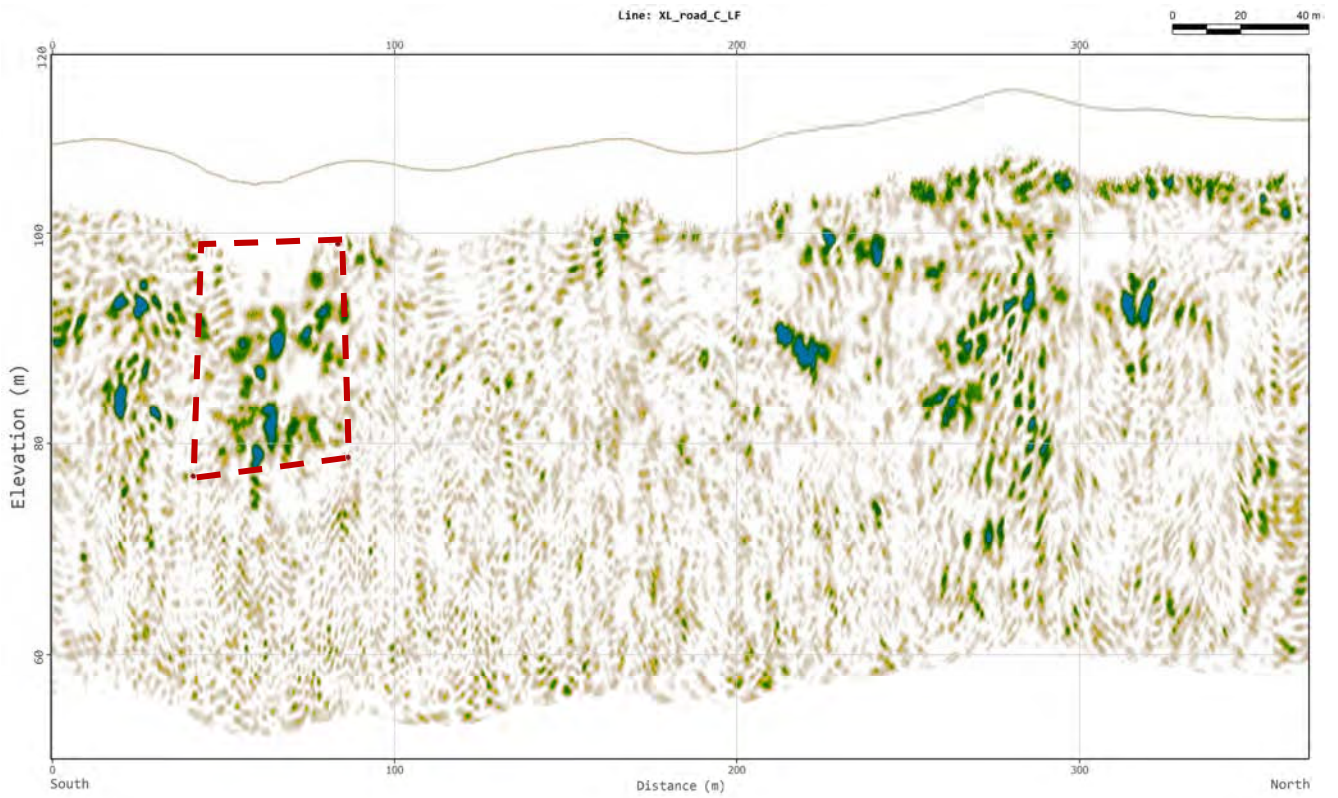
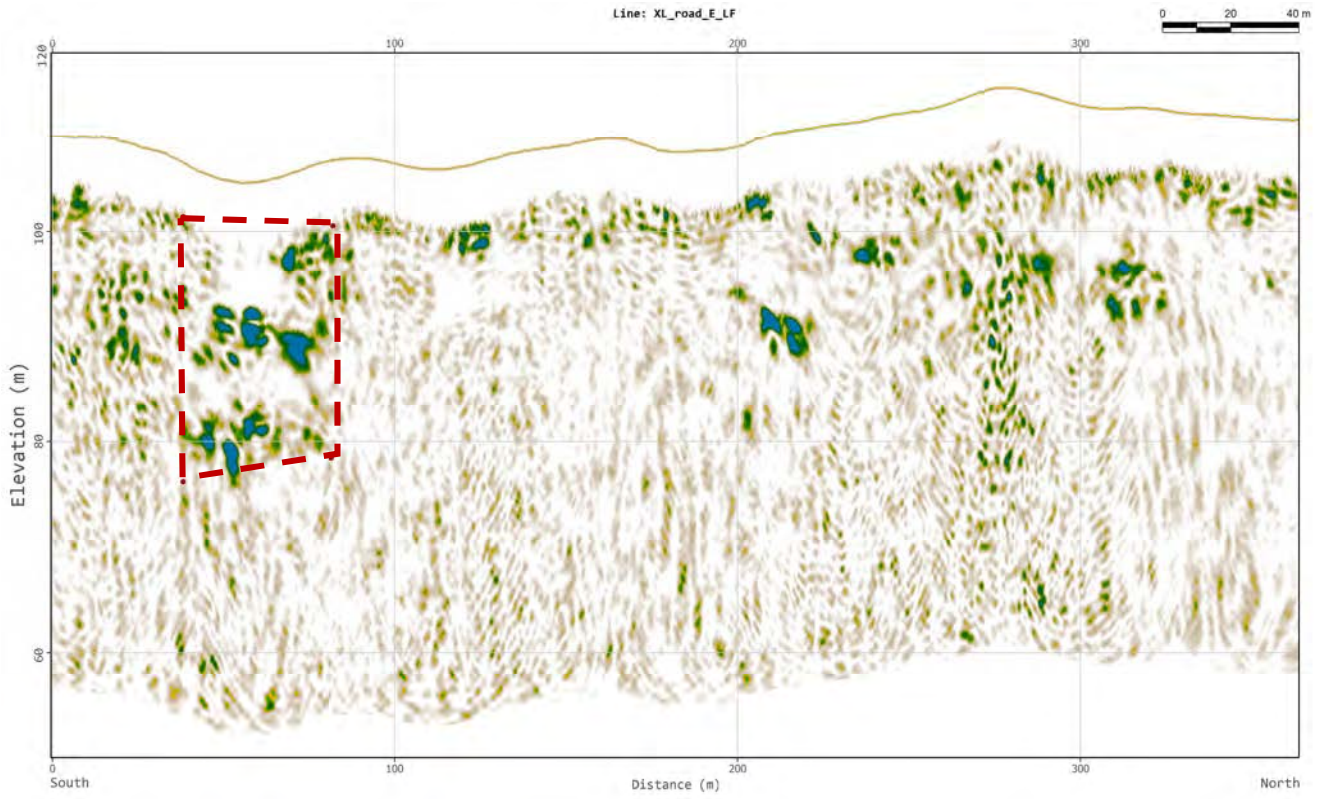


4.1.14 Region of Interest I

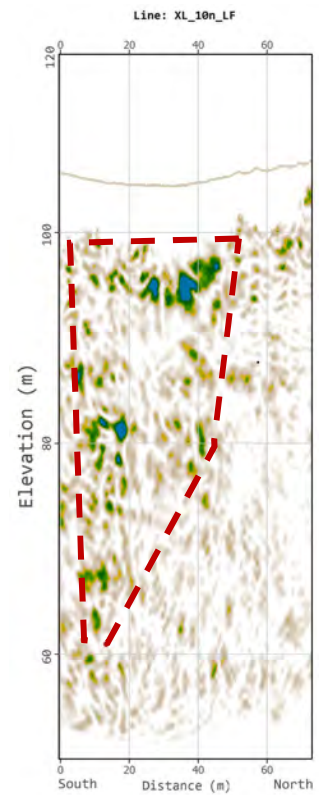
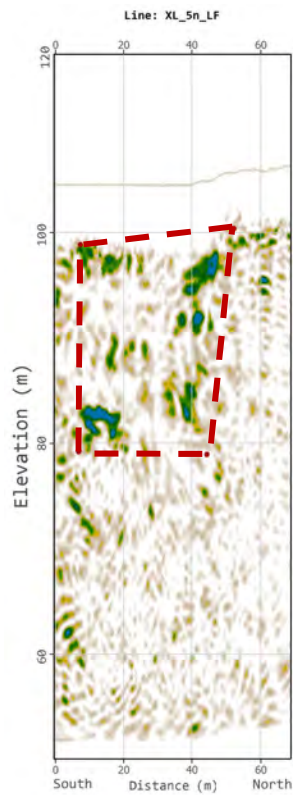
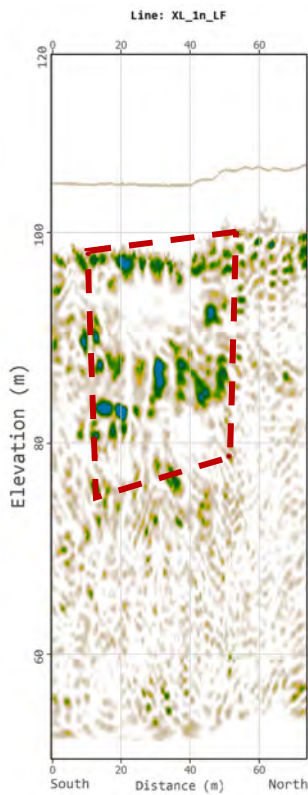
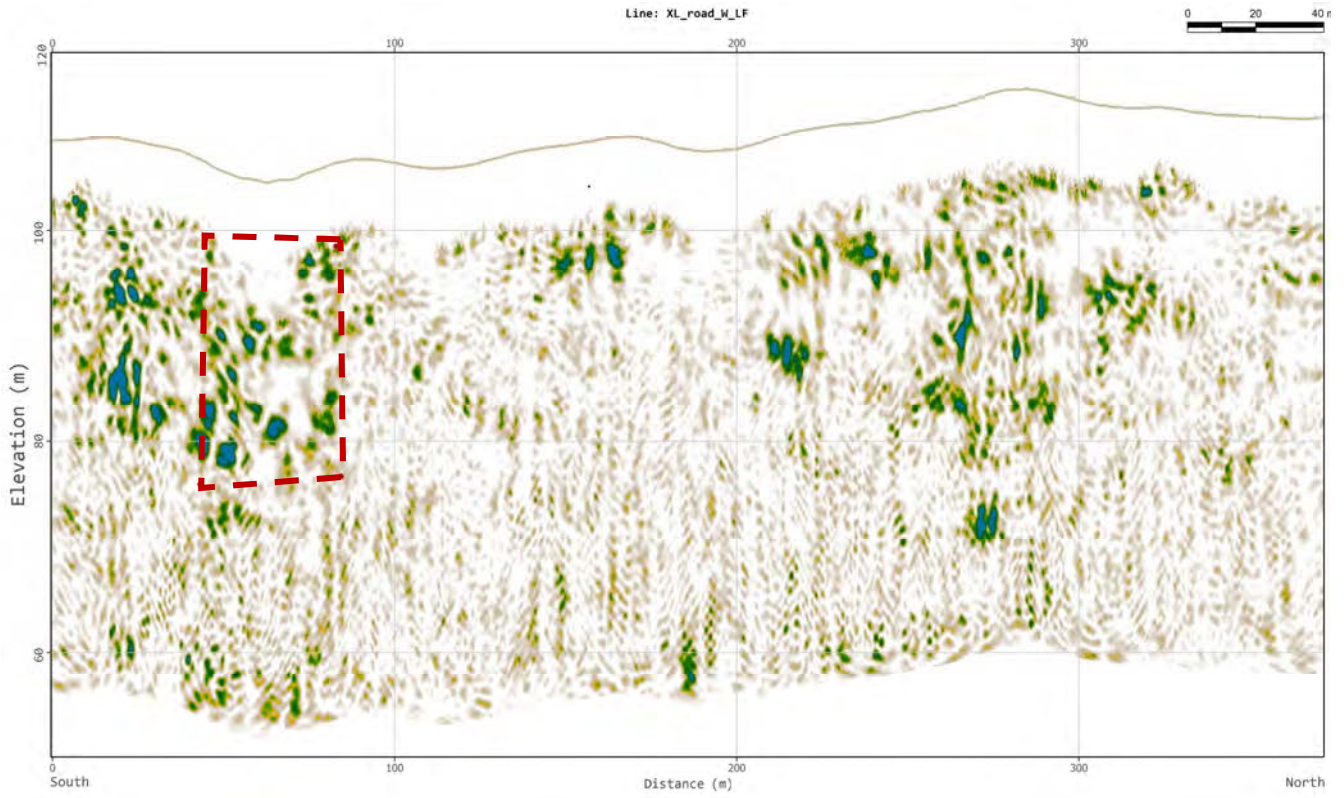
Confidence:	High
Characterization:	Complex zone of non-isolated and high-energy scattering

COORDINATES OF THE FEATURE (NAD 83, UTM 20N)		
EASTING (m)	NORTHING (m)	ELEVATION (m)
504463	4980761.7	99.4
504438.1	4980792.8	99.8
504437.1	4980792.7	78.8
504463.3	4980760.3	77.4
504461.6	4980760.8	98.9
504437.1	4980791.3	99.1
504435.5	4980792.8	78.6
504462.9	4980758.7	76.9
504461.3	4980760	98.7
504437.3	4980788.6	98.5
504436.9	4980789	76.9
504461.7	4980757.4	76.3
504447.6	4980759.9	98.1
504446.2	4980761.8	78.8
504420.3	4980790.4	78.8
504419	4980791.8	100
504445.1	4980759	98.8
504445.3	4980758.9	79.2
504418.4	4980785.2	78.9
504413.9	4980790.5	100.2
504410.9	4980788.5	99.4
504418.3	4980785.4	79.7
504435.2	4980759.6	61
504438.7	4980754.4	61.3
504441.1	4980750.9	98.9





Touquoy Open-Pit Mine: Detection of Underground Mine Workings Using Ground-Penetrating Radar



5 SUMMARY

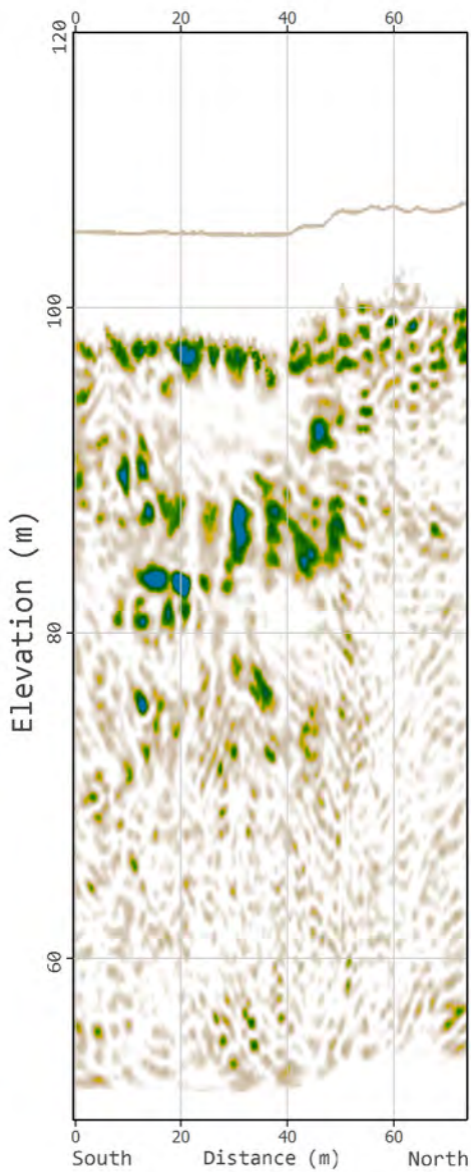
The strategic deployment of the rough-terrain ground-penetrating radar with the lowest available central frequency, survey design with lateral redundancy or verification, and purpose-tailored processing workflow produced an interpretable dataset showing numerous isolated or localized high-amplitude events. In summary, the GPR survey discovered:

- 3 faults; zones with a substantial sub-vertical scattering
- 10 zones of interest (Zol); interpreted as probable underground mine workings
- 1 region of interest (RoI); interpreted as complex networks of likely underground workings

These events were binned, *a priori*, into probable underground workings or geological categories and are detailed in this report.

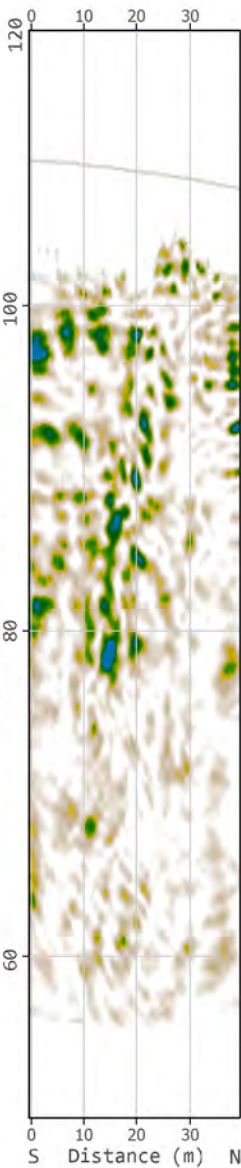
LOW FREQUENCY DATA

Line: XL_1n_LF

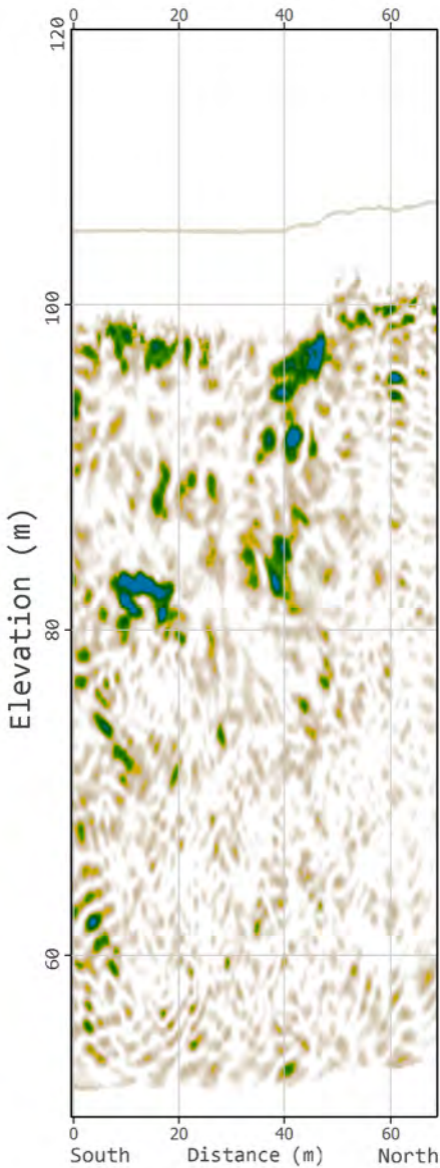


Line: XL_1s_LF

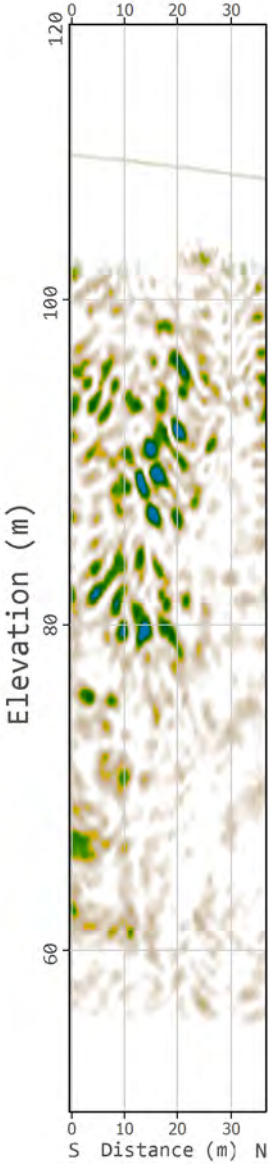
Elevation (m)



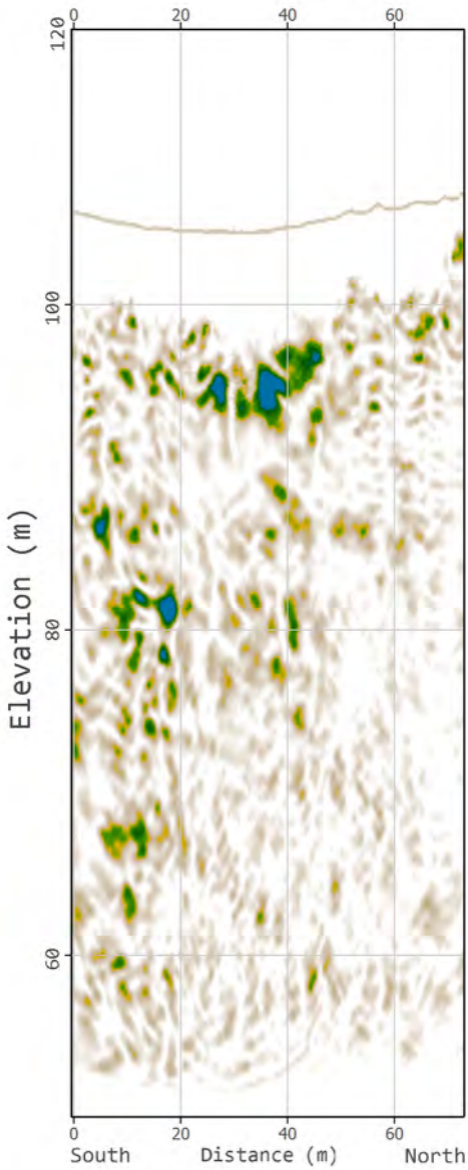
Line: XL_5n_LF



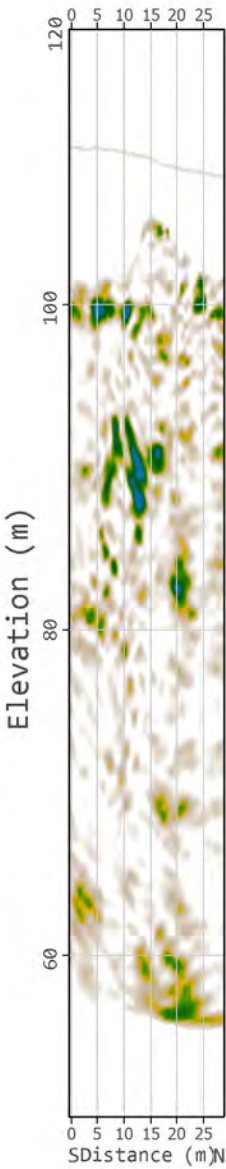
Line: XL_5s_LF



Line: XL_10n_LF

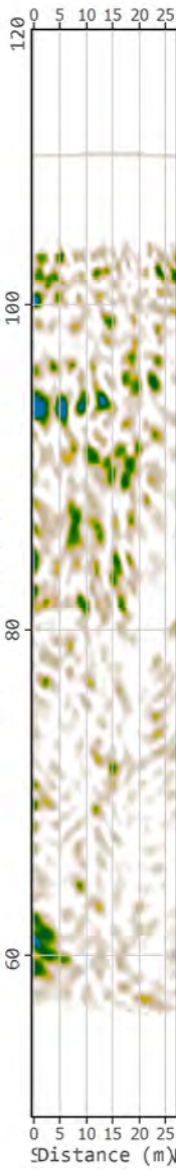


Line: XL_10s_LF

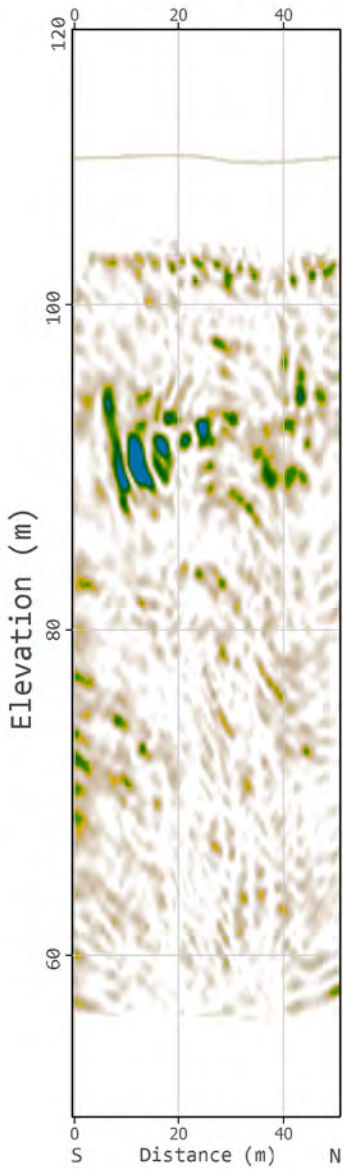


Line: XL_33_LF

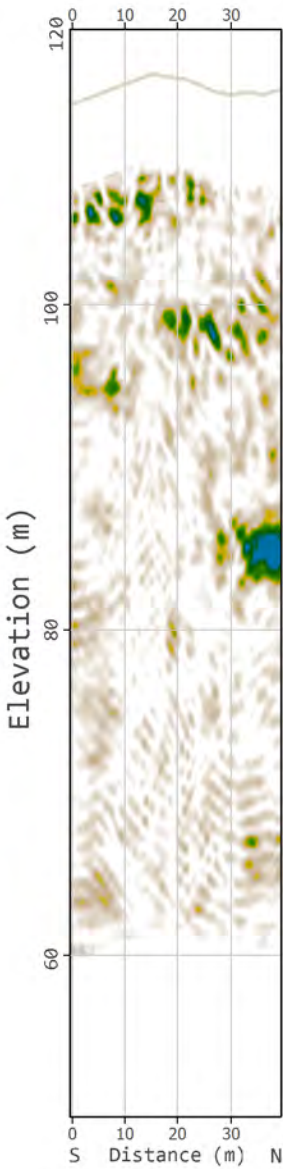
Elevation (m)



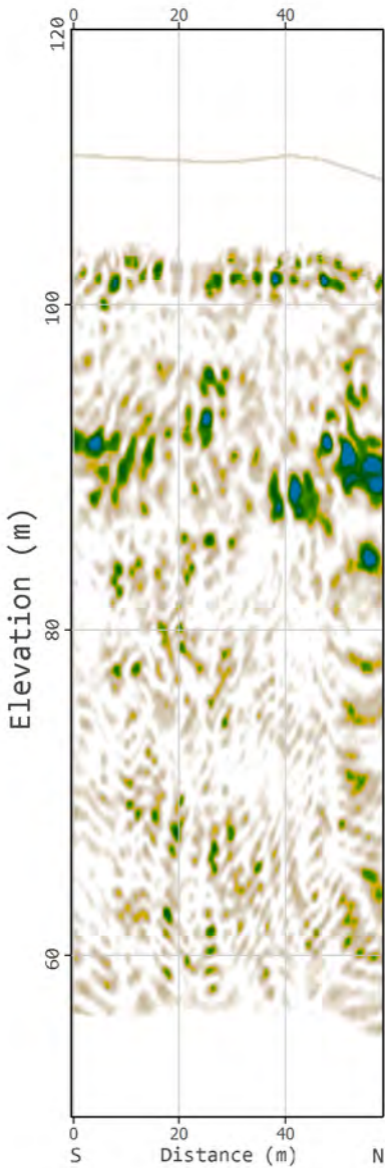
Line: XL_38_LF



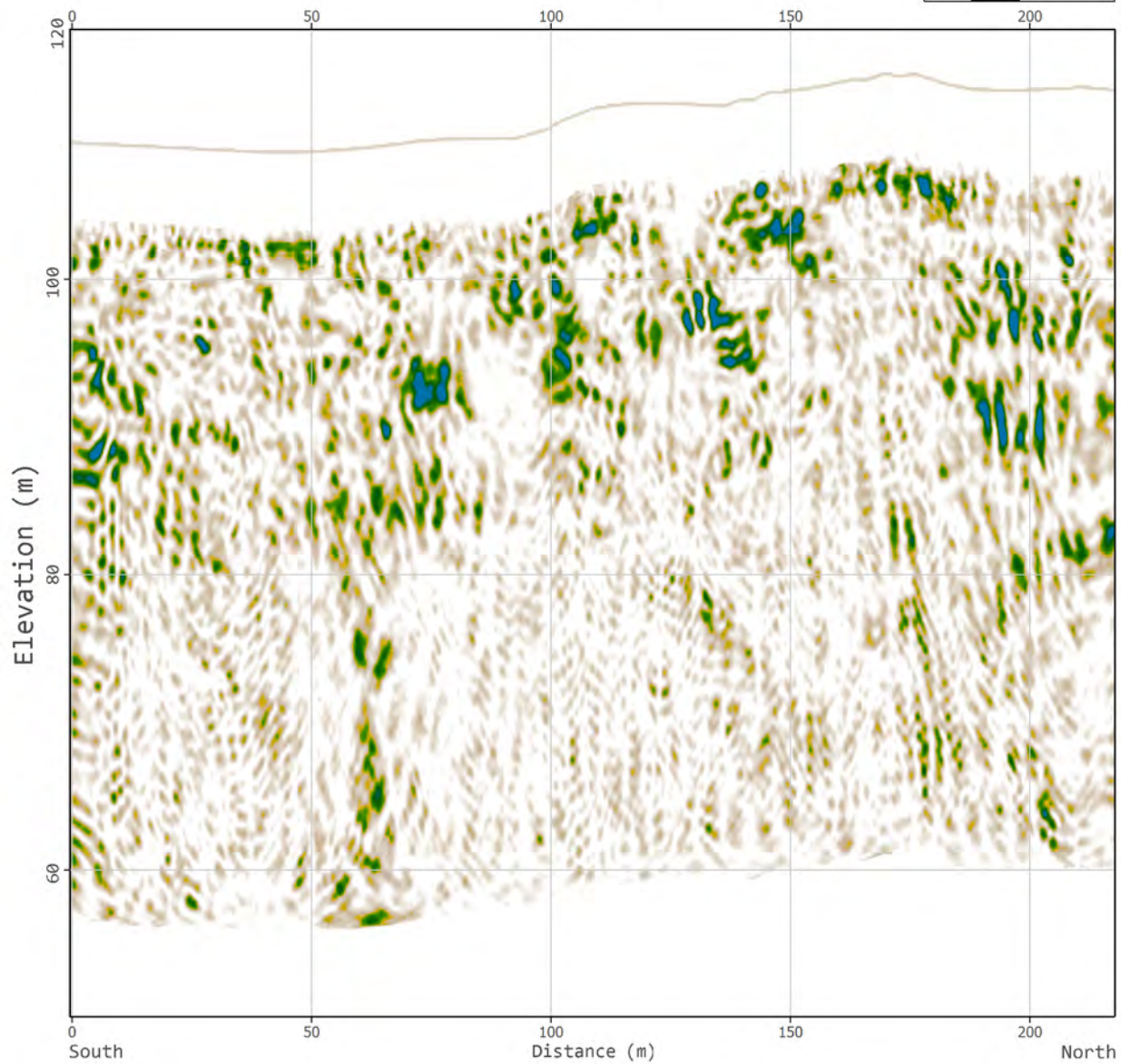
Line: XL_43n_LF



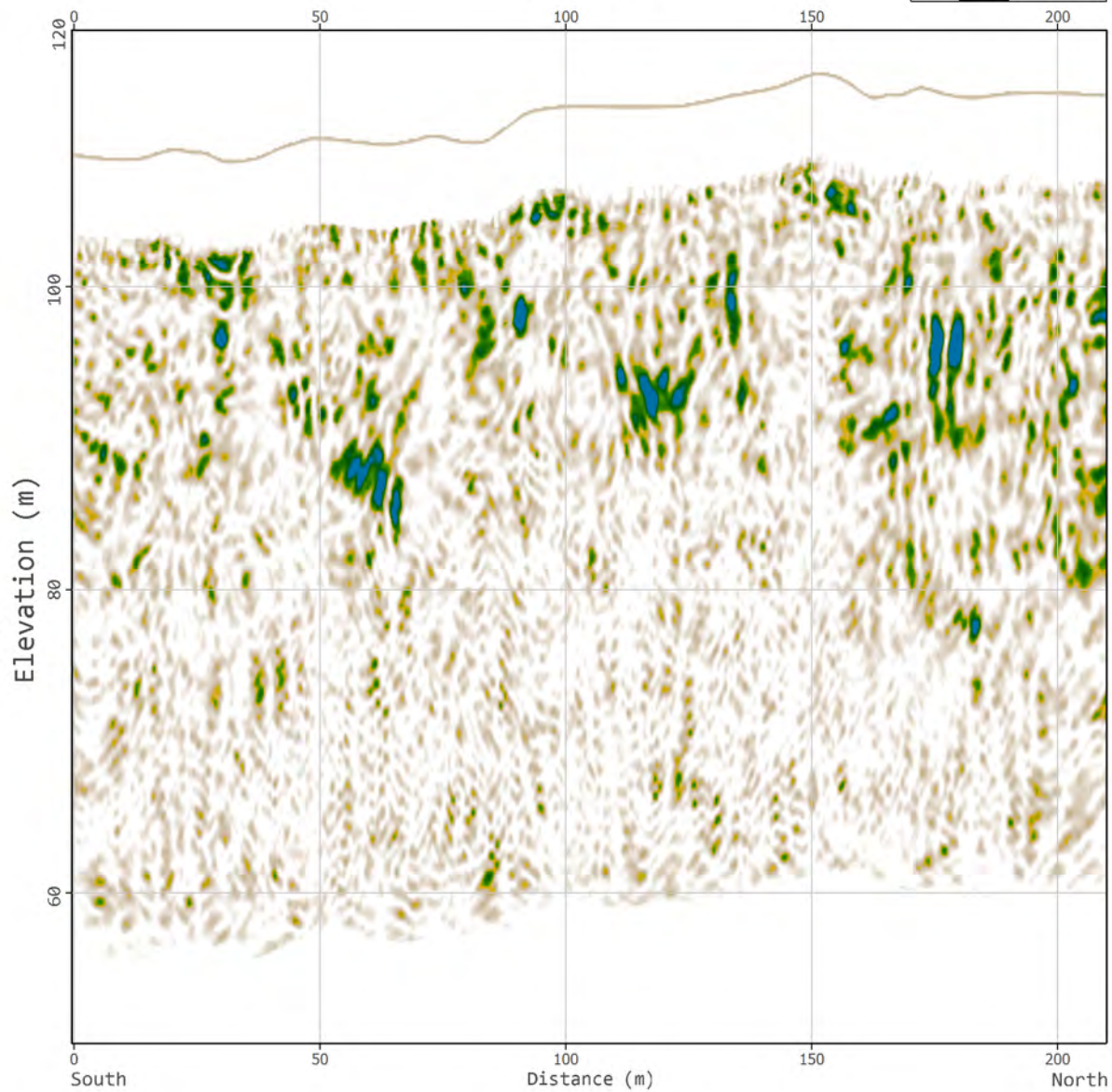
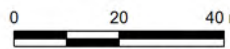
Line: XL_43s_LF



Line: XL_50_LF

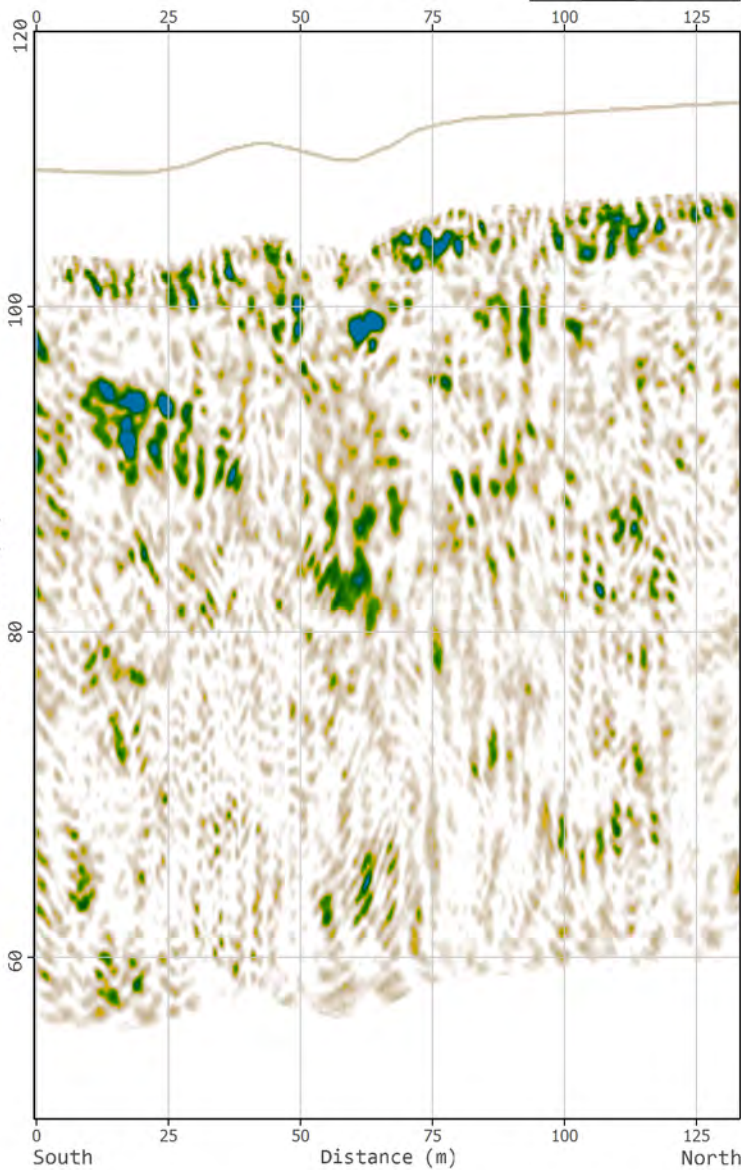


Line: XL_55_LF

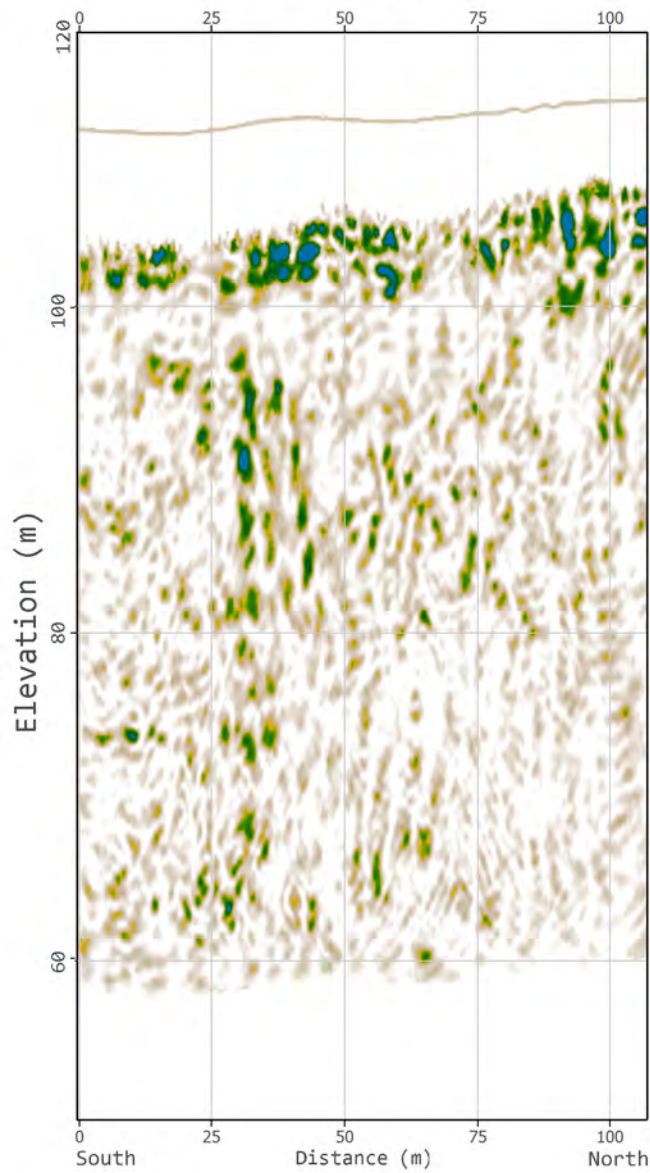


Line: XL_60_LF

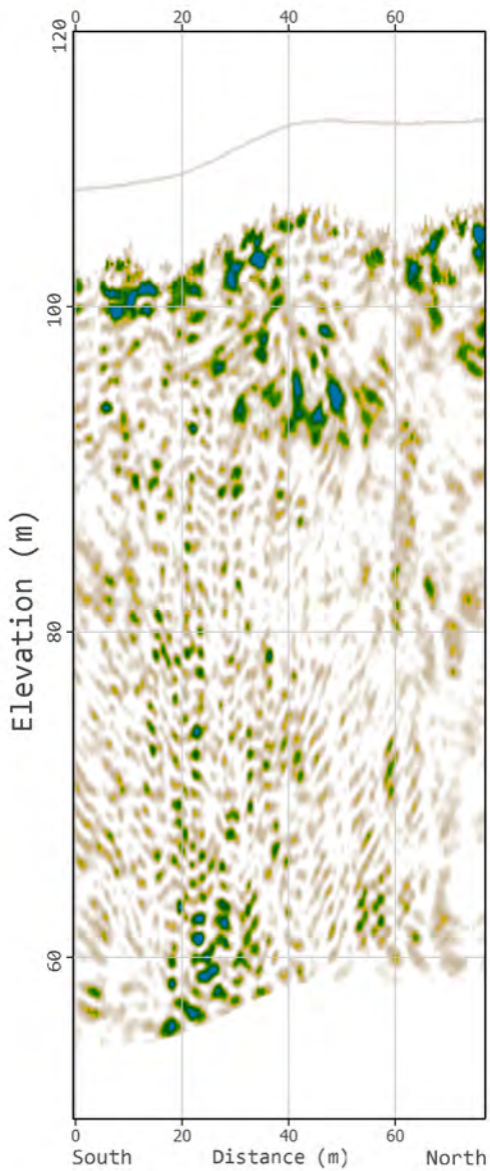
0 20 40 m



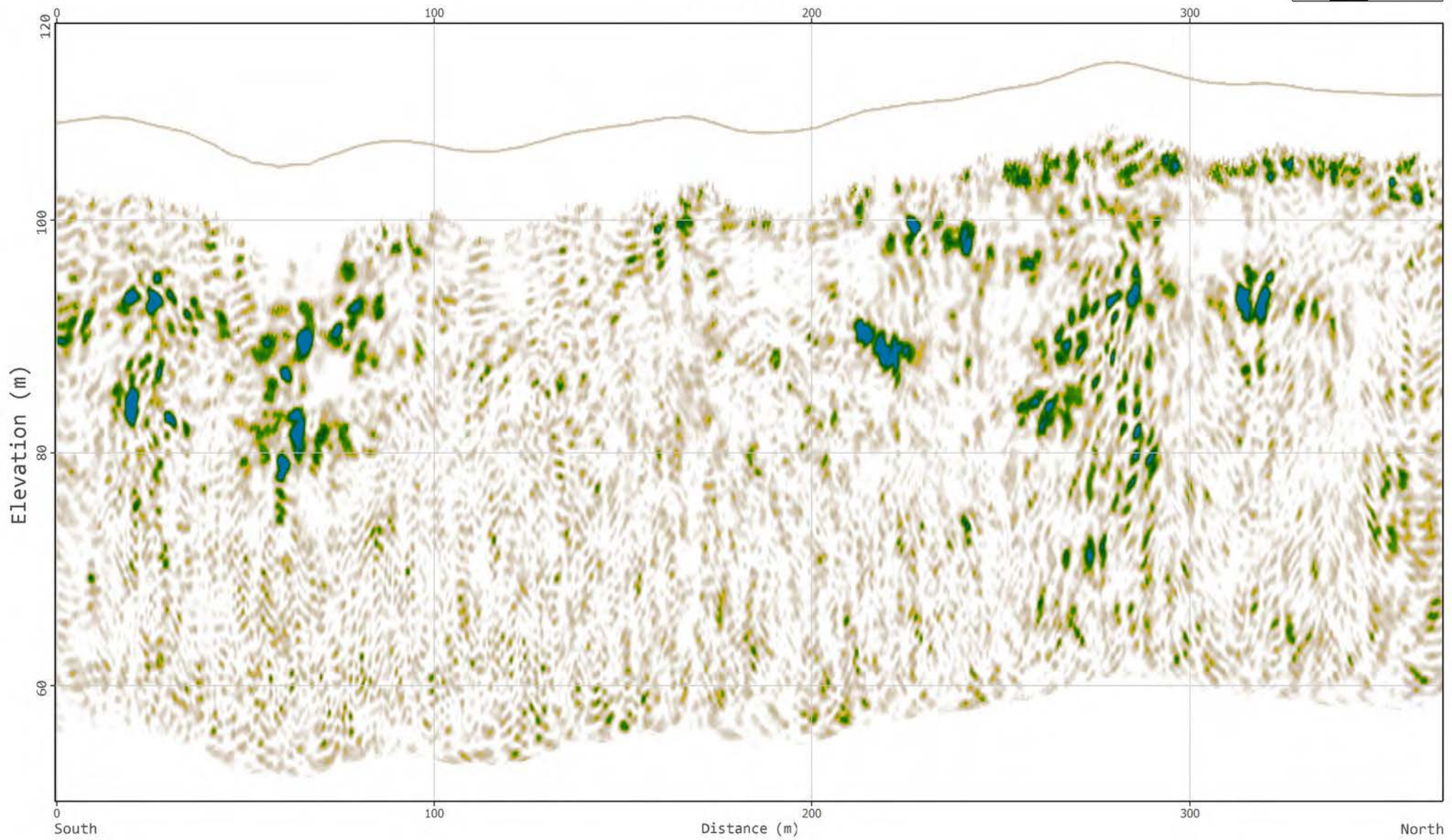
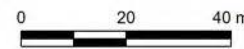
Line: XL_berm_LF



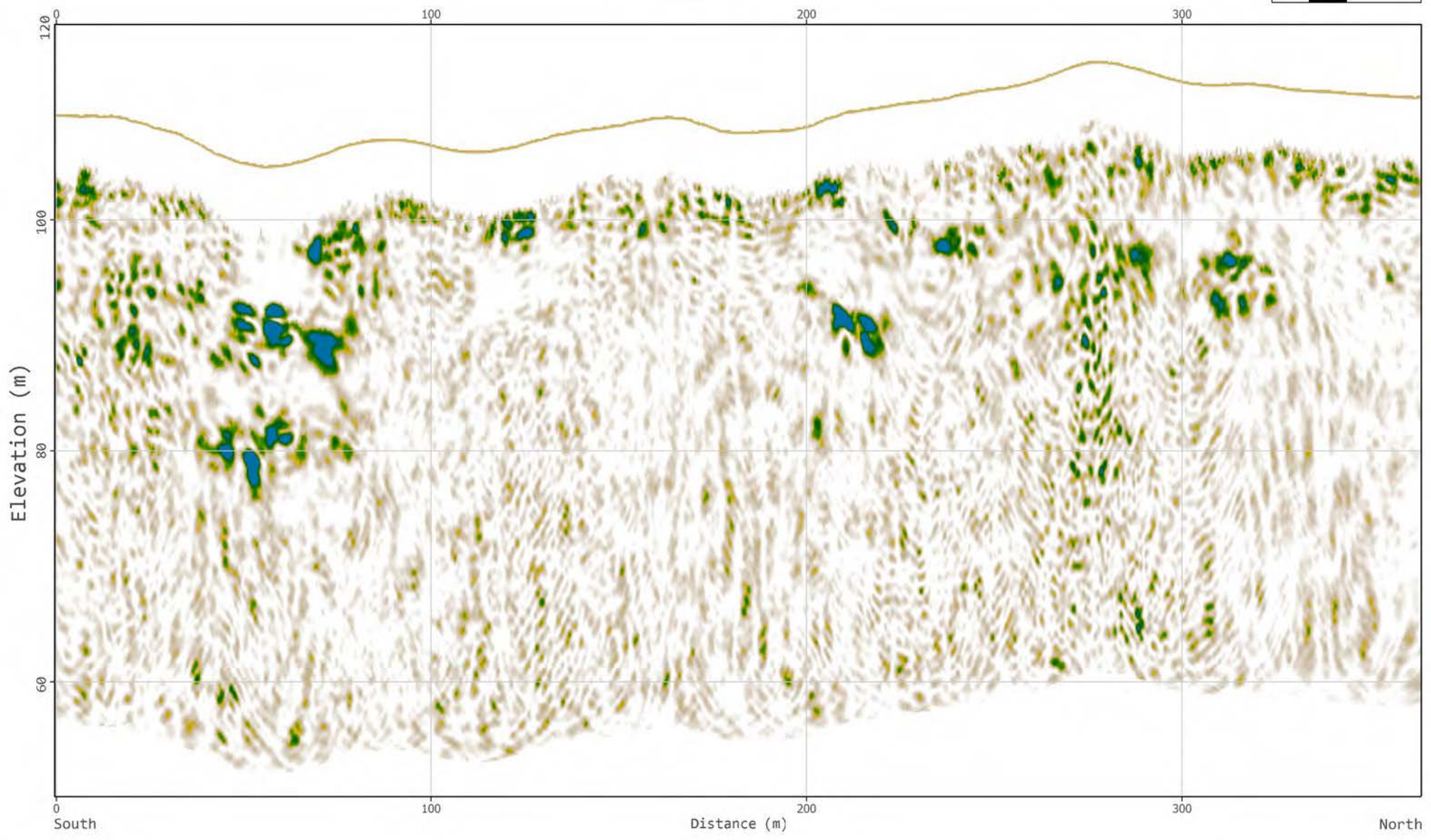
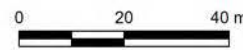
Line: XL_ramp_berm_LF



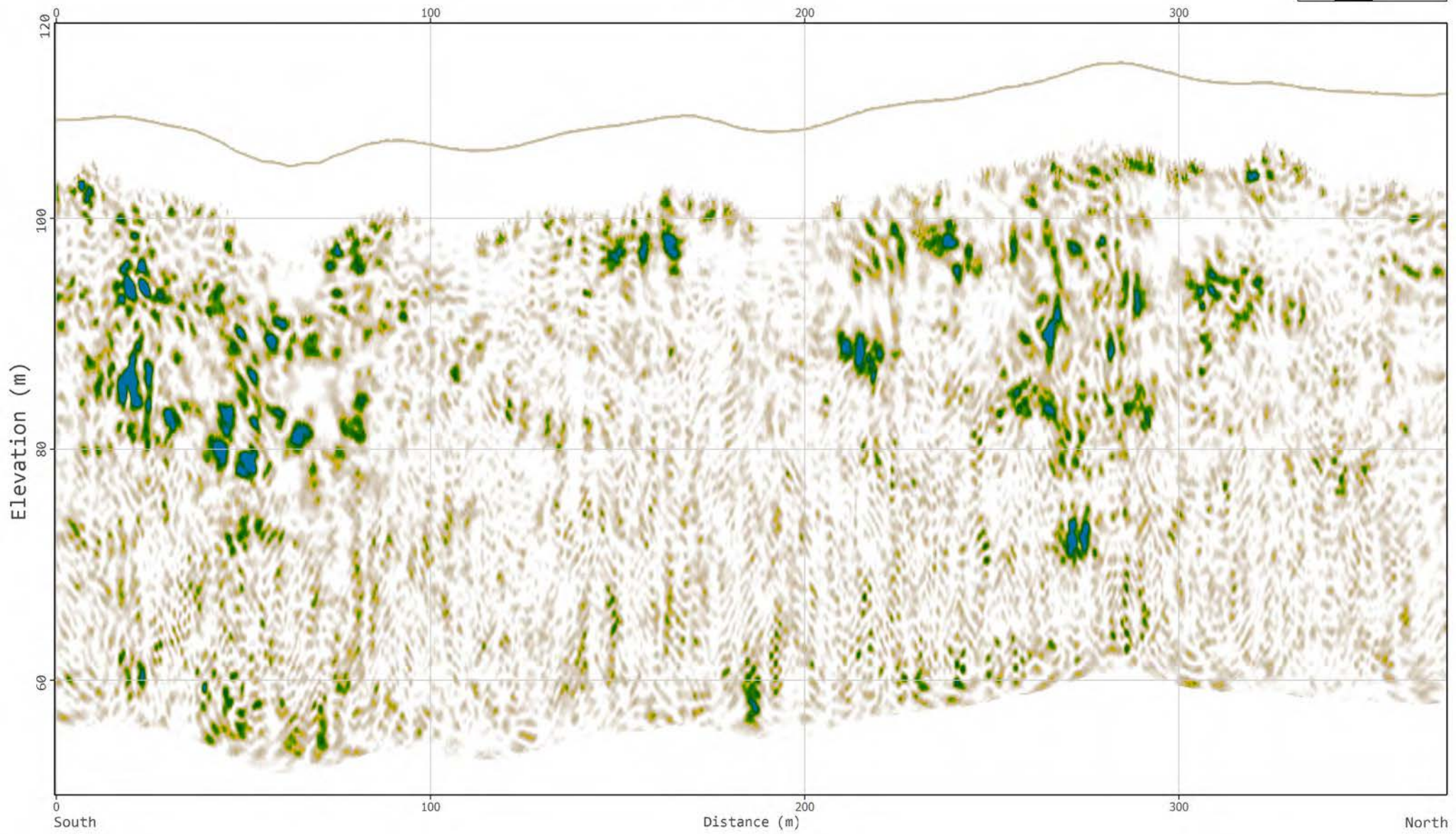
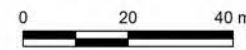
Line: XL_road_C_LF



Line: XL_road_E_LF

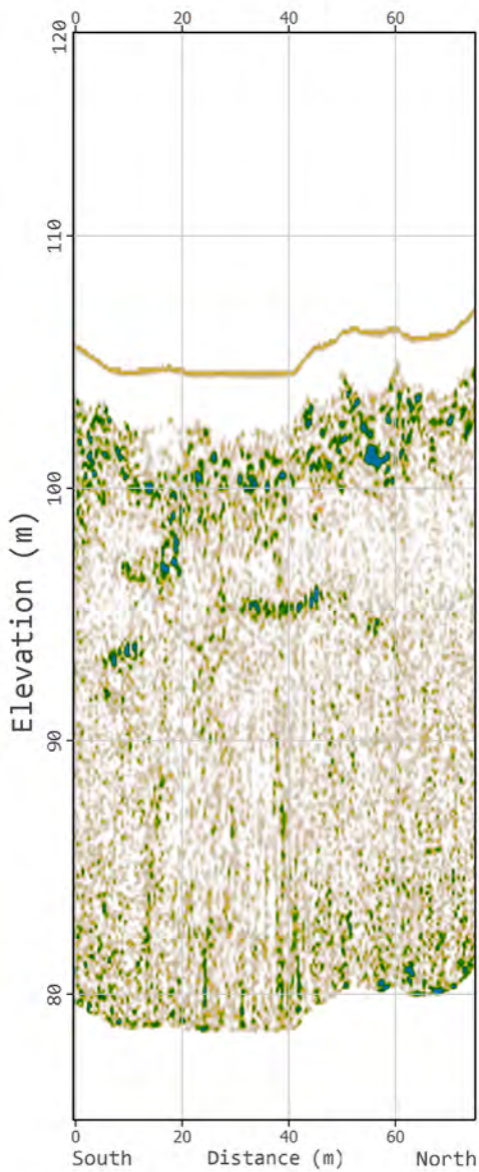


Line: XL_road_W_LF

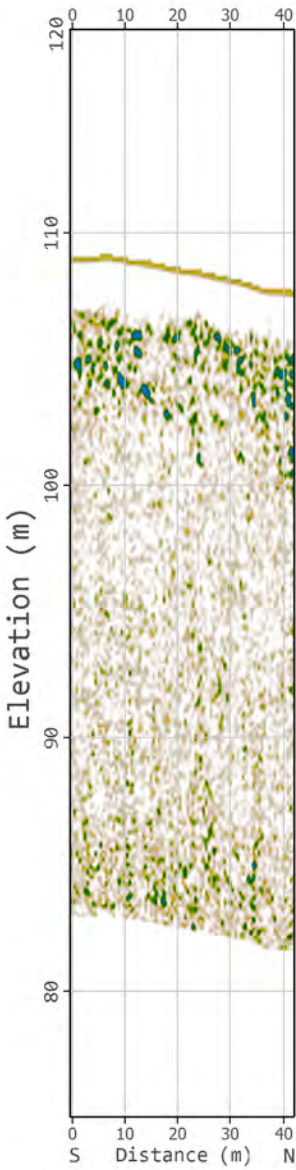


HIGH FREQUENCY DATA

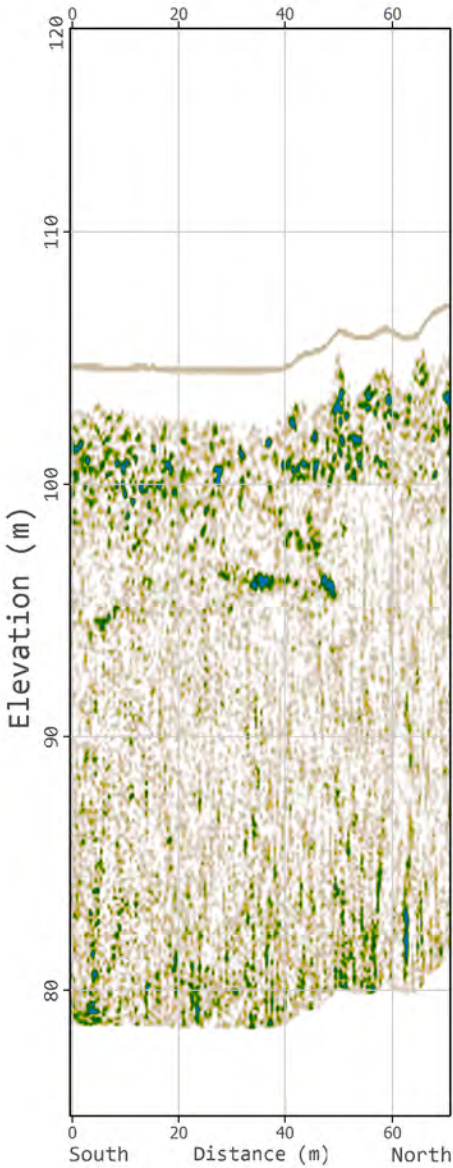
Line: XL_1n_HF



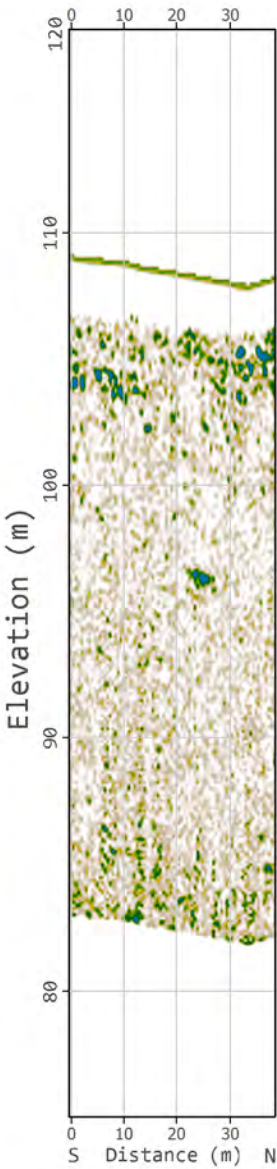
Line: XL_1s_HF



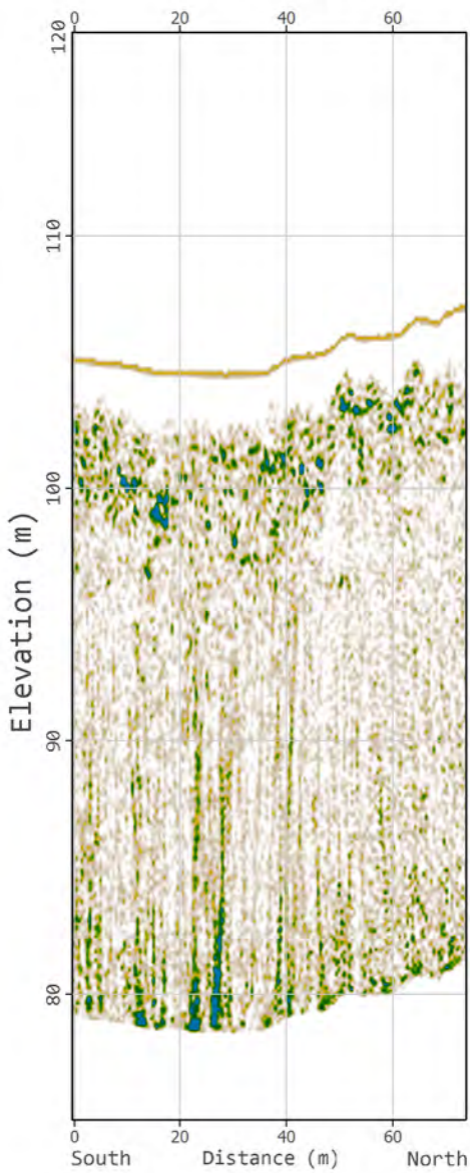
Line: XL_5n_HF



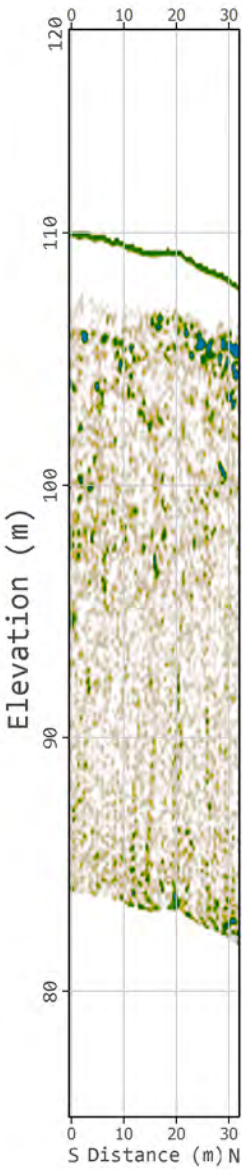
Line: XL_5s_HF



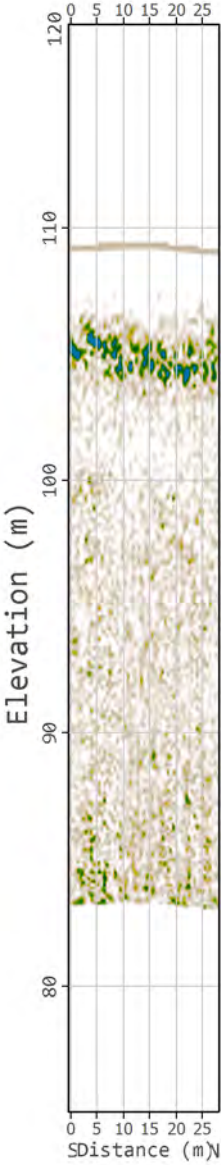
Line: XL_10n_HF



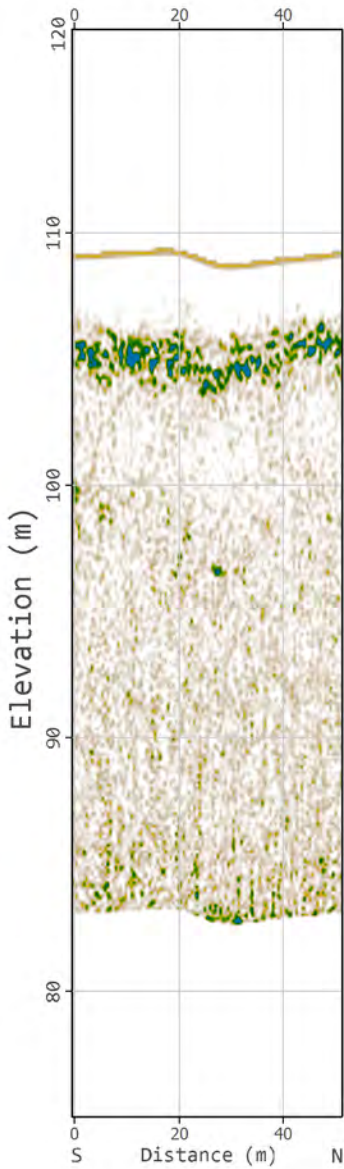
Line: XL_10s_HF



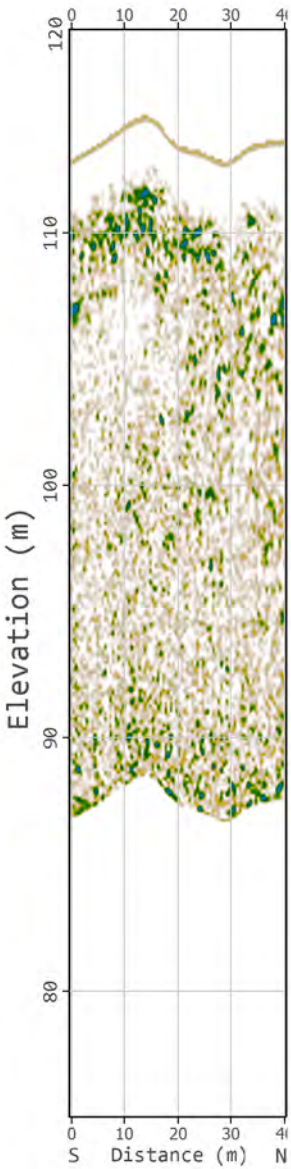
Line: XL_33_HF



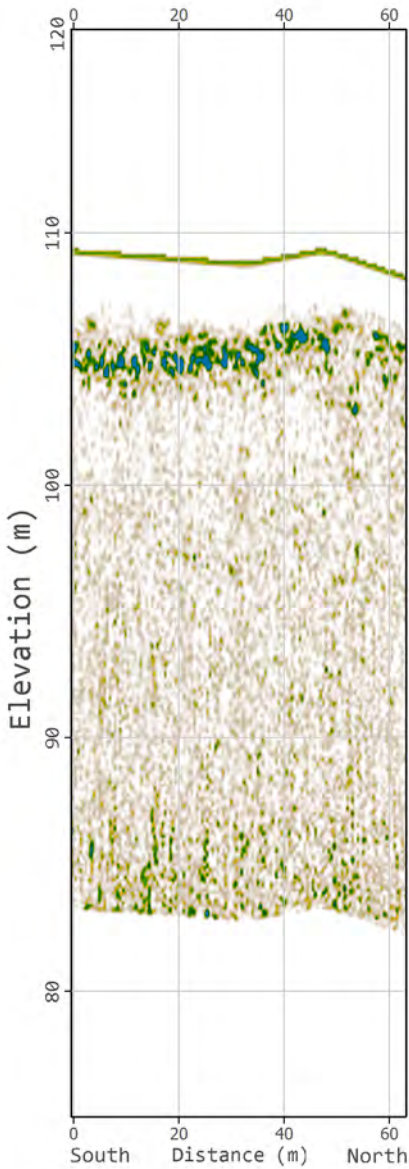
Line: XL_38_HF



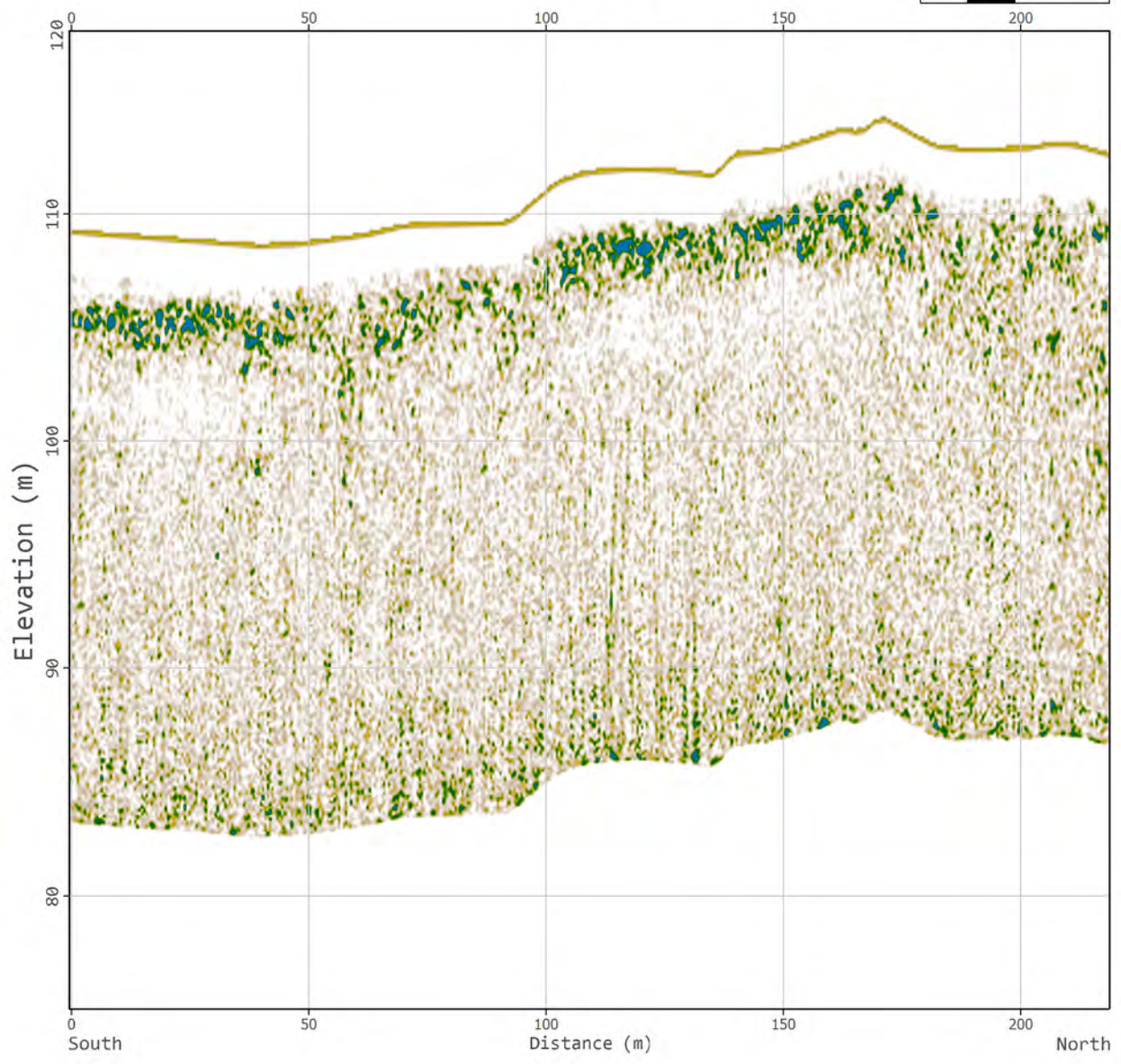
Line: XL_43n_HF



Line: XL_43s_HF

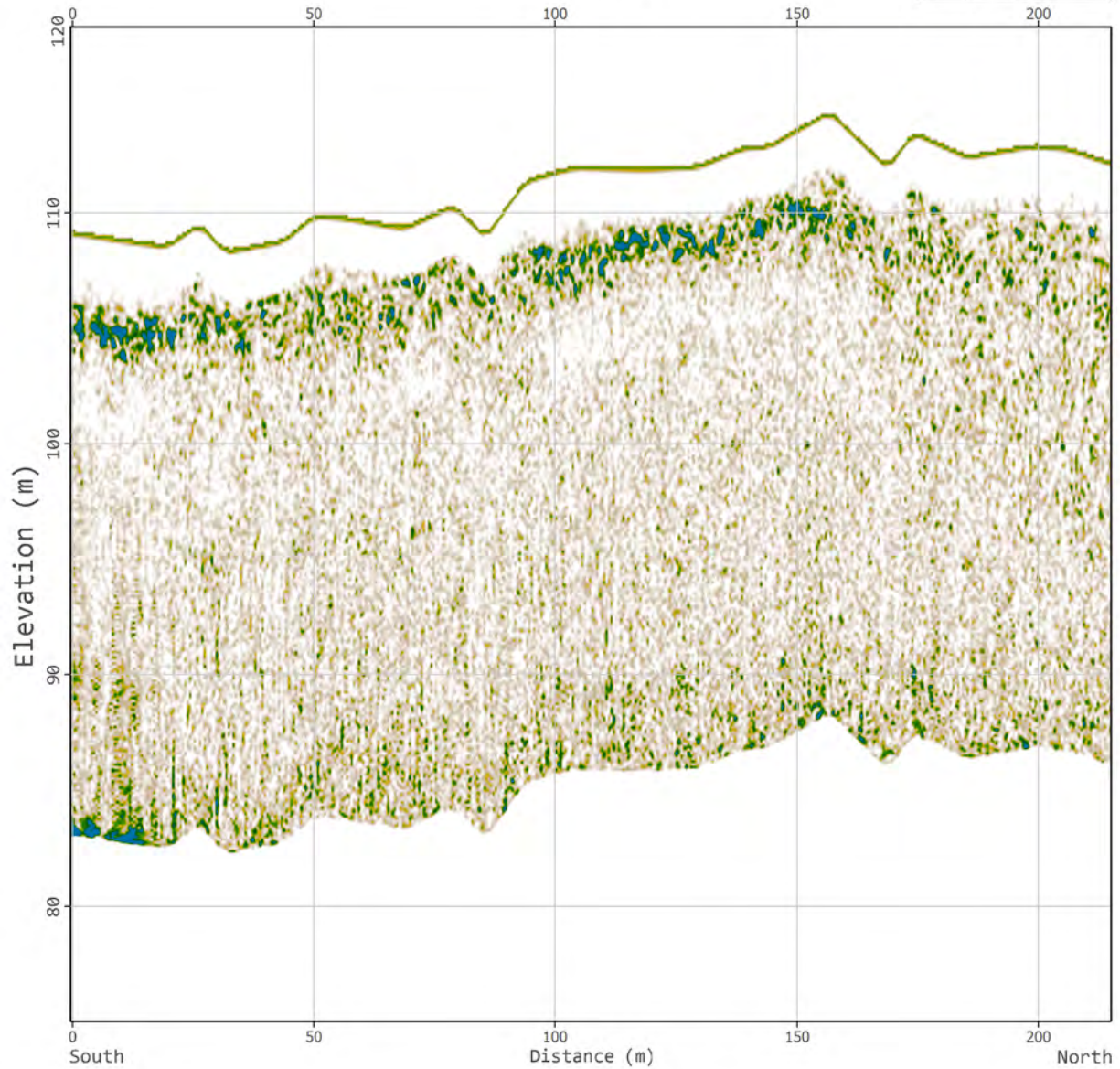


Line: XL_50_HF



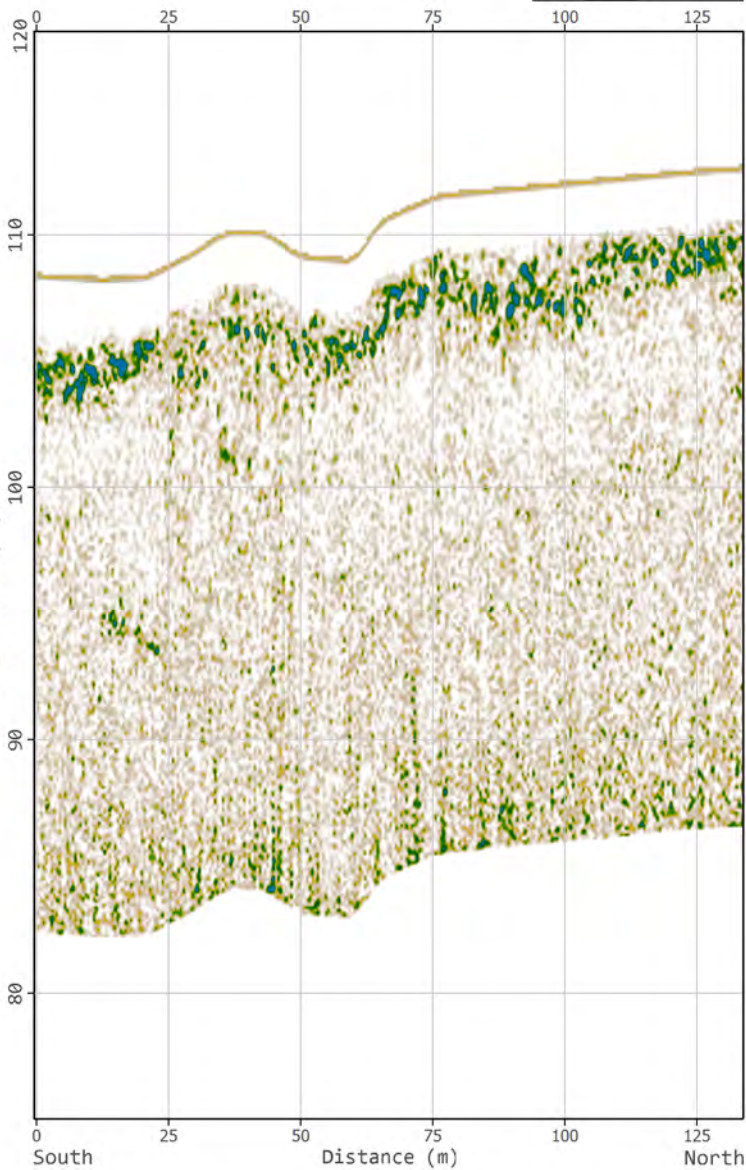
Line: XL_55_HF

0 20 40 m

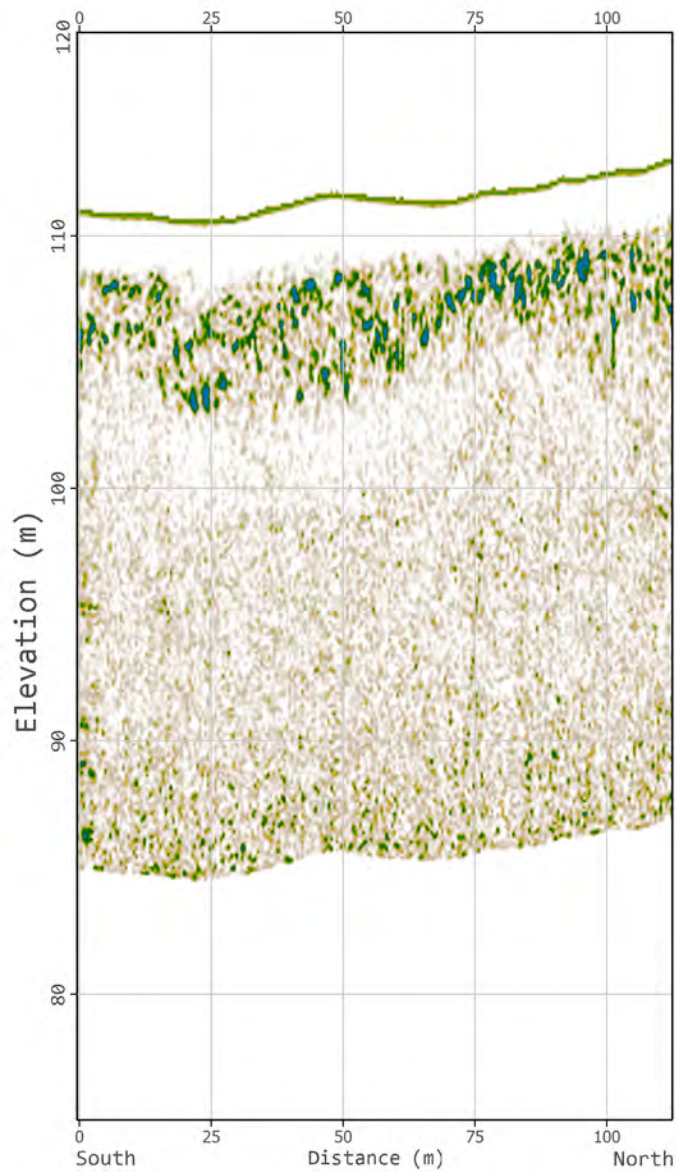


Line: XL_60_HF

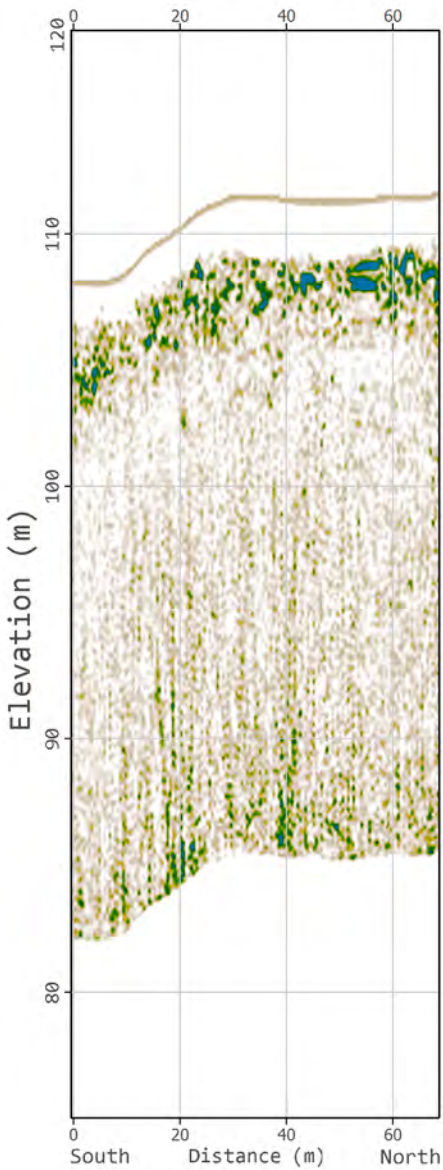
0 20 40 m

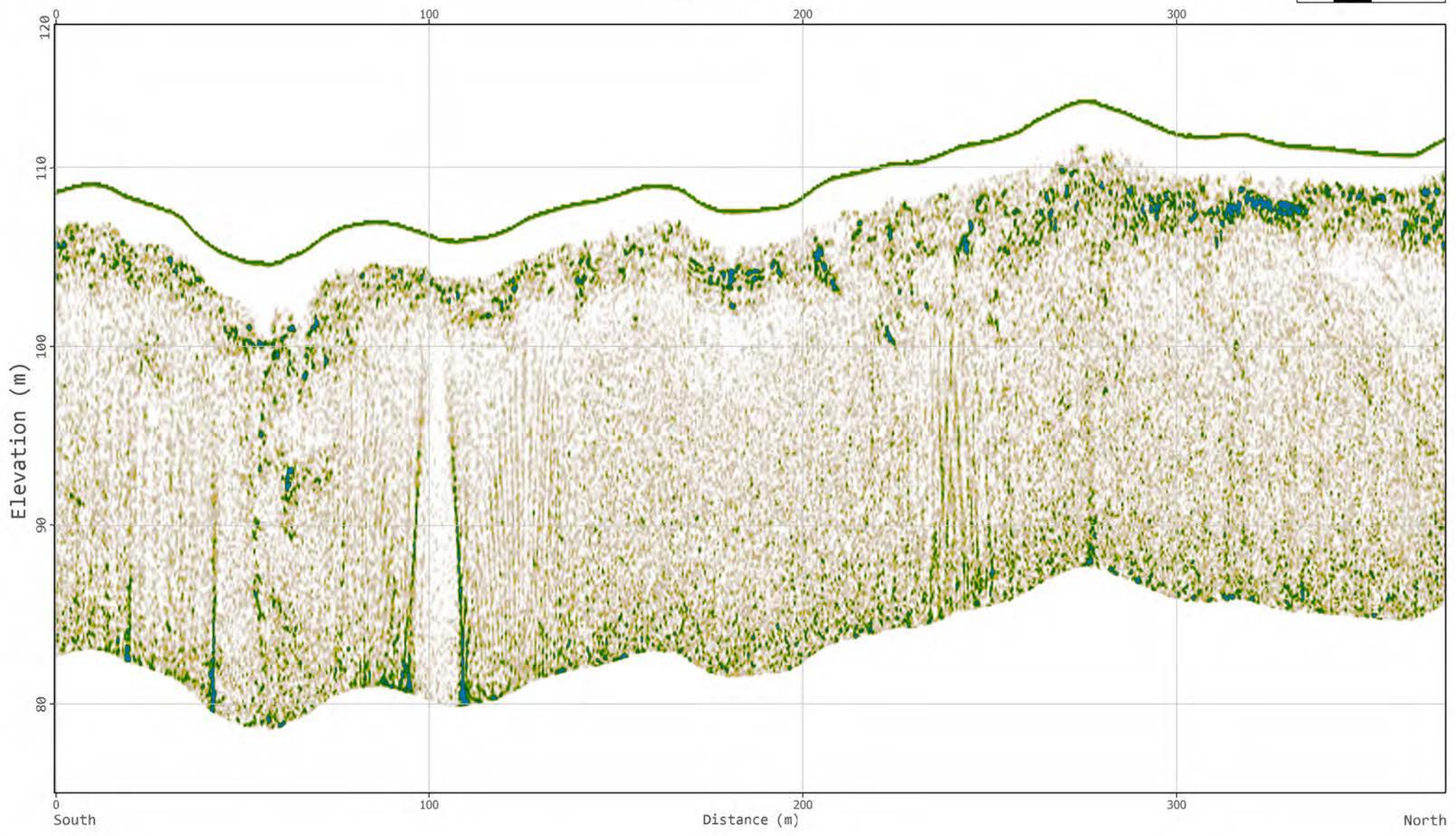


Line: XL_berm_HF



Line: XL_ramp_berm_HF





Line: XL_road_E_HF

0 20 40 m

